USGS Research on Mineral Resources—1987 Program and Abstracts

Third Annual V. E. McKelvey Forum on Mineral and Energy Resources

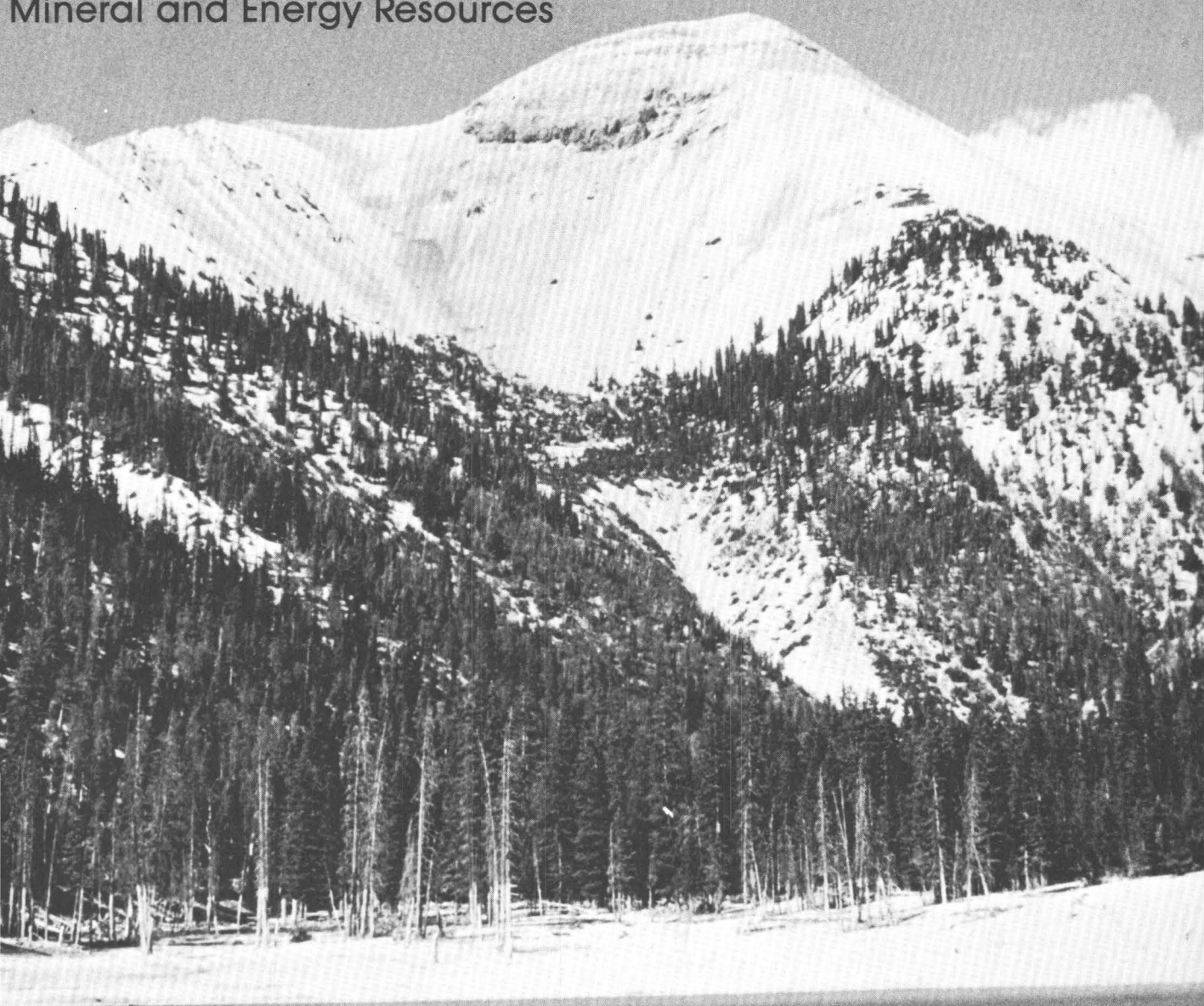

U.S. Geological Survey Circular 995

Ash-flow tuffs and lava flows in the Mount Belknap caldera, Utah.

USGS Research on Mineral Resources—1987 Program and Abstracts

Edited by Janet Somerville Sachs

Third Annual V. E. McKelvey Forum on Mineral and Energy Resources

U.S. Geological Survey Circular 995

DEPARTMENT OF THE INTERIOR
DONALD PAUL HODEL, Secretary

U.S. GEOLOGICAL SURVEY
Dallas L. Peck, Director

Free on application to the Books and Open-File Reports Section,
U.S. Geological Survey, Federal Center, Box 25425, Denver, CO 80225

A society's wealth depends on the use it makes of raw materials, energy, and especially ingenuity.

—V. E. McKelvey
1916–1987

Foreword

The first two V. E. McKelvey Forums, in 1985 and 1986, were exceptionally well-attended by industrial, State and Federal government, and academic members of the earth science community. This participation resulted in many positive contributions to U.S. Geological Survey programs in mineral and energy resources. Through active exchanges of ideas between Geological Survey scientists and the people attending the Forums, we learned firsthand about the changing needs of the mineral and energy industries, and we found new ways to make significant improvements in our programs.

The Forum is named for Vincent E. McKelvey in recognition of his lifelong contributions to research, development, and administration in mineral and energy resources as a scientist, as Chief Geologist, and as Director of the Geological Survey. We were very fortunate to have Vince attend the first two Forums. The meeting is an annual event, and the subject matter alternates yearly between mineral and energy resources. Though the format of the meeting may change from year to year, the primary purpose will remain the same—to encourage direct communication between Geological Survey scientists and earth scientists in the industrial, academic, and government communities.

Current programs in mineral-resource investigations at the Geological Survey include strategic and critical minerals, wilderness mineral evaluations, regional mineral assessments, and geochemical and geophysical research on new exploration techniques. The topics of papers at the 1987 Forum span a very wide range of research; precious- and base-metal studies in ultramafic deposits in Alaska, geophysical research on disseminated gold deposits in Nevada, minerals in agriculture, isotopic research on mineral systems, nuclear borehole logging for critical metals, and the role of aqueous systems in the formation of mineral deposits are representative of the 95 papers for the Forum.

I am extremely pleased with the success of the two previous Forums, and I look forward to a highly useful and productive 1987 meeting. All of us at the Geological Survey welcome this opportunity to discuss our research with our colleagues in industry, academia, and government and to hear about ways we can better serve the mineral-resource needs of the public.

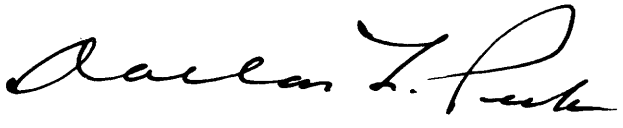

Dallas L. Peck
Director

PROGRAM CHAIRMEN

(Semicolon indicates change in chairmanship)

Technical Session 1

Gary R. Winkler, Charles H. Thorman; Thomas G. Hildenbrand, David A. Lindsey

Technical Session 2

Byron R. Berger, Edwin H. McKee; Donald J. Grybeck, Frederick S. Fisher

Technical Session 4

Bruce R. Lipin, Lawrence J. Drew

PROGRAM

Tuesday Afternoon, March 10, 1987

4:00 Registration (East Lobby)
5:00 Ice-breaker/Cash Bar Mixer (East Lobby)

Wednesday Morning, March 11, 1987—Technical Session 1

8:00 Welcome and opening remarks (Dallas L. Peck and Robert M. Hamilton)
8:10 Keynote Address: "International perspective on mineral resources" (Prof. Dr. Martin O. C. Kürsten, President, BGR, Hannover, Federal Republic of Germany)
8:50 Overview of USGS mineral-resource program and activities (Glenn H. Allcott)
9:00 Application of deposit models in U.S. Geological Survey programs (Dennis P. Cox and Donald A. Singer)
9:20 Tectonic setting of some Cretaceous and Cenozoic structural and magmatic systems of the Western United States (Warren B. Hamilton)
9:40 Post-Laramide magmatism in the U.S. Cordillera (Robert L. Christiansen)
10:00 Coffee break
10:20 The role of regional aeromagnetic and gravity data in mineral-resource investigations, southeastern Nevada (H. Richard Blank)
10:40 Central San Juan caldera cluster, Colorado—New stratigraphic and structural interpretations and implications for mineralization (Peter W. Lipman and Marvin A. Lanphere)
11:00 Quantitative analysis of fluid-inclusion gases—Applications to studies of ore deposits (Gary P. Landis, Albert H. Hofstra, David L. Leach, Jr., and Robert O. Rye)
11:20 Sulfide solubilities in buffered systems at elevated pressures and temperatures and their depositional implications (J. Julian Hemley, Gary L. Cygan, and William M. d'Angelo)
11:40 $^{40}Ar/^{39}Ar$ thermochronology of mineral deposits—Information on age, duration, number of episodes, and temperature of mineralization (Lawrence W. Snee)
12:00 McKelvey Forum Luncheon (Harry A. Tourtelot, presiding)
Welcome by Colorado State Geologist (John W. Rold)
Luncheon Address: "The appropriate role of government in mineral-resource research" (Sen. Harrison H. Schmitt, Consultant, Albuquerque, NM)

Wednesday Afternoon, March 11, 1987—Technical Session 2

2:00 New geochemical guides to Au-rich Co-Cu lodes in the Blackbird mining district, Lemhi County, Idaho (J. Thomas Nash and Gregory A. Hahn)
2:20 Some features of the composition and distribution of geochemical types of placer gold in the Koyukuk-Chandalar mining district, Alaska (Edwin L. Mosier, John B. Cathrall, John C. Antweiler, and Richard B. Tripp)
2:40 Epithermal gold mineralization in the Republic of Palau (James J. Rytuba, William R. Miller, and Edwin H. McKee)
3:00 "Mesothermal" gold—A metamorphic connection? (William J. Pickthorn, Richard J. Goldfarb, and David L. Leach, Jr.)
3:20 Coffee break
3:40 Ophiolites, metallogenic models, and terrane models—Interrelations observed in the Arabian Shield and potential for "cryptic" mineralization (John S. Pallister)
4:00 Geological setting of two sediment-hosted hydrothermal mineral localities in Escanaba Trough, Gorda Ridge (Janet L. Morton, William R. Normark, Mark L. Holmes, and Mitchell Lyle)
4:20 The Red Dog Pb-Zn-Ag deposit, Alaska—An example of nonexhalative processes in the formation of syngenetic massive sulfides (Jeanine M. Schmidt and Robert A. Zierenberg)
4:40 Comparative studies of modern and ancient sediment-hosted massive sulfides (Wayne C. Shanks III)

Wednesday Evening, March 11, 1987—Technical Session 3

7:30–10:30 Seventy-four poster papers and authors, with kegs on tap

Thursday Morning, March 12, 1987—Technical Session 4

8:00 Preliminary geophysical well-log analysis of the geothermal alteration of alluvial sediments in the Salton Sea basin, California (Frederick L. Paillet and Roger H. Morin)
8:20 Mapping contact-metamorphic aureoles in Extremadura, Spain, using Landsat Thematic Mapper images (Lawrence C. Rowan, Carmen Anton-Pacheco, David W. Brickey, Marguerite J. Kingston, Alba Payás, Norma Vergo, and James K. Crowley)
8:40 Neogene-Quaternary volcanism and mineralization in the Central Andes (George E. Ericksen, Robert L. Smith, and Robert P. Koeppen)
9:00 Geographic information system requirements in mineral-resource assessment—Lessons learned through cooperative research (John L. Dwyer, Stanton H. Moll, Charles M. Trautwein, James E. Elliott, Robert C. Pearson, Walden P. Pratt, and J. Thomas Nash)
9:20 Mineral-resource assessment process and results, Petersburg project area, southeastern Alaska (David A. Brew, Donald J. Grybeck, John B. Cathrall, Susan M. Karl, Richard D. Koch, David F. Barnes, Andrew Griscom, and Henry C. Berg)
9:40 Coffee break
10:00 Panel Discussion: "Future trends in mineral-resource research—Perspectives from government, industry, and academia" (Glenn H. Allcott, moderator; T S Ary, Robert C. Horton, Richard W. Hutchinson, William C. Kelly, Gregory E. McKelvey, and Larry D. Fellows, panelists)
11:30 Concluding Address (Dr. Samuel S. Adams, Head, Geology and Geological Engineering Department, Colorado School of Mines, Golden, CO)
12:00 Adjournment of Technical Sessions (Glenn H. Allcott)

Thursday Afternoon, March 12, 1987—Workshops and USGS Open-House

1:30 Departure from Sheraton Denver Tech Center
2:00 USGS Open House: Denver Federal Center, Lakewood
Denver West Office Park, Golden
Workshops: Microcomputer systems in geologic map compilation and drafting (Richard B. Taylor, Gary I. Selner, and Bruce R. Johnson)
Fractal geometry—Concepts and application to geologic structure and mineral-resource analysis (Christopher C. Barton)
4:00 Conclusion of Forum

Posters (Technical Session 3)

[Initial number is booth number]

I. Investigations of Mineralizing Processes and Mineralized Systems

A. Studies Focused on Geochemistry and Mineralogy

1. Sanford, R. F., Geochemistry of precious- and base-metal veins, Lake City area, Colorado
2. Wanty, R. P., Fitzpatrick, J. J., and Goldhaber, M. B., Geochemical and crystallographic constraints on the formation of the vanadium-uranium ores of the Colorado Plateau
3. Asher-Bolinder, Sigrid, and Whitney, Gene, Mechanism of lithium enrichment in the Popotosa Formation, Socorro County, New Mexico
4. Hearn, P. P., Jr., Sutter, J. F., and Belkin, H. E., Authigenic K-feldspar—An indicator of the geochronology and chemical evolution of mineralizing fluids in carbonate-hosted lead-zinc deposits
5. Church, S. E., Studies of lead isotopes in sulfide deposits from accreted terranes in the North American Cordillera
6. Spirakis, C. S., and Heyl, A. V., A link among ^{34}sulfur-rich pyrite in greenish-grey shales, ferric iron from smectite as it converts to illite, kinetics of sulfur redox reaction, and the genesis of Mississippi Valley-type deposits
7. Philpotts, J. A., Kane, J. S., Aruscavage, P. J., Kirschenbaum, H., Johnson, R. G., Dorrzapf, A. F., Jr., Brown, Z., and Mee, J. S., Geochemical aspects of ocean-floor hydrothermal-vent fluids and massive sulfide chimneys from the southern Juan de Fuca Ridge
8. Chaffee, M. A., Chemical zoning of mineral deposits as an exploration technique—The Red Mountain, Arizona, porphyry copper system
9. Gray, Floyd, Page, N. J, and Moring, B. C., Petrology and platinum-group element variation in zoned ultramafic complexes, Klamath Mountains, Oregon and northern California
10. Moring, B. C., Page, N. J, and Oscarson, R. L., Platinum-group element mineralogy of the Pole Corral podiform chromite deposit, Rattlesnake Creek terrane, northern California
11. Zientek, M. L., and Oscarson, R. L., Textural association of platinum-group minerals from the J-M Reef, Stillwater Complex, Montana

B. Studies Focused on Petrology and Field Relations

12. Duffield, W. A., Relations between cassiterite-bearing veins and rhyolite layers, Black Range area, southwestern New Mexico
13. Lange, I. M., Nokleberg, W. J., Aleinikoff, J. N., and Church, S. E., Genesis and tectonic setting of volcanogenic massive sulfide deposits, eastern Alaska Range, Alaska
14. Gamble, B. M., Gold veins of the Seward Peninsula, Alaska
15. Tosdal, R. M. and Smith, D. B., Some characteristics of gneiss-hosted gold deposits of southeastern California
16. Schmidt, R. G., Payás, Alba, Gumiel, Pablo, and D'Agostino, J. P., The Saxapahaw, North Carolina, gold occurrences—Search for a deposit model and new remote sensing techniques
17. Zierenberg, R. A., Koski, R. A., Shanks W. C., III, Seyfried, W. E., Jr., and Strickler M. D., Comparison of the Turner-Albright ophiolite-hosted massive sulfide, southwestern Oregon, to active hydrothermal deposits on the southern Juan de Fuca Ridge
18. Bove, D. J., Hon, Ken, and Rye, R. O., Evolution of the Red Mountain alunite deposit, Lake City caldera, Colorado
19. Clark, S. H. B., Potential for sedimentary exhalative base-metal deposits in Cambrian-Ordovician shelf carbonates of western Vermont and southern Quebec
20. Ayuso, R. A., and Ratte, C. A., Epigenetic uranium mineralization in the Precambrian Mount Holly complex, Vermont
21. Wenrich, K. J., Verbeek, E. R., Sutphin, H. B., Van Gosen, B. S., and Modreski, P. J., The Apex Mine, Utah—A Colorado Plateau-type solution-collapse breccia pipe
22. Himmelberg, G. R., Loney, R. A., and Nabelek, P. I., Petrogenesis of gabbronorite at Yakobi and northwest Chichagof Islands, Alaska
23. Bawiec, W. J., Zientek, M. L., and Attanasi, E. D., Three-dimensional geologic model of the Mouat nickel-copper prospect, Stillwater Complex, Montana, and its application to mineral-resource assessment
24. Larsen, C. E., and Force, E. R., A worldwide paleoclimatic model for Quaternary shoreline placer deposits of titanium minerals
25. Sidder, G. B., Alteration and mineralization in the Monterrosas copper-iron deposit, Peru
26. Breit, G. N., Meunier, J. D., Rowan, L. E., and Goldhaber, M. B., Alteration related to red bed copper mineralizing brines and other fault-controlled solutions in Lisbon Valley, Utah, and the Slick Rock district, Colorado
27. Stollenwerk, K. G., and Eychaner, J. H., Neutralization of acidic ground water near Globe, Arizona

C. Studies of Marine Systems

28. Escowitz, E. C., and Grosz, A. E., Heavy minerals of the mid-Atlantic inner Continental Shelf
29. Hein, J. R., Morgenson, L. A., Fleischman, Charlaine, Schwab, W. C., and Clague, D. A., Composition and distribution of cobalt-rich ferromanganese crusts from the Pacific
30. Holmes, M. L., and Morton, J. L., Regional structure and distribution of hydrothermal activity within Escanaba Trough, southern Gorda Ridge
31. Koski, R. A., Zierenberg, R. A., Kvenvolden, K. A., and Shanks, W. C., III, Mineralogy and chemistry of hydrothermal sulfide and petroleum deposits from Escanaba Trough, Gorda Ridge

D. Studies Involving Microorganisms

32. Lovley, D. R., Microbial transformations of iron minerals
33. Repetski, J. E., Briskey, J. A., Armstrong, A. K., Smith, Fred,

II. Mapping and Mineral-Resource Assessments

III. Geophysical Surveys and Other Geophysical Investigations

IV. Geochemical Investigations

V. Information Systems

Third Annual V. E. McKelvey Forum on Mineral and Energy Resources

USGS Research on Minerals Resources—1987
Programs and Abstracts

Edited by Janet Somerville Sachs

Applications of Digital Mapping and Geographic Information Systems to Earthquake Hazards Reduction, Wasatch Front, Utah

Robert Alexander and Thomas Dinardo

The U.S. Geological Survey is conducting experiments to determine the feasibility of applying digital map data bases and geographic information systems to earthquake hazards reduction in the Salt Lake City-Wasatch Front corridor, Utah. Preliminary work included input of geologic, hydrologic, and other map data relevant to the earthquake hazard within the Sugar House quadrangle, east-central Salt Lake County, UT.

This 7.5-min quadrangle was the source of the digital line graph and digital elevation model data products to which all other data types were registered. More than two dozen types of data were entered into the project data base, including the surface trace of the Wasatch fault, potential liquefaction zones, predicted land stability during an earthquake, surface hydrologic features, topography, slope, flood zones, landslide and mudflow zones, land use, lifelines, and critical or response facilities, such as schools and hospitals.

Preliminary analyses of the data bases include automated measuring and mapping of school locations and residential areas that coincide with high-potential earthquake hazard zones, lifelines crossing potential fault rupture zones, and undeveloped land that lies outside identified multihazard zones. Many other kinds of analyses can be performed on these and similar data sets, addressing scenarios that included preearthquake planning for response and recovery, loss estimation, and hazard mitigation through land use planning where the opportunity exists to guide new development away from the areas of greatest potential hazard.

Recommendations are drawn from the Sugar House quadrangle experiments on how to apply digital technology to the development of a cooperative information management system in the impacted region. Through planned sharing of data and the use of appropriate data standards, such a system will assist in efficient implementation of earthquake hazard reduction measures.

A New Tin-Bearing Base- and Precious-Metal Province in the U.S. Virgin Islands

H. V. Alminas, R. E. Tucker,[1] R. T. Hopkins, J. M. Nishi, and R. P. Christian

A regional geochemical study of the U.S. Virgin Islands (St. Thomas, St. John, and St. Croix) has delineated extensive areas with anomalous concentrations of Au, Ag, Te, Sb, Bi, As, Pb, Sn, Cu, Zn, and Ba. The anomalies appear to be structure related and transect all exposed rock types on the islands.

The U.S. Virgin Islands are part of the northeastern portion of the Greater Antilles island arc and are located to the east of Puerto Rico. In addition to the main islands, about 50 smaller islands, which are concentrated mainly near St. Thomas and St. John, are within the study area.

The most detailed geologic map of St. Thomas and St. John published to date is that produced by Donnelly (1966). As mapped by Donnelly, the two northern islands consist of island-arc-related Cretaceous and Tertiary volcanic, volcanoclastic, carbonate, and plutonic rocks.

St. Croix was mapped by Whetten (1966), who indicated that the island is underlain by strongly folded Upper Cretaceous sedimentary rocks, which have undergone low-grade metamorphism, and by gently folded unmetamorphosed Tertiary sedimentary rocks. Igneous intrusions of Late Cretaceous and early Tertiary age with contact metamorphic aureoles occur in the sedimentary rocks.

[1]Colorado School of Mines, Golden, CO.

Outcrops, B-horizon soils, and stream sediments were sampled during the course of the geochemical study. In addition, heavy-mineral concentrates and oxalic acid leachates were derived from the soil and stream-sediment samples. Only the two derivative sample types were found to be effective in delineating the base- and precious-metal mineralization. Outcrop samples were effective in detecting the precious-metal assemblage.

The most extensive anomalies are those of Pb, Sn, and Cu, which decrease in intensity and extent in the major islands in the order of St. Croix, St. John, and St. Thomas. Precious-metal anomalies on these islands show the reverse order.

Scanning electron microscope, electron microprobe, and X-ray diffraction investigations indicate that, in the weathering environment, most of the Sn occurs as poorly crystallized cassiterite incorporating blebs of native Sn, native Pb, and euhedral crystals of a Sn-Cu alloy. Vugs filled with Sn chloride commonly occur within the native Sn and Pb blebs. Much of the Pb occurs in native form associated with chloride, carbonate, oxide, and sulfide forms. The Cu is found in native, oxide, chloride, silicate, and alloy forms. Most of the Au is found in native form with some occurrences of a Au-Ag telluride. The Ag is found in native telluride, chloride, sulfide, widespread iodide, and Au-Ag telluride forms.

References Cited

Donnelly, J. W., 1966, Geology of St. Thomas and St. John, U.S. Virgin Islands: Geological Society of America Memoir 98, p. 85–176.

Whetten, J. D., 1966, Geology of St. Croix, U.S. Virgin Islands: Geological Society of America Memoir 98, p. 177–239.

U.S. Geological Survey's Federal Land Information System

Raymond E. Arndt, Thomas L. Johnson, and Donald O. Ohlen

The U.S. Geological Survey is implementing the Federal Land Information System (FLIS), formerly called the Federal Mineral Land Information System. FLIS is a data base networking system which uses geographic information system technology to allow Federal policymakers and resource managers to evaluate more efficiently surface- and mineral-resource development issues at the national, State, and regional levels.

FLIS program activities are directed to users' needs, in that a geographic index of FLIS data sources with query capabilities will be made available. System outputs are tailored to user requests and include spatial display products and statistical summaries. Data conversion and networking capabilities are being developed and demonstrated for Federal lands in Alaska and New Mexico. The FLIS program has ongoing cooperative activities with other Federal agencies, including the Bureau of Land Management and the Bureau of Mines offices in those two States.

The principal categories of data in use or being considered for use in FLIS statewide data bases are Federal ownership (surface and mineral reservations), restrictions to exploration and mining of federally owned minerals (legal and management withdrawals), mineral-resource potential and occurrence, surface-resource information (water, soils, land use and land cover, and terrain derivatives), and cartographic detail. At present, U.S. Geological Survey, Bureau of Land Management, and Bureau of Mines are the primary suppliers of data for these statewide data bases.

Mechanism of Lithium Enrichment in the Popotosa Formation, Socorro County, New Mexico

Sigrid Asher-Bolinder and Gene Whitney

Sedimentation, Li geochemistry, and clay mineralogy combined to provide a source, a concentrator, and a trap for Li in tuffs of the Popotosa Formation, central New Mexico. These Li-rich tuffs (80–3,850 ppm Li) occur in the closed-basin rocks of the Socorro paleobasin, a late Oligocene through Miocene precursor of the Rio Grande rift. The 7- to 18-m.y.-old airfall and waterlain tuffs were erupted from postcaldera-resurgence vents near the paleobasin margin. Tuffs deposited in playa sediments are thicker, more zeolitic, and more Li rich than are tuffs deposited on alluvial flats.

Li is leached preferentially from rhyolitic and dacitic volcanic glasses by fresh and alkaline ground waters. Li forms no salts in nature and has the lowest cation exchange capacity of the alkaline metals; however, it shows limited substitution for Mg in clay minerals. Airfall ashes have high porosity and permeability, which make them susceptible to leaching of Li and other cations by ground water flowing downbasin to the playa where evaporative concentration occurs.

The thicknesses of the airfall portions of the playa tuffs correlate with their whole-rock lithium contents ($r = 0.71$, $n = 13$ samples), suggesting that thicker, hence, volumetrically larger, ashes were leached of more Li by ground waters moving through the tuffs to the basin center than were thinner ones. Thus, the source of Li in Popotosa tuffs may be the tuffs themselves.

Li-rich playa tuffs consist of dioctahedral smectite, quartz, plagioclase, varying amounts of calcite and clinoptilolite, and traces of mordenite, gypsum, biotite, and dolomite. Li is contained in dioctahedral smectites, which have identical X-ray diffraction traces no matter what their Li content. When interlayer cations of high-Li smectites were exchanged for Sr, much of the Ca, Na, and K were replaced by Sr. However, the Mg and Li values remained constant because they are structural elements of the octahedral layer. Cation exchange coefficients of the clay fractions range from 0.90 to 1.75 meq/g and are proportional to a clay fraction's Li content. Li^{+1} occupies sites in the octahedral layer normally held by Al^{+3} or Mg^{+2}, leading to a net negative octahedral layer charge, balanced by the addition of Ca, Na, and K to the smectite interlayers.

Whole-rock chemistries of high-Li playa tuffs are similar to those of their cogenetic volcanic flows except for Li and Mg enrichment and K depletion. Li is elevated as much as 58 times, and Mg is 10 times higher in the tuffs than in the cogenetic flows. If Li in the tuffs was brought to the playa by ground-water dissolution and movement through the ashes, then why are calcium and sodium levels not elevated? and why do K values drop an order of magnitude in the playa facies, the center of evaporative concentration? Independent observation suggests that K in the flows was elevated by K metasomatism that did not affect the playa tuffs. However, the playa tuffs probably were enriched originally in Ca and Na by ground-water flow through the tuffs. Because those elements were not incorporated structurally into the dominant diagenetic phase smectite, their final concentrations were controlled by postdiagenetic events. Some Na

Mount Baldy, a 12,082-ft peak in the Tushar Mountains of west-central Utah. It is within the 19-Ma Mount Belknap caldera and is composed of alkali-rhyolite ash-flow tuffs and volcanic domes containing anomalous quantities of Mo, U, Be, and Li. Westward, beyond Mount Baldy, lie Beaver Valley and the Mineral Mountains along the eastern margin of the Basin and Range province.

and Ca and K presently are held as interlayer cations in the smectites; more of those cations may have been held as soluble salts in the tuffs, later removed by fresher waters introduced by intrabasin horsting, paleobasin breaching, and rainwater.

A delicate balance between ground-water inflow and tuff leaching and evaporative concentration and incorporation of Li into neoforming smectite was maintained to achieve high structural Li values in these dioctahedral smectites. Paleobasin breaching occurred 4–7 m.y. ago; Li still in solution or in exchangeable sites would have been removed or replaced by other cations in fresher open-basin system waters.

Epigenetic Uranium Mineralization in the Precambrian Mount Holly Complex

Robert A. Ayuso and Charles A. Ratte[1]

Epigenetic uranium-bearing veins and pegmatitic pods and lenses are disseminated widely in the Precambrian Mount Holly Complex in the Green Mountains in Vermont. These occurrences represent probably the largest bedrock uranium occurrences known in New England. Mineralized rocks at Okemo Mountain and Jamaica are on the eastern flank of the Green Mountains anticlinorium and may be related to the Taconic orogeny (about 440 m.y.) and to the Acadian orogeny (about 380 m.y.).

Disseminated uranium mineralization is found in a wide variety of rock types ranging from feldspathic gneisses and pegmatite-rich rocks at Jamaica to cataclastically deformed rusty quartzites, schists, and calcsilicates at Okemo Mountain. In both areas, but especially the latter, a significant association exists between highly mineralized areas and quartz-tourmaline rocks. The veins are mineralogically simple and vary in width from about 10 cm to a few meters. They contain uraninite, small amounts of brannerite, and uranophane as the important uranium-bearing minerals. At Okemo Mountain, uranium veins are hosted by epidote-chlorite-garnet-white mica-tourmaline-quartz rocks. Mineralized rocks are concentrated near shear zones in rusty quartzitic schists (epidote-tourmaline-magnetite-pyrite-hematite-chlorite-white mica-quartz) and granitic gneisses (epidote-tourmaline-microcline-perthite-quartz). In the Jamaica area, the host rocks range from quartzitic and schistose rocks (garnet-chlorite-biotite-white mica-quartz), which are generally similar to those in Okemo Mountain, to thinly banded feldspathic gneisses (epidote-allanite-microcline-perthite-quartz) and pegmatite-rich gneisses (allanite-epidote-white mica-perthite-quartz).

Bulk rock compositions of the mineralized units are highly variable. No strong correlations between uranium content and silica or between uranium and most other major elements are observed. High values for Fe_2O_3/FeO are found in many of the mineralized samples. Values for U_3O_8 range from 0.2 to 0.6 percent in the mineralized veins, and anomalous values as high as 22.0 percent have been recorded. Ratios of thorium to uranium vary from <0.01 to >10. Trace element variations are not related to the uranium content of the rocks. Total rare earth element (REE) content of the host rocks is widely variable and is relatively low (generally <300 ppm for total REE content, except in some samples where it is as high as 1,500 ppm). The most significant trace element covariation at Okemo Mountain is that for uranium and boron, which is in agreement with the observed association of mineralized veins and quartz-tourmaline rocks.

The low total content of REE in the mineralized zones and their uncorrelated nature with respect to uranium argue against an origin of the widely disseminated mineralization by direct derivation from anatectic melts. The mineralized areas are best characterized as products of pegmatitic rocks remobilized by oxidized and boron-rich fluids formed in response to the Taconian and (or) Acadian orogenies. Migration of these fluids probably was controlled by the regional development of fractures and shear zones.

Three-Dimensional Geologic Model of the Mouat Nickel-Copper Prospect, Stillwater Complex, Montana, and Its Application to Mineral-Resource Assessment

W. J. Bawiec, M. L. Zientek, and E. D. Attanasi

Deposits of magmatic Ni-Cu sulfides are concentrated near the base of the Stillwater Complex, an Archean mafic to ultramafic layered intrusion exposed on the northern edge of the Beartooth Mountains, MT. Extensive drilling and more limited underground development work, done largely by the Anaconda Minerals Company, has delineated the subsurface extent of one of these deposits in the Mountain View area, the Mouat Ni-Cu prospect.

[1]Vermont State Geologist, Waterbury, VT 05676.

The three-dimensional interpretation of the geology of this deposit is based on 1:1200-scale surface mapping, 1:120- and 1:240-scale core logging of approximately 90,000 ft of core from 110 drill holes, 1:240-scale adit mapping, and Ni-Cu concentration data from the drill holes. Computer-generated graphics are used to illustrate the geology of this deposit.

The three-dimensional structural interpretation of this area shows that the rocks of the Stillwater Complex are folded into a broad syncline cut by several generations of faults. The sulfides are concentrated at the lower contact of the Basal series with the underlying metasedimentary rocks and within very discontinuous, irregularly shaped Stillwater-associated sills and dikes that intrude the metasedimentary rocks. The base of the Stillwater Complex in this area shows considerable relief over short distances; as a result, the thickness of the Basal series ranges from 0 to over 450 ft. Metasedimentary rock xenoliths, the largest over 800 ft in length, occur within the Basal series and the Peridotite zone of the Ultramafic series. The oldest faults trend northeasterly and have near-vertical dips. These faults are cut by northwesterly trending, near-vertical faults showing left-lateral offset. The left-lateral northwesterly trending Verdigris fault, in turn, cuts all previous faults. Apparent offsets of these faults are less than 500 ft. Two high-angle reverse faults, the Lake and the Bluebird faults, show the greatest offset and truncate the Mouat deposit on the southwest and the northeast.

As part of this study, several attempts were made to estimate the tonnage and grade of the explored part of the deposit. Because of the inclined attitude of the stratigraphy and increasing depth, the sulfide deposits in the deepest parts of the syncline were not evaluated. The sulfide accumulations at the base of the Basal series showed the greatest continuity; therefore, the grade and tonnage computations concentrated on rock units near this contact. Data on Cu and Ni concentrations were analyzed and examined in 25-ft intervals above the base of the Basal series and below the Basal series in the metasedimentary rock by using 25- x 25-ft and 100- x 100-ft mining blocks. The intensity of faulting and the very irregular shape and distribution of mineralized footwall sills and dikes made it extremely difficult to use geostatistical methods. Therefore, conventional grade interpolation procedures were applied to Ni and Cu data. Only two fault-bounded blocks contained sufficient data (number of drill holes or surface exposure of the contact) to credibly estimate grade-tonnage relations. One fault-bounded block lying directly west of the Verdigris fault contains 17.1 million–22.3 million short tons of ore having an average grade of 0.5 percent combined Ni and Cu. In a smaller fault-bounded block farther to the west, 2.4 million–5.3 million short tons of ore having an average grade of 0.5 percent combined Ni and Cu are thought to be present.

Role of Regional Aeromagnetic and Gravity Data in Mineral-Resource Investigations, Southeastern Nevada

H. Richard Blank

Southeastern Nevada is a miogeosynclinal province that has undergone late Mesozoic compression followed by mid- to late-Cenozoic extension concommitant with calc-alkaline and bimodal magmatism. At least 50 percent of the bedrock is covered with surficial deposits. Because base- and precious-metal deposits here commonly are associated with plutons emplaced during tectonic modifications of the miogeosyncline, an important objective of mineral-resource evaluation is the delineation of concealed intrusive bodies and of regional structures that may impact the exploration rationale. For this task, use of recently compiled aeromagnetic and gravity maps can be of considerable benefit.

Sources of strong magnetic anomalies include Cenozoic volcanic and Precambrian crystalline basement rocks as well as target plutons. However, the Precambrian basement and magnetically transparent Paleozoic carbonates generally have positive density contrasts, whereas the Mesozoic-Cenozoic volcanic and sedimentary rocks have negative density contrasts, with respect to Mesozoic-Cenozoic plutons. Thus, gravity data used in conjunction with magnetic data serve as a powerful discriminator.

Long-wavelength aeromagnetic anomalies primarily reflect topographic relief of the magnetic basement (whether it consists of Precambrian or younger rocks). Long-wavelength gravity anomalies record basement relief and carbonate surface relief, the latter dominated by Basin-Range faulting. Major discordances between aeromagnetic and gravity trends probably indicate that the terrane has been extended highly and that the magnetics "see through" suprajacent rocks and record structures of an autochthonous basement. Examples of magnetic basement that seems to bear no relation to Basin-Range structure are the Grant Range–Railroad Valley basement, believed to be associated,

at least in part, with granitoid rocks of Mesozoic age, and the basement northeast of Las Vegas Valley, a possible decapitated core complex.

In some places, potential field data suggest that the locus of igneous activity was confined to sites of modern intermontane basins, and it can be inferred that magma invaded high-level structural discontinuities of extensional origin. Large volcanotectonic structures, such as those of the Indian Peak caldera complex and the Caliente cauldron and their associated hypabyssal intrusions, have strong aeromagnetic and gravity signatures; the Pioche Pb-Ag district apparently is truncated by Indian Peak ring faults and may extend to the east buried at considerable depth beneath alluvium and caldera infill volcanics. Elsewhere, it is possible to infer that mineralized plutons have shallow concealed extensions. Examples are granitic bodies in the Patterson Pass area of the Schell Creek Range, the pluton of the Freiburg district in the Worthington Mountains, and the Troy Canyon pluton of the Grant Range.

Mineral Deposit Density—A Useful Tool for Mineral-Resource Assessment

James D. Bliss, W. David Menzie, Greta J. Orris, and Norman J Page

Mineral deposit density (MDD) is the number of deposits per unit area. When calculated for a single deposit type, such densities are hypothesized to be similar for large regions of comparable geology and thus provide a basis for mineral-resource assessment. This tool is particularly useful in the methodology developed for the Alaska Mineral Resource Assessment Program, which seeks to provide a quantitative, probabilistic estimate of the mineral endowment. Estimation of the mineral endowment includes (1) delineation of tracts permissive for the presence of deposit types that are known or suspected to occur within the map area, (2) use of descriptive and grade and tonnage models of these deposit types, and (3) estimation of the number of undiscovered deposits within identified tracts. Two basic approaches, standard statistical methods and expert judgment, have been used to estimate numbers of undiscovered deposits in tracts. MDD are basic data that can be used by either approach.

Based on well-explored regions (that is, ones in which essentially all deposits of the type of interest have been found), the MDD for that specific deposit type can be derived. The development of MDD depends on (1) insuring that deposits in the MDD are compatible with those in the grade and tonnage models and (2) establishing boundaries that contain all deposits in control regions by using concise operational rules based on geological, geochemical, and geophysical criteria that can be applied generally. MDD is computed for the control region by dividing the number of deposits by the size of the region. An initial estimate of the number of deposits that occur in a tract of land may be obtained by multiplying the MDD by the area of the tract. The estimate may then be adjusted to more precisely reflect specific geologic conditions in, and exploration history of, the tract by using either statistical models or expert opinion.

MDD for low-sulfide Au-quartz vein deposits in four large regions generally has similar values. This deposit type typically forms at moderate depth and temperatures in metasedimentary and metavolcanic rocks of predominantly greenschist facies on the flanks of batholithic complexes. Preliminary MDD's (deposit per square kilometer) for areas with low-sulfide Au-veins are

1. Sierra Nevada Foothills, CA—4.6 $x10^{-3}$,
2. Klamath Mountains, CA-OR—4.3 $x10^{-3}$,
3. Meguma Group of Nova Scotia, Canada—5.4 $x10^{-3}$, and
4. Victoria, Australia (for example, Bendigo, Ballarat)—5.0 $x10^{-3}$.

Preliminary MDD's also have been developed for podiform chromite, silica-carbonate mercury, and bedded barite. MDD's for bedded barite deposits and low-sulfide Au veins are being used in the the mineral-resource assessments of the Tonopah 1° x 2° quadrangle, Nevada, and the Wiseman 1° x 3° quadrangle, Brooks Range, AK, respectively.

Evolution of the Red Mountain Alunite Deposit, Lake City Caldera, Colorado

Dana J. Bove, Ken Hon, and R. O. Rye

The Red Mountain alunite deposit, one of the largest in the U.S. with 70 million metric tons of alunite, formed on the eastern margin of the 23.1-Ma Lake City caldera. Several texturally and temporally distinct high-K dacite intrusions (63–65 percent SiO_2) cut earlier postcaldera collapse high-K dacite lavas (63–66 percent SiO_2) on Red Mountain. Almost all the rocks were alunitized late in the caldera cycle, and over one-half of the surface exposures display evidence of hydrothermal brecciation.

Alunitization occurred in two large, roughly conical centers with roots extending more than 250 m

beneath the surface. Alunitized rocks change outward into argillized and propylitized postcollapse lavas and downward through argillic and potassic zones that are dominantly within dacite intrusions. Four 260- to 1,000-m drill holes intersect the area, but drill hole coverage does not permit direct observation of the transition between the alunite and argillized zones. Multiple stages of alunite are present and include (1) early fine to slightly coarser grained alunite replacing feldspar phenocrysts with quartz-pyrite alteration of the groundmass, (2) irregular flooding of alunite in groundmass and previously altered phenocrysts, and (3) late, fracture-controlled alunite veinlets. In argillically altered rocks, kaolinite overprints earlier sericite ± pyrite. The potassic zone is defined by secondary K-feldspar ± biotite ± pyrite, which is overprinted by sericitic and kaolinitic alteration near the top of the zone. Weak "porphyry-type" mineralization with anomalous amounts of molybdenum (and minor molybdenite) occurs throughout a 1,000-m drill hole, with highest molybdenum values (100-300 ppm) in the zone of potassic alteration. Elevated concentrations of Cu, Pb, and Zn also were detected, but only rare, finely disseminated sphalerite and chalchopyrite could be identified.

Mass balance calculations show large additions of sulfur from the hydrothermal system. This sulfur is present primarily as SO_3 within alunitized rocks and as FeS_2 within the potassic and argillic zones. Al_2O_3 and K_2O were removed during alunitization, and Sr was enriched due to the stabilization of a strontium-phosphate phase. Water was added to all the alteration zones as secondary hydrous alteration minerals. Potassium and rubidium were added to the potassic zone, and a slight gain in Al_2O_3 was observed in kaolinite-altered rocks. Only Zr and TiO_2 remained relatively immobile in the system.

Hydrogen, oxygen, and sulfur stable isotope data constrain the origin of alunite and the source of fluids and sulfur. Each stage of alunite has distinctly different isotopic compositions as do different generations of pyrite. Stage 1 $\delta^{34}S$ SO_4 and $\delta^{18}O$ SO_4 values range from 6.9 to 10.7 per mil and 6.0 to 9.7 per mil, respectively; Stage 2 values range from 19.7 to 27.2 per mil and 10.3 to 13.9 per mil, respectively; Stage 3 δ^3SO_4 values range from −3.3 to −3.9 per mil. Pyrite, which is cogenetic with Stage 1 alunite, has $\delta^{34}S$ values ranging from −5.8 to −8.7 per mil, while pyrite in the argillic assemblage has values of −1.0 to 2.1 per mil. Although interpretation is hampered by lack of experimental isotopic fractionation factors for alunite in hydrothermal systems, the data suggest that Stage 1 alunite formed from sulfate derived from a magmatic sulfur source at temperatures above 350°C, and Stage 2 alunite formed from the same sulfur source at lower temperatures. In contrast, late Stage 3 alunite is probably of supergene origin or was derived from the surficial oxidation of H_2S.

We propose an origin for the Red Mountain alunite deposit where a large lateral influx of meteoric water from the adjacent resurgent dome of the Lake City caldera enters a zone of hot, dry rock above a dacite magma emanating large volumes of SO_2 and H_2S gases. Fluid mixing occurred, creating an initially superheated acidic solution that permeated the overlying dome complex, and caused the formation of most of the alunite, periodicaly producing hydrothermal brecciation.

Alteration Related to Red Bed Copper Mineralizing Brines and Other Fault-Controlled Solutions in Lisbon Valley, Utah, and the Slick Rock District, Colorado

G. N. Breit, J. D. Meunier,[1] E. L. Rowan, and M. B. Goldhaber

Zones of red bed-type Cu enrichment along faults in Lisbon Valley, southeastern Utah, and the Slick Rock district, southwestern Colorado, were examined to evaluate the solutions responsible for the Cu mineralization. These fault-controlled fluids formed economic Cu deposits in the Cretaceous Dakota Sandstone along the Lisbon Valley fault and a zone of Cu enrichment in the Jurassic Morrison Formation along the structurally contiguous Dolores zone of faults. Fluid-inclusion studies of calcite in the fractures and isotopic and chemical studies of authigenic minerals in sandstones surrounding the faults indicate that three distinct solutions moved sequentially along the faults. These fluids not only formed the Cu deposits, but also precipitated calcite, barite, and dolomite and dissolved Fe oxides in zones up to 5 km from the faults.

Calcite, barite, and Cu minerals precipitated from the earliest of the solutions. This water had a $\delta^{18}O$ of about 0 per mil [Standard Mean Ocean Water (SMOW)], an average temperature of 95°C, and a dissolved solid content greater than 8 weight

[1]CREGU, Nancy, France.

percent NaCl equivalent. Fluid inclusions with different salinities indicate that this brine mixed with a dilute ground water during growth of the calcite. Collectively, the data suggest that the saline water was a connate water from the underlying Pennsylvanian Hermosa Formation. The Hermosa within the study area includes about 1,000 m of bedded evaporites. This saline water extracted copper from the Hermosa or from the red beds that occur between the evaporites and the Dakota and Morrison Formations. Interaction of the brines with the intervening clastic rocks is indicated by the Sr isotope composition of barite within the fault zones ($^{87}Sr/^{86}Sr$ of 0.7103). The Rb/Sr values of brines in the Hermosa are too low to account for the $^{87}Sr/^{86}Sr$ value of 0.7103. A likely source of Sr, in addition to the evaporites, are feldspars and clays in the clastic sediments. The extent of alteration by the brines is reflected by the decrease of $^{87}Sr/^{86}Sr$ in authigenic barite with increasing distance from the faults. The decrease in $^{87}Sr/^{86}Sr$ suggests mixing between Sr contained in the brines (0.7103) with Sr in the host sandstones (0.7080).

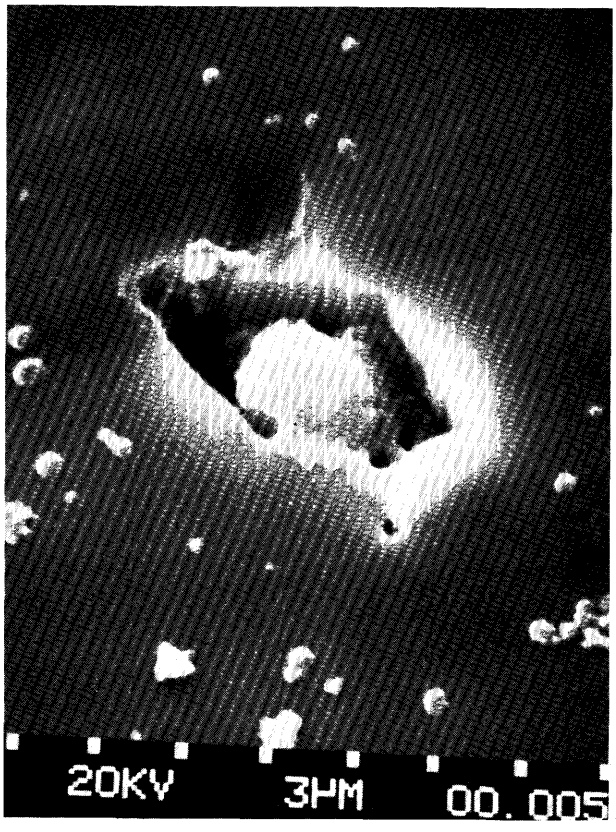

The scanning electron microscope photograph of a 12-μm-long fluid inclusion in quartz from the Santa Rita porphyry copper deposit, New Mexico. The inclusion contains a NaCl daughter mineral (cubic form). Various salts from the evaporated brine solution drape the NaCl crystal and form blebs around the opened inclusion.

Simultaneous with or shortly after the first brine, a second solution moved through the Dolores zone of faults. This water had an estimated $\delta^{18}O$ of –8 per mil (SMOW), which suggests that a component of the solution was meteoric water. As it moved through the sandstones, this solution precipitated dolomite. The solution also contained dissolved organic acids (probably derived from petroleum) that bleached red sandstones through which the solution passed. Flow of this solution was restricted to sandstones south of the Dolores zone of faults due to changes in permeability possibly related to the precipitation of calcite by the earlier brine. The $^{87}Sr/^{86}Sr$ of the dolomite is similar to the ratio in fracture-filling barite. The similar Sr isotope ratios and the O isotope compositions of the carbonate minerals indicate that this solution may have been a product of mixing between the earlier brine and the meteoric water described below.

The final solution to move through the fractures was a very dilute ground water that precipitated calcite within the Dolores zone of faults. This solution had a temperature of 50°C and a $\delta^{18}O$ near – 16 per mil (SMOW).

These solutions were forced upward by Laramide tectonism when uplift of anticlines cored by the Hermosa evaporites expelled fluids along fractures. Waters with isotopic and chemical compositions similar to these solutions currently exist within the Hermosa and overlying units.

Mineral-Resource Assessment Process and Results, Petersburg Project Area, Southeastern Alaska

David A. Brew, Donald J. Grybeck, John B. Cathrall, Susan M. Karl, Richard D. Koch, David F. Barnes, A. Griscom, and Henry C. Berg[1]

The Petersburg project region encompasses 16,300 km^2 and includes all the Petersburg, about one-third of the Port Alexander, and about one-tenth of the Sumdum 1:250,000-scale map areas, southeastern Alaska. Although the region contains only three mines that produced any commodities (barite, garnet, and gold), it contains a wide variety of metallic mineral occurrences and has long attracted the attention of prospectors and mineral exploration companies.

The mineral-resource assessment (MRA) was done by an expert panel of regional geologists, economic

[1]USGS retired.

geologists, geochemists, and a geophysicist, who had participated collectively in 44 person-months of fieldwork between 1978 and 1982. In the course of the MRA process, 17 types of deposits were identified as being present and (or) geologically permissible, and, by using the procedures described below, 28 areas of interest were identified.

The identification of the 28 areas was based on sequential data collection, data analysis, compilation, preliminary interpretation, and, finally, on the judgment of the expert panel. The information used came from the following sources: regional geology, economic geology, bedrock geochemistry, stream sediment geochemistry, panned concentrate geochemistry, geophysics:aeromagnetic, geophysics: gravity, geophysics:high-altitude aeroradiometric, geophysics:low-altitude aeroradiometric, and telegeology:Landsat and other high-altitude images. The basic data from all but one of these sources and a few preliminary interpretative maps were released. The most useful of the unreleased maps were (1) the interpretation of the geologic map showing the rock units and structural situations permissive for the 17 different types of deposits, (2) various stream sediment, panned concentrate, and bedrock geochemical maps depicting combinations of elements in various innovative ways, and (3) the preliminary aeromagnetic interpretation.

The 28 areas of mineral resource interest were classified in four main categories, which have as a common factor permissive geology for a specific mineral-deposit type. The criteria for each category are

1. A mine (with or without production); significant stream sediment, panned concentrate, and (or) bedrock geochemical anomalies; and both with and without significant geophysical anomalies;
2. One or more prospects or metallic mineral occurrences; significant stream sediment, panned concentrate, and (or) bedrock geochemical anomalies; and both with and without significant geophysical anomalies;
3. Significant stream sediment, panned concentrate, and (or) bedrock geochemical anomalies; and both with and without significant geophysical anomalies; and
4. Significant geophysical anomalies.

Only one of the three areas in Category 1 contains identified (inferred, paramarginal) resources. Undiscovered (hypothetical, submarginal) resources are contained in the other two areas in Category 1 and in several of the areas in Category 2. The remaining areas have undiscovered (speculative) resources. The information available in the MRA process did not justify applying statistical methods of estimating the number, size, and grade of the deposits that may be present in the region.

Geoelectric, Gravity, and Aeromagnetic Studies in the Delta, Utah, Quadrangle

David L. Campbell, Victor F. Labson, and Robert J. Bisdorf

The Conterminous United States Mineral Assessment Program (CUSMAP) does integrated geologic, geophysical, and geochemical studies at 1:250,000 scale to make mineral-resource assessments of selected 1° x 2° quadrangles. Work on the Delta, UT, quadrangle began in March 1986 and is scheduled to continue for 4 yr. Here, we report results to date from the geophysical part of the effort.

Gravity and aeromagnetic data were compiled and used together with a preliminary geologic map to guide geoelectric work in the first field season. This geoelectric work consisted of 23 magnetotelluric (MT) soundings and 50 audiofrequency magnetotelluric (AMT) soundings. In addition, 139 direct-current vertical electric soundings (VES) were used that had been made in the quadrangle earlier. All three methods show electrical resistivity versus depth under each site. MT soundings see deepest (often to more than 10 km depth) but take more time to make than the shallower AMT and VES soundings (1–2 MT soundings per day versus 3–6 AMT or VES soundings per day). MT and AMT soundings were made in conjunction with each other near Desert Mountain to investigate the depth and lateral extent of an inferred caldera and to the south of Whirlwind Valley to investigate a buried wishbone-shaped structure seen on the gravity map. VES were used to map thicknesses of sediments in the Tule Valley and northern Fish Springs Flat. Minor slingram and very low frequency geoelectric work also was begun in the historical Tintic mining district.

Profiles made by contouring resistivities from sounding to sounding show that the Desert Mountain caldera contains up to 2 km of electrically conducting (<100-ohm-m) surficial material, probably water-saturated sedimentary and volcanic rocks. Many of the soundings show 10–30 m of very conductive (<20-ohm-m) surficial material, probably representing sediments shed from the Sheeprock and Simpson Ranges to the north and deposited in glacial Lake Bonneville. The profiles also show zones of 50- to 500-ohm-m material embedded in

the caldera fill that may represent blocks of Paleozoic country rock that were brecciated and engulfed during Tertiary volcanic episodes. Such megabreccia zones appear from preliminary geologic mapping to characterize much of the Tintic-Deep Creek volcanic belt. The outcropping central core of the Desert Mountain caldera consists largely of electrically resistive (>1,000 ohm-m) intrusive rocks; the sides of this core are steep and possibly fault bounded.

Geoelectrical soundings can be used to further constrain gravity and magnetic models along selected profiles. Such a procedure was used to model a major fault of presumed Basin-Range age that the gravity map shows to be buried under Snake Valley midway between the Deep Creek and Fish Springs Ranges.

Geophysical work in the first year of this study has added information on structural and lithologic settings in the Delta quadrangle but has not given any direct evidences of mineralization. The role of geophysics in the Delta CUSMAP study, for the most part, will be to define and investigate bedrock structures in the more than 50 percent of the quadrangle that is covered by lacustrine and alluvial sediments.

Chemical Zoning of Mineral Deposits as an Exploration Technique—The Red Mountain, Arizona, Porphyry Copper System

Maurice A. Chaffee

The physical and chemical processes that produce a large hydrothermal mineral deposit (an economic or subeconomic enrichment of one or more minerals) or system (the deposit plus the surrounding rocks affected during the formation of the deposit) create chemical and mineralogical zones—areas that are enriched or depleted in various constituents—in these systems. This paper describes a chemical zoning study conducted at Red Mountain, about 80 km south of Tucson, AZ, where drilling to depths of more than 1,700 m has identified a remarkably complete porphyry Cu system. This system occurs within a gently dipping stack of predominantly felsic to intermediate volcanic rocks of Late Cretaceous to early Tertiary age that have been intruded by irregular bodies of porphyritic rocks.

For this study, samples of drill core were collected at about 15-m intervals from seven drill holes that comprise an east-west fence across the entire system. The samples were analyzed for 41 different elements. Evaluation of the spatial distributions of these elements indicates that chemical zoning is clearly present. This zoning of elements (for example, Mg and Li) can be used to help identify and correlate lithologic units. The zoning of elements or of ratios of elements also can be used to identify mineralogical and alteration zones; for example, Ba for barite, Co:Ni for pyrite, and Rb:Sr for advanced argillic alteration. Other elements (for example, Co, Mn, Ni, and Zn) can be used to identify the extent of chemical weathering.

Three general areas of mineralization are recognized within the Red Mountain system. The deepest of the three consists of a chalcopyrite-pyrite deposit similar in configuration to the San Manuel-Kalamazoo, AZ, deposit. The limbs of this deposit converge to an apex about 800 m below the present surface. A deposit containing sparse hypogene enargite and extensive supergene chalcocite is present near the surface. Between these two deposits are roughly concentric zones for such elements as Ag, As, Cu, K, Mn, Sb, and Zn. Minerals typical of potassic and phyllic alteration zones in porphyry Cu systems are also present at Red Mountain.

The distributions of the elements suggest that the Red Mountain system was formed in the following stages: (1) after deposition of the volcanic sequence, the top of the area was subjected to solutions that leached Ca and Na, (2) Fe was remobilized as part of an early "barren" pyrite event, (3) solutions enriched in Ag, As, Au, B, Ba, Bi, Cd, Co, Cs, Cu, Hg, Li, K, Mo, Pb, Rb, S, Sb, Sn, Sr, Te, Tl, U, W, Zn, and possibly Mn moved upward and formed the deep chalcopyrite deposit, the upper enargite deposit, and the intermediate zones, (4) the enargite deposit, which was associated with advanced argillic alteration, was converted to a chalcocite blanket as a result of supergene enrichment, and (5) the area of the system was uplifted, eroded, and weathered.

Anomalies of Ag, As, B, Ba, Bi, Hg, Mo, Pb, Sb, Sn, Te, and Tl are found in the outer fringes of this large system and are not strongly remobilized. As a result, any or all of the elements in this suite should be particularly useful in the search for deep-seated porphyry Cu deposits such as that at Red Mountain.

The recognition and understanding of chemical zoning can be a valuable technique in the search for new deposits, particularly deposits not exposed at the surface. Although this discussion emphasizes a zoned Cu system, the basic multielement chemical

zoning concept developed here should be applicable to exploration for many other types of mineral deposits.

Digital Mosaicking and Merging of Dissimilar Data Sets—GLORIA, Magnetic, and Bathymetric

Pat S. Chavez, Jr., James W. Schoonmaker, Jr., and Jeffery A. Anderson

Data from the GLORIA (Geological Long-Range Inclined Asdic) digital imaging system have become an important component within the U.S. Geological Survey for offshore mapping. Digital processing techniques to correct the geometric and radiometric distortions inherent in the original data have been developed and are operational. Until recently, the processed results have been in long strips on track-line format that were film mosaicked into 2° quadrangle areas for visual analysis. One disadvantage of film mosaics is that a new film mosaic must be made if a different type of enhancement or processed result is generated. Also, it is extremely difficult to digitally merge the sonar image data in track-line format with other types of data. To overcome these problems, procedures were developed to correct geometrically the individual long track-line strips of sonar image data to make digital mosaics of 2° quadrangles.

One of the major advantages of digital mosaicking over film mosaicking is that it allows the data, in quadrangle format, to be merged and combined with other image and nonimage data sets for digital analysis. In this project, we have merged the magnetic and bathymetric data, which were collected every 2 min at nadir locations during the GLORIA cruise, with the sonar image data. The magnetic and bathymetric data were converted first from vector to raster format with the same pixel size and geometric projection (Universal Transverse Mercator) as the sonar image data. A spatial filtering technique then was used to interpolate a surface through these data points. Special attention had to be given to the density and distribution of the data points (high density in the along-track direction and low density in the across-track direction). The resultant "image" products then were used individually and with the sonar image data for digital and visual analysis. The procedure for mosiacking the GLORIA sonar image data is more difficult than those required for other types of remotely sensed data, such as satellite images, because geometric control is available only at nadir locations. Currently, no information exists about the pointing characteristics of the imaging system; that is, pitch, roll, yaw. As with other data sets, the geometric corrections for digital mosaicking involve the identification of control points and the generation of the transformation file using these control points and the actual resampling of the image file using the transformation. Because control points are available *only* at nadir locations, the first step becomes much more involved. The second step is straightforward and very similar, or identical, to those used on other remotely sensed data. Also, because of the radiometric quality of the sonar image data, especially at far-range locations, additional work is required to get an acceptable tone match between the various track lines. An interactive digital stenciling or feathering capability was developed to optimize this stage of the process, which is similar to the feathering technique used on film mosaics.

Post-Laramide Magmatism in the U.S. Cordillera

Robert L. Christiansen

Three post-Laramide continental tectonomagmatic associations can be defined by the compositions, distributions, and tectonic settings of igneous rock suites. One is a classic arc, which produces predominantly basaltic to andesitic and subordinately dacitic to rhyolitic magmas in continental margin belts near active subduction zones. Another, generally more silicic, has few or no basalts but produces abundant andesites to rhyolites; compositions—broadly calc-alkalic but more potassic than the arc suites—typically evolve from andesites to voluminous rhyolites, either in belts across interior regions of tectonic extension or near the coast in association with the migrating ends of a transform system. A third embraces basaltic, alkalic, and bimodal rhyolite-basalt suites, which occur in regions of tectonic rifting or in cratonic foreland zones adjacent to the andesite-rhyolite belts. Each association is characterized by different types of mineral deposits.

Major contractional deformation ended in most of the U.S. Cordillera by 55–50 Ma. From 55 to 43 Ma, arc magmatism spanned from coastal Canada to central Oregon. Coeval basalts in coastal Washington and Oregon are oceanic in origin and were accreted to the continent later. The continental interior Challis andesite-rhyolite belt accompanied extension between the northern Cascades and the Rocky Mountain front in Montana and northwestern Wyoming,

with voluminous ash-flow calderas in the central part. Contemporaneous alkalic centers evolved on the Great Plains of Montana, northern Wyoming, and northwestern South Dakota. In the southern Cordillera, arc magmatism was active in western Mexico; continental interior magmatism spanned northward into western Texas and southern New Mexico.

From 43 to 37 Ma, arc magmatism persisted northward from central-western Oregon. Northern Cordilleran extension and magmatism stepped southward to the Tuscarora belt, reaching from central Oregon into northern Nevada and northwestern Utah; only minor activity continued in the Challis belt. In the southern Cordillera, continental interior andesites extended northward to central Colorado and westward to southeastern Arizona, with some voluminous rhyolites in southern New Mexico.

From 37 to 21 Ma, the Cascade arc spanned from coastal Canada to northwestern Nevada. To the east, from central Oregon to northern Nevada, southern Idaho, and southwestern Montana, is the John Day-Lewis & Clark belt of relatively small bimodal trachyandesites and rhyolites. Voluminous andesite-rhyolite magmatism jumped southward to a belt crossing central Nevada and splitting into two branches in western Utah; it produced voluminous ash-flow calderas, mainly after 34 Ma. Beginning about 28 Ma, major caldera activity moved to another belt overlapping this one on the south; activity continued until about 21 Ma. To the southeast, caldera-related eruptions occurred in Colorado and southwestern New Mexico between 34 and 27 Ma; less voluminous andesite-rhyolite volcanism reached southeastern California by 35–32 Ma. By 26–21 Ma, andesites to rhyolites erupted from Sonora to the southern Coast Ranges (now offset by the San Andreas fault), voluminous rhyolites erupted in southeastern Arizona, and mafic andesites and basalts became common in New Mexico and Colorado. Alkalic centers developed on the adjacent Cordilleran foreland and Colorado Plateau.

Between 21 and 17 Ma, the continental margin arc became continuous except for a gap of 400 km in southeastern California, where subduction had ceased; part of this arc has been disrupted by later translation and rotation in southern California. Since 17 Ma, the arc has retreated northward with lengthening of the Pacific-North American transform system; andesites and rhyolites have erupted near the migrating Mendocino triple junction. Distributed extension to the east has been accompanied by basaltic and bimodal magmatism. Between 17 and 14 Ma, a linear rift from central Nevada to western Idaho and eastern Washington erupted progressively more voluminous basalts northward. A 21- to 6-Ma belt of rhyolitic ash-flow calderas extended east-west across southern Nevada. During Basin and Range faulting since 14–10 Ma, magmatism has concentrated toward the margins of extending regions.

Studies of Lead Isotopes in Sulfide Deposits From Accreted Terranes in the North American Cordillera

S. E. Church

Recent studies of the composition of Pb in sulfide minerals from stratiform or sediment-hosted (SH) and from volcanogenic massive sulfide (VMS) bodies in accreted terranes in the North American Cordillera have shown that the primary source of Pb in these deposits is the crust. Specifically, the Pb isotope data indicate that the Pb in these sulfide systems reflects the interaction of the hydrothermal fluids with crustal sediments. In the case of SH deposits, Pb in the sulfide minerals reflects hydrothermal convection and deposition within the unconsolidated sediment pile. Pb from sulfide minerals in Cyprus-type VMS deposits represents hydrothermal convection within the oceanic crust and may reflect either a mantle-Pb composition or a mixture between mantle and sediment Pb. In contrast, the Pb isotope signature from Besshi- and Kuroko-type VMS deposits represents predominantly a crustal sediment Pb. Comparison of the average Pb isotope compositions found within the Devonian SH and VMS deposits in the Brooks Range differ significantly from that found in Devonian VMS deposits in the Alaska Range. Similarly, the isotopic composition of Pb in Triassic-Jurassic VMS deposits of the Klamath Mountains differs from VMS deposits of the same age found in southeastern Alaska.

Variations in the average composition of Pb from calc-alkaline volcanic rocks (CAVR) from the active continental margin of the Pacific Basin also vary significantly. The studies of Pb isotopes in CAVR rocks has resulted in a general model that invokes admixing sediment Pb with melts derived from the subducted oceanic crust to form mixing arrays between the mantle and sediment-Pb compositions. Because the Pb isotope composition of the mantle and the crust are variable on a regional scale, valid interpretations of the Pb isotope data seem plausible only when comparisons are based on a regional geological model. Regional variations of the isotopic

composition of Pb in modern oceanic sediments are reflected in CAVR from active volcanic arcs; for example, large variations have been found in the composition of Pb in CAVR's from the Cascade Range, the Lesser Antilles, and Japan and reflect the average composition of sediment Pb derived from the Western United States, the Brazilian craton, and the Asian craton, respectively, during Quaternary time. Thus, these rocks reflect the average composition of Pb in sediments derived from the present crustal geometry; sediment Pb, therefore, can be used to constrain models for accreted terranes because they accurately reflect the geometry of the rocks in the source.

Studies of the isotopic composition of Pb from SH and VMS sulfide systems from the Western United States and Alaska indicate that Pb isotopes from deposits of the same age within a district are generally uniform and that the average composition of Pb from ores within the district can be used as a Pb isotope signature, or "fingerprint." Similar work by Godwin and others (1982) also has shown regional variations of Pb isotopes from VMS deposits in the Canadian Cordillera. Regional variation between deposits of the same type and age within the North American Cordillera presumably reflects the average composition of Pb in sediments deposited in the sedimentary basin. Pb isotope data may be used to place limits on the extent of movement of accreted terranes in western North America.

Reference Cited

Godwin, C. I., Sinclair, A. J., and Ryan, B. D., 1982, Lead isotope models for the genesis of carbonate-hosted Zn-Pb, shale-hosted Ba-Zn-Pb, and silver-rich deposits in the northern Canadian Cordillera: Economic Geology, v. 77, p. 82–94.

Potential for Sedimentary Exhalative Base-Metal Deposits in Cambrian-Ordovician Shelf Carbonates of Western Vermont and Southern Quebec

Sandra H. B. Clark

Occurrences of sulfide minerals in the Cambrian-Ordovician carbonate-siliciclastic shelf terrane east of the Proterozoic basement of the Adirondack Mountains have been known at least since the 1870's. The occurrences are near the line between the shelf sequence and the deeper water basinal deposits to the east. Study of one of these occurrences at Lion Hill, which is about 3 mi north of Brandon, VT, resulted in a new interpretation of the genesis as sedimentary exhalative, analogous to the Irish carbonate-hosted zinc-lead deposits and indicated potential for additional deposits in the shelf sequence. Zinc-lead-copper mineralization at Lion Hill is primarily in the Lower Cambrian Monkton Quartzite, a mixed carbonate-siliciclastic tidal-flat sequence. Trace amounts of sulfide minerals also occur in the stratigraphically overlying Winooski Dolomite and underlying Dunham Dolomite. The Lion Hill deposit is on the overturned east limb of the Middlebury synclinorium, and host rocks are strongly deformed and metamorphosed to greenschist facies assemblages. The predominant ore mineral is sphalerite with smaller amounts of galena and chalcopyrite. Two mineralized zones that have been identified in drill core are along bedding-schistosity planes and are elongate at about N. 70° W., which is approximately perpendicular to the fold axes. The two zones contain about 500,000 tons of mineralized rock. The ore minerals occur predominantly as metamorphic segregations within schistosity surfaces, indicating pretectonic or, at the latest, syntectonic mineralization. Evidence for possible timing of mineralization relative to the deposition of host rocks comes from several sources. The association of layered magnetite iron formation with the lead-zinc mineralization suggests syngenetic deposition. Rarely preserved pretectonic textures indicative of mineralization during diagenesis include intergranular disseminated sulfides and dilatant fracture fillings by material, including sphalerite, that flowed in a plastic state. Discordant masses and veinlets indicate that some of the mineralization was epigenetic. The Lion Hill deposit differs from Mississippi Valley-type (MVT) deposits in scarcity of gangue minerals and lack of abundant open-space filling or evidence of paleokarst. Lead-isotope and fluid-inclusion studies (Nora K. Foley, U.S. Geological Survey, written commun., 1986) also suggest that the Lion Hill deposits are more like the sedimentary exhalative zinc-lead deposits of Ireland, which are stratabound and stratiform, than MVT deposits. Overthickening of the Monkton Quartzite at Lion Hill and abrupt lithologic changes indicate possible crustal instability during sedimentation and synsedimentary faulting. Mineralizing fluids may have ascended along growth faults and deposited sulfides in unconsolidated sediments of a shallow-water marine environment. The escape of some metal-bearing fluids onto the seafloor could account

for the associated iron formation. Forceful injection of fluids produced mineralized fractures and other locally discordant features.

Applications of Deposit Models in U.S. Geological Survey Programs

Dennis P. Cox and Donald A. Singer

In 1986, the U.S. Geological Survey published Bulletin 1693, which contains 87 deposit model descriptions by 38 authors (Cox and Singer, 1986). These are derived from data on 3,900 individual deposits distributed in 111 countries. Tonnage and grade models for 60 of these types also are presented. Many of these models have been applied in domestic programs beginning with Alaska Mineral Resource Assessment in 1975 and internationally in Colombia in 1982. Currently, these models are finding increasing acceptance in the conterminous U.S. resource assessment programs and, in some (particularly Reno quadrangle), are being used in initial program planning stages. The deposit model framework is being used in the preparation of some commodity and regional resource reports for the Decade of North American Geology Series. In the Geological Survey's international program, deposit models are an integral part of resource assessment. Our collection of deposit models was adopted enthusiastically by the Geological Survey of Japan for use in their Deep Seated Resource Assessment Project, and Japanese geologists contributed important data for several deposit models. In Costa Rica, 14 models were applied in a 1:500,000-scale resource assessment; detailed field work was carried out on the characteristics of local epithermal gold deposits that were determined to be of the Sado type. In Papua New Guinea, a report has been prepared describing deposit models that are known or likely to be discovered in that country. These include a model for Lihir Island gold, a unique deposit type insofar as is presently known.

Future applications include an assessment of tin resources based on deposit models being carried out by the International Strategic Minerals Inventory Working Group. In additionl, new models are being developed with special attention to nonmetallic deposits, and detailed subdivisions of some models, such as volcanogenic manganese, are being prepared.

Reference Cited

Cox, D. P., and Singer, D. A., eds., 1986, Mineral deposit models: U.S. Geological Survey Bulletin 1693, 379 p.

Geochemists sampling organic-rich lower paleozoic carbonaceous limestones at the Horse Canyon disseminated gold deposit, Nevada. They are studying the thermal maturity of the organic material and its effect on the ore-forming process.

Geochemical Anomalies and Mineral-Deposit Models

Dennis P. Cox, Donald A. Singer, and Paul B. Barton

During the preparation of a compendium of mineral deposit models (Cox and Singer, 1986), we constructed a matrix relating 87 deposit types to 50 chemical elements. In addition to providing the geochemical associations, the matrix contains a ranking of the frequency with which each anomalous element is associated with each deposit type. In this preliminary study, the assignments of numerical values to the occurrence frequency were based only on the experience of the three authors. The ranked matrix was subjected to factor analysis to examine how compatible it is with our intuitively held relations of geochemistry and mineralization processes. Factor analysis was used, first, to reveal relations among elements and, second, to reveal relations among deposit types.

In the first analysis, each of the 50 elements was treated as a variable, and the 87 deposit types, as samples. Because of the high degree of similar affiliations among the 50 elements, a parsimonious grouping of elements into six factors reflects 50 percent of the variability among the elements (table 1). The elements are ordered by the strength of the correlation (factor loading) between element and factor. Multiple elements correlated with the factors suggest that not every element need be measured to reflect the factor. Note that the following factor group names, applied to the same factor numbers as table 1, are only for convenience and are not congruent with conventional geochemical usage—(1) lithophile group, (2) base- and precious-metal group, (3) siderophile group, (4) biogenic group, (5) chalcophile group, and (6) alkalic group.

The second analysis examined the relations among deposit types by treating each of 80 deposit types as a variable and the 50 elements as samples. Alluvial and bauxite deposit types were excluded. Six factors (groups) were required to reflect 60 percent of the variability of deposit types shown by geochemical anomalies (table 2). Most base- and or precious-metal deposit types were associated with the first factor; the second factor contains deposit types associated with ultramafic rocks; the third factor has mostly iron or high Fe-bearing deposits; most Sn- and W-bearing deposits and Climax Mo are associated with the fourth factor; hot spring Au and Hg, Sb vein, and carbonate-hosted Au-Ag deposits are associated with the fifth factor; and phosphate- and U-bearing deposit types are associated with factor six.

Sn polymetallic vein, porphyry Sn, and low-F porphyry Mo deposit types are associated with the first (base- and precious-metal) factor rather than the fourth (Sn-W vein, skarn, Climax Mo) deposit factor. This dichotomy for Sn and Mo results from the fact that the first group is associated with geochemically simple calc-alkaline rocks, whereas the second group is related to high-silica granite systems that contain a distinctive, highly evolved geochemical suite. Although Homestake Au-type deposits are associated predominantly with factor 1, an association also exists with the fifth (hot spring) factor.

In addition to being a powerful exploration tool, geochemistry offers a quick and relatively reliable

Table 1

FACTOR 1	FACTOR 2	FACTOR 3	FACTOR 4	FACTOR 5	FACTOR 6
Ta	Pb	Ni	C	Hg	Zr
Rb	Ag	PGE	Se	Sb	Ti
Cs	Zn	Cr	U	Tl	Sr
Sn	Cu	Co	NH3	(Au)	P
W	Au	Mg	V	(As)	(-As)
Li	(Mn)	(K)		(Ca)	(Th)
Nb	(Te)			(Te)	(REE)
Th	(-Na)				
F	(K)				
Be					
REE					
B					
(U)					
(Mo)					

'()'=Secondary

Table 2

FACTOR 1	FACTOR 2	FACTOR 3	FACTOR 4	FACTOR 5	FACTOR 6
Creede epithermal vein	Dunitic Ni-Cu	Algoma Fe	W veins	Almaden Hg	Phosphate, upwelling type
Low sulfide Au-quartz vein	Komatiitic Ni-Cu	Superior Fe	Sn greisen	Hot-spring Hg	Phosphate, warm current type
Porphyry Cu-Au	Merensky Reef PGE	Fe skarn	Sn skarn	Hot-spring Au-Ag	Sandstone U
Polymetallic veins	Stillwater Ni-Cu	Volcanic-hosted magnetite	W skarn	Sb veins	Quartz pebble conglomerate Au-U
Polymetallic replacement	Synorogenic-Synvolcanic Ni-Cu	Bushveld Fe-Ti-V	Replacement Sn	Carbonate-hosted Au-Ag	Volcanogenic U
Cu skarn	Limassol Forest Co-Ni	Blackbird Co-Cu	Climax Mo	(Homestake Au)	
Replacement Mn	Noril'sk Cu-Ni-PGE	(Gold on flat faults)	Rhyolite-hosted Sn	Silica-carbonate Hg	
Zn-Pb skarn	Alaskan Cr-Pt	Olympic Dam Cu-U-Au	(Sn-polymetallic vein)		
Porphyry Cu	Podiform chromite	(Besshi massive sulfide)	(Volcanogenic U)		
Porphyry Cu, skarn-related	Bushveld Cr	(Stillwater Ni-Cu)			
Sn-polymetallic vein	Diamond pipes				
Porphyry Mo, low-F	Lateritic Ni				
Comstock epithermal vein	Carbonate-hosted asbestos				
Sado epithermal vein	Serpentine-hosted asbestos				
Epithermal quartz-alunite Au	Unconformity U-Au				
Sedimentary exhalative Zn-Pb	(Southeast Missouri Pb-Zn)				
Homestake Au					
Porphyry Sn					
Volcanic-hosted Cu-As-Sb					
Au-Ag-Te veins					
Cyprus massive sulfide					
Epithermal Mn					
Kuroko massive sulfide					
Sandstone-hosted Pb-Zn					
Kipushi Cu-Pb-Zn					
Besshi massive sulfide					
Sediment-hosted Cu					
Southeast Missouri Pb-Zn					
(Sb veins)					
Basaltic Cu					
Volcanogenic Mn					
(Olympic Dam Cu-U-Au)					
(Blackbird Co-Cu)					
Gold on flat faults					

NOT ACCOUNTED FOR	NOT INCLUDED
Carbonatite	Bauxite, laterite type
Porphyry Cu-Mo	Bauxite, karst type
Sedimentary manganese	Placer Au-PGE
Bedded barite	Placer PGE-Au
Emerald vein	Shoreline placer Ti
Appalachian Zn	Diamond placer
	Alluvial placer Sn

"( )" Secondary Factor

way to identify the general type of deposit at an early stage of exploration. This is our first attempt to generate a comprehensive compilation; subsequent efforts can be improved substantially by incorporation of additional input from experienced exploration geochemists.

Reference Cited

Cox, D. P., and Singer, D. A., eds., 1986, Mineral deposit models: U.S. Geological Survey Bulletin 1693, 379 p.

CRIMS—Development of Multiple Automated Mapping Capabilities at the Rocky Mountain Mapping Center, Denver, Colorado

Thomas Dinardo, Michael Crane, and K. Lea Ginnodo

The Rocky Mountain Mapping Center (RMMC), Denver, CO, is responsible for meeting the thematic cartography production requirements of the Central Region of the U.S. Geological Survey. Until recently, these production requirements dealt mainly with the traditional mapping efforts of the Geologic Division. Now, these requirements are being augmented by the needs of a number of other Survey programs including Wasatch Front Earthquake Hazards Reduction, Conterminous United States Mineral Assessment, National Water Quality Assessment, Regional Aquifer System Analysis, and Geographic Information System research and applications activities.

To better meet these responsibilities, RMMC has developed a Central Region Integrated Mapping System (CRIMS). CRIMS is a software system that is designed to support the automated generation of thematic map products by providing interfaces to RMMC's array of high-accuracy cartographic plotting equipment. Input to CRIMS may derive from digital line graph files, Scitex scanning, and manually digitized data files. The development of CRIMS greatly enhances RMMC's digital thematic cartographic production capabilities and ability to respond to the requirements placed on it.

Relations Between Cassiterite-Bearing Veins and Rhyolite Lavas, Black Range Area, Southwestern New Mexico

Wendell A. Duffield

Cassiterite-bearing veins cut late Oligocene rhyolite lava flows and domes in the Black Range area of southwestern New Mexico, and cassiterite-rich placer deposits occur in streams that drain areas underlain by this rhyolite. Although bedrock and placer occurrences are too small and dispersed to have prompted much commercial production, the origin of the cassiterite has been the subject of many research projects during the past half century. These projects have focused on the cassiterite-bearing

veins and have led to two theories for the origin of the Sn mineralization, one that postulates a direct genetic link between the veins and the host rhyolite and another that views the veins as the product of a hydrothermal event younger than and not directly related to the emplacement and cooling of the rhyolite lava. My ongoing study of the rhyolite emphasizes geochemical and physical aspects of volcanology and provides considerable evidence that the veins formed during cooling of newly emplaced lava and that the Sn came directly from such lava as it degassed and devitrified.

Geologic mapping and isotopic geochronology indicate that a minimum of 30 km^3 of rhyolite was emplaced over an area of about 300 km^2 during half a million years or less. The rhyolite has a silica content of 77–78 percent and is essentially uniform in major-element composition throughout the lava field. Apparently, a large reservoir of homogeneous silicic magma underlay the region in late Oligocene time. Contents of Ba and Sr as low as 10 and 3 ppm, respectively, and of Th and Rb as high as 40 and 460 ppm, respectively, attest to the highly chemically evolved character of the rhyolite magma. Sn content is 1–4 ppm in devitrified parts of the rhyolite (nearly the entire volume of lava), and other workers report values as high as 28 ppm in hydrated vitrophyre, material that may reflect more nearly the original Sn content of the magma. Thus, the devitrified rock is a possible source for the Sn in cassiterite; mass-balance calculations indicate that about 1–2 ppm of Sn in the rhyolite lava is equivalent to the Sn known in cassiterite of bedrock and placer occurrences.

Bedrock cassiterite was deposited in such open spaces as vesicles and cooling joints, and nearly all of these occurrences are located in the outermost parts of lava flows, where steep gradients in temperature, vapor pressure, and vapor composition favor mineral deposition in a cooling degassing lava. Other researchers report that fluid inclusions in cassiterite and associated vein minerals formed at 750–100°C, temperatures that reflect vapor-dominated and hot-water mineralizing environments, and that coexisting cassiterite, bixbyite, and pseudobrookite lining vesicles in the outer zone of a lava flow were deposited from a vapor phase somewhat hotter than 500°C. These reports are consistent with the hypothesis that Sn deposition began immediately after emplacement of lava and continued during cooling to near-ambient temperature. Two-feldspar geothermometry applied to phenocrysts in the lava suggests that preeruption magmatic temperature was about 815°C. Absence of Sn mineralization in an overlying ash-flow sheet of $^{40}Ar/^{39}Ar$ age identical to that of the lava also argues for Sn deposition during cooling of the host lava. All characteristics of the mineralization seem explicable through a direct genetic link between the cassiterite-bearing veins and their host rhyolite; one need not invoke a subsequent hydrothermal event.

Geographic Information System Requirements in Mineral-Resource Assessment—Lessons Learned Through Cooperative Research

John L. Dwyer,[1] Stanton H. Moll,[1] Charles M. Trautwein, James E. Elliott, Robert C. Pearson, Walden P. Pratt, and J. Thomas Nash

The Geologic and the National Mapping Divisions of the U.S. Geological Survey have been involved formally in cooperative research and development of computer-based geographic information systems (GIS's) applied to mineral-resource assessment objectives since 1982. Experience in the Conterminous United States Mineral Assessment Program (CUSMAP) projects including the Rolla, MO, Dillon, MT-ID, Butte, MT, and Tonopah, NV, 1° by 2° quadrangles has resulted in the definition of processing requirements for geographically referenced geological, geophysical, geochemical, and mineral-resource data that are common to these studies.

The diverse formats of data sets collected and compiled for regional mineral-resource assessments necessitate capabilities for digitally encoding and entering data into appropriate tabular, vector, and raster subsystems of the GIS. Although many of the required data sets are either available or can be provided in a digital format suitable for direct entry, their utility is largely dependent on the original intent and consequent preprocessing of the data. In this respect, special care must be taken to ensure that digital data type, encoding, and format will meet assessment objectives.

Data processing within the GIS is directed primarily toward the development and application of models that can be used to describe spatially geological, geophysical, and geochemical environments either known or inferred to be associated with specific types of mineral deposits. Consequently, capabilities to analyze spatially, aggregate,

[1]TGS Technology, Inc., Earth Resources Observation System Data Center, Sioux Falls, SD 57198.

and display relations between data sets are principal processing requirements. To facilitate the development of these models within the GIS, interfaces must be developed among vector-, and raster-, and tabular-based processing subsystems to reformat resident data sets for comparative analyses and multivariate display of relations.

Metallogenic Maps of Massive Sulfide Occurrences in the Western United States

Robert L. Earhart

Maps that show the distribution of volcanogenic massive sulfide occurrences and their host rocks are being compiled for the Western United States by teams of geologists from the U.S. Geological Survey, State Surveys, and industry. The maps are being published in the Geological Survey's Miscellaneous Field Studies map series, and, upon completion, the data will be combined to produce a Western United States metallogenic map of massive sulfide occurrences that shows the distribution of deposits with respect to tectonostratigraphic features.

Each State map contains a summary text that discusses the geologic setting of the occurrences and an accompanying table that provides critical information about the localities shown on the map. Detailed information compiled in a dBase III format and published in a Geological Survey open-file report, further supplements map data and provides updated information for the Geological Survey Mineral Resource Data System. Some of the maps will be drafted digitally by using programs developed for the IBM PC and compatible microcomputers (Selner and others, 1986). The maps, along with the supplementary information, will provide detailed information on individual occurrences and an overview of massive sulfide distribution with respect to age, host lithologies, and regional and local tectonic frameworks.

The metallogenic map of massive sulfide occurrences in Arizona (Donnelly and Conway, 1986) is an example of the State maps and related data bases. Massive sulfide deposits in Arizona have been the sources of important amounts of gold, silver, copper, and zinc.

All known massive sulfide occurrences in Arizona formed between 1.7 and 1.8 b.y. Three-fourths of the occurrences are clustered in volcanic and volcano sedimentary rocks of the Yavapai Series in central and western Arizona. Most deposits are associated with felsic volcanic rock or were formed near contacts of mafic and felsic strata. The massive sulfides in nearly one-half the occurrences show a close spatial association with chemical sediments, including oxide facies iron formation and ferruginous chert. The compilation of data from the records of the massive sulfide occurrences in Arizona is utilized in plotting the distribution of rocks of appropriate age and lithology on the map. As a result, the State map delineates geologic terranes that may be favorable for new discoveries.

References Cited

Donnelly, Michael, and Conway, Clay, 1986, Metallogenic map of volcanogenic massive sulfide occurrences in Arizona, *with* contributions by Paul Handverger, edited by R. L. Earhart: U.S. Geological Survey Miscellaneous Field Investigation Map, MF–1853B, 1:1,000,000 scale.

Selner, G. I., Taylor, R. B., and Johnson, B. R., 1986, GSDRAW and GSMAP—Prototype programs for the IBM PC or compatible microcomputers to assist compilation and publication of geologic maps and illustrations: U.S. Geological Survey Open-File Report 86–42, 40 p.

Mineral Deposits in Neogene-Quaternary Eruptive Centers in the Central Andes

George E. Ericksen, Robert L. Smith, and Robert P. Koeppen

Eruptive centers, which include collapse calderas, composite cones, and flow-dome fields in the Neogene-Quaternary volcanic complex of the central Andean region of northwestern Argentina, western Bolivia, northern Chile, and southern Peru, are potential targets for hydrothermal mineral deposits. This volcanic complex extends over an area of about 300,000 km^2 within a 1,000,000-km^2-area that is one of the world's great mineral provinces. Because many deposits of Cu, Pb, Zn, Sn, W, Sb, Bi, Ag, and Au in this area are chiefly of pre-Pliocene age, it had been believed that most of the Neogene-Quaternary volcanic rocks represented postmineralization cover. However, recent studies have shown that important metalliferous deposits as young as Pleistocene are associated with the eruptive centers. Mineral deposits in these centers were emplaced during the waning phases of

volcanic activity, and available radiometric ages show that they were emplaced chiefly within an interval of not more than 1 m.y. after the major eruptive phase of the center. Our studies in the central Andes, beginning in 1978, have been focused on a better understanding of the relation between types of mineral deposits and the geochemistry of associated igneous rocks. We examined the possibility that some minor elements in igneous rocks might be utilized in exploration for tin deposits. Such stable minor elements as Ta, Th, Rb, and Hf are indicators of Sn-anomolous magmas. These magmas are widespread in the Bolivian tin belt but have not been found in the Chilean copper belt, suggesting that there may be real magmatic control of differences between types of mineralization.

Epithermal Ag-Au deposits are by far the most economically important type of deposit associated with Neogene-Quaternary volcanic centers, chiefly collapse calderas, in the central Andes, and we believe that the potential for finding similar deposits in other eruptive centers is great. Other types of deposits present in the Neogene-Quaternary volcanic complex of the central Andes are (1) hydrothermal and exhalative Pb-Ag, Cu, Mn, and native S deposits and presumed magnetite-hematite flows in the upper parts of composite cones, (2) Ag-Au deposits associated with altered and brecciated porphyry stocks exposed in deeply eroded composite cones, (3) polymetallic Sn, Pb-Zn, and Ag-Au deposits associated with brecciated and hydrothermally altered porphyry stocks that are not associated with known volcanic landforms, (4) Ag-Au deposits in intensely altered volcanic rocks at sites of fossil geothermal spring systems, and (5) wood-tin veins and supergene U deposits in ash-flow tuffs within and near collapse calderas. In addition, the volcanic rocks and associated thermal springs contain abundant water-soluble salts and are the chief sources of the widespread saline deposits of this region, which include major resources of Li and B.

Heavy Minerals of the Mid-Atlantic Inner Continental Shelf

Edward C. Escowitz and Andrew E. Grosz

Economically valuable heavy-mineral assemblages have been identified in grab samples from the mid-Atlantic inner continental shelf. Typically, the heavy-mineral assemblages include ilmenite, leucoxene (altered ilmenite), rutile, zircon, monazite, sillimanite, and staurolite. High heavy-mineral content in surficial sediments of particular geomorphic features, such as shore parallel shoals and submerged channels, has led to speculation of economic deposits. Analyses of vibracores, nominal length 5 m, now confirm the vertical continuity of high heavy-mineral concentrations offshore of Cape Charles, VA, and Cape May, NJ.

Heavy-mineral (specific gravity > 2.96 gm/cm^3) content for the surficial 6 m of sediment comprising Smith Island Shoal (approximately 20 km west of Cape Charles) has an average value greater than 2.5 percent, whereas the upper 3 m exceeds 3.0 percent. In-situ economic heavy minerals at Smith Island Shoal have been estimated to be on the order of 10^6 metric tons using presently available vertical control. This estimate is based on the following assumptions: (1) 6 m thick, 10 km long, 3 km wide, equivalent deposit dimensions for rectangular solid estimate, (2) 50 percent of the seafloor volume is sediment, (3) 2.7 gm/cm^3 average density of sediment, and (4) 1 percent of the deposit mass is economic heavy minerals. This estimate probably is conservative because deeper vertical control is likely to show deposit thickness exceeds 6 m, the length of the vibracore device used for this study (did not penetrate the deposit), and preliminary analysis of seismic reflection profiles indicates that deposit equivalent horizontal dimensions are likely to exceed those used for this estimate.

Heavy-mineral concentration values for cores from an inner continental shelf study area offshore of Cape May have a maximum value of 5.1 percent for a 1.56-m vertical unit and exceed 3.0 percent for vertical units greater than 2 m at two other sites. Areas of high heavy-mineral concentration have a shore parallel trend but lie between Holocene shoals. High values also are associated with a relic channel approximately 25 km southeast of Cape May and were found to have a trend parallel to the recent channel between Cape May and Cape Henlopen, DE.

Application of Crystal Chemistry to the Geochemistry of Vanadium

Howard T. Evans, Jr.

Vanadium ores generally are deposited under reducing conditions, in which trivalent vanadium behaves like trivalent iron; for example, in the titaniferous magnetite ores (for example, in South Africa) vanadium does not occur as discrete minerals, but is present as a minor constituent in spinellike oxides (magnetite, coulsenite). When released from

such a state by hydrothermal or weathering action, vanadium displays a bewildering variety of reactions and forms numerous mineral phases because of its great sensitivity to two prominent environmental parameters, acidity and oxidation potential. To understand this behavior, it is necessary to follow the changes in the valence and structural states of the element.

A simplified diagram (fig. 1) shows a field in which acidity varies on the abcissa and oxidation state on the ordinate. The appropriate environment for the occurrence of many vanadium minerals can be indicated qualitatively on the diagram. Most vanadium minerals are highly colored, and those with mixed valences are generally black. Proper location of such phases on the diagram often can be made only by crystal chemical techniques, including crystal structure analysis.

High-temperature vein minerals form mostly in the upper left region of the diagram, where vanadium forms tetrahedral VO_4^{3-} groups similar to those of phosphate PO_4^{3-} (vanadinite is isostructural with apatite). In the United States, a major source of vanadium is the mineralized sandstones of the Colorado Plateau, where a completely different, low-temperature, aqueous environment prevails and representatives from all parts of the diagram are found. The primary ore is mainly montroseite VO(OH), which is analogous to goethite FeO(OH), but, on exposure to air-laden ground water, vanadium passes up through the diagram to the top, where the mineral form depends on local acidity and other cations present. When vanadium and uranium become fully oxidized, they become bound together in the insoluble carnotite type of structure, which is a layer complex built from linear O-U-O and double square pyramidal O_3-V-O_2-V-O_3 groups. The higher coordination state of the latter is typical of more acid environments. Without uranium, oxidized vanadates in acid medium form soluble, brightly colored polyvanadate salts (pascoite), which are leached rapidly.

At the upper right of the diagram, there occurs an important group of mixed 4+/5+ vanadium oxide minerals, which are analogous to a class of compounds known in solid state chemistry as "vanadium bronzes." Several different structure motifs are known, but, generally, they consist of VO_5 and VO_6 groups joined into chains, which are linked laterally to form sheets, with large interlayer or channel spaces. Varying amounts of delocalized electrons in the chains are charge balanced by varying concentrations of interlayer cations. One structure is represented by hewettite with a layer composition V_3O_8, whose structure we have examined in some detail. Another type is straczekite with a V_2O_5 layer. A newly analyzed structure type is found in melanovanadite, which also has a V_2O_5 layer but with a structure completely different from that of straczekite.

On the basis of crystal chemistry, we are able to classify rationally the 110 known vanadium mineral species and, on the diagram, to trace the course of weathering of the original montroseite ore from one species to the next as oxidation state rises and acidity swings either to alkaline or acid environments.

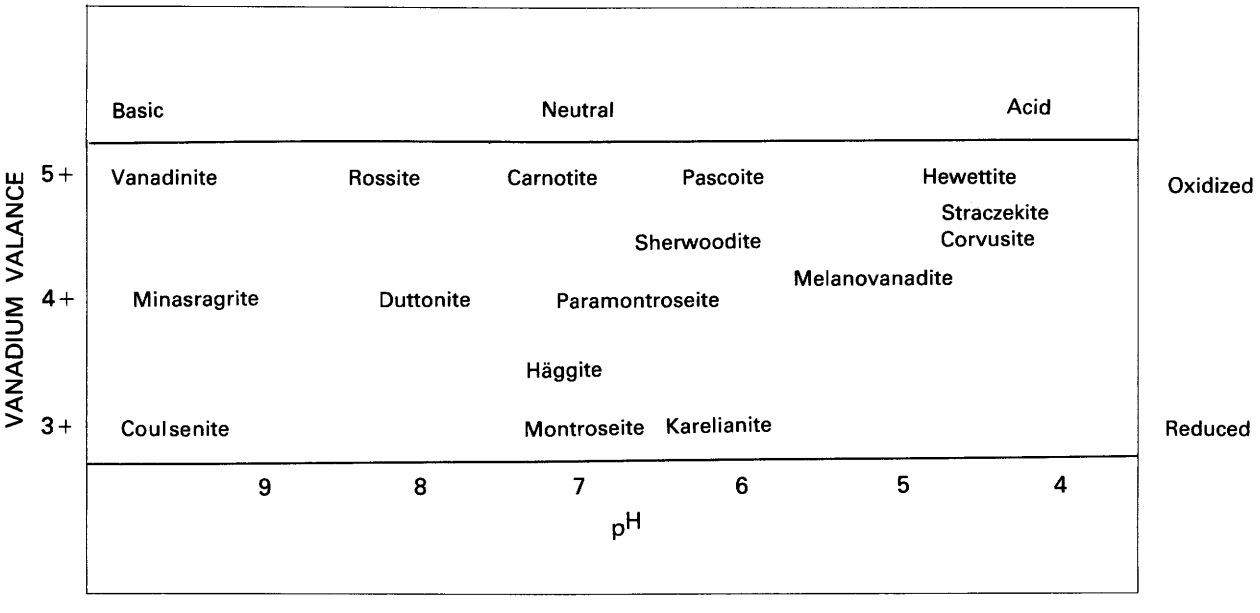

Figure 1. Approximate conditions of formation of some vanadium minerals in the valence-acidity field.

The Geophysical Character of Solution-Collapse Breccia Pipes on the Coconino Plateau of Northern Arizona

Vincent J. Flanigan, R. Michael Senterfit, Pam Mohr, and Karen J. Wenrich

The potential for economic mineral resources associated with solution-collapse breccia pipes has focused research on the nature and physical character of these geologic features. Numerous pipes are exposed on canyon walls, and occurrences of hundreds more are strongly suspected within the plateaus of northern Arizona. The pipes originated from solution caverns developed in the Mississippian Redwall Limestone accompanied with subsequent successive caving of younger Paleozoic rocks. High-grade U ore in association with potentially economic concentrations of Ag, Pb, Zn, Cu, Co, and Ni constitute the main mineral resources of these collapse breccia pipes.

Based upon common surface expression and electrical characteristics, two physical models of breccia pipes are proposed for those pipes present on the Coconino Plateau. These two models are subsets of a basic geologic model and are related to the differences of character of the Kaibab Limestone collapse cone surrounding the throat of the breccia pipe. One model is a circular depression of 100 m or more in diameter at the center of a slight topographic high lying within an extended depressed area. An electrical cross section of this model suggests alternate conductive-resistive zones across the collapse cone, with the most conductive zone located over the throat of the pipe. At the surface of the Kaibab Limestone, the second model is quite similar to the first but differs in that the central area over the throat of the pipe is a small hill at the middle of a depression 500 m or more in diameter. An electrical cross section of the second model is very similar to the first model, except that the throat of the pipe is capped with a resistant plug of Kaibab Limestone. In the second model, the throat of the pipe apparently did not stope upwards through the Kaibab, but may have been covered by a circular block of relatively undisturbed Kaibab that later dropped into the underlying throat. Conductive zones outside of the central conductive zone or throat area probably are related to ring fracturing developed when the Kaibab plug dropped. Common physical features of the two models include circular drainage, concentrically inward-dipping strata, anomalous vegetation, and alteration of the exposed rocks by hydrothermal fluids.

New Geophysical, Geochemical, and Geological Investigations of Northern Appalachian Zinc-Lead Sulfide Deposits of New York State

Jules D. Friedman and Felix E. Mutschler[1]

Combined remote sensing geophysical, geological, and geochemical investigations of northern Appalachian ZnS-PbS deposits of the Shawangunk, NY, district have begun to answer old questions about the spatial distribution, tectonic control, mode, temperature, and age of origin of these orthoquartzite-hosted deposits. At the same time, our investigations also have raised new questions about their relation to Mississippi Valley-type (MVT) deposits and to similar sulfide deposits of Hercynian age along the Iapetus geosuture zone from Ireland to Scandinavia.

The Shawangunk deposits are represented by 10 or more small ore bodies and occurrences that we relocated, sampled, and analyzed in relation to Thematic Mapper, radar, aeromagnetic, and isostatic gravity maps. The mineralized bodies consist mostly of open-space and vein fillings in the Silurian Shawangunk Formation, the basal unit above the Taconian unconformity. The ZnS-PbS ore bodies and occurrences are localized along the northeast-trending Shawangunk Mountain, a northwest-dipping monoclinal ridge marking the easternmost margin of the Silurian Salina sedimentary basin. The proximity of the basement in this area is evidenced by a northeast-trending aeromagnetic high and associated isostatic gravity low near Ellenville that might reflect a detached piece of faulted gneissic basement beneath the Taconian unconformity at a depth of a few kilometers.

Most of the ore bodies and occurrences are located within a few kilometers of the exposed trace of the Taconian unconformity surface where it intersects N. 55–60° W.-striking fractures observed on optically and geodetically corrected radar mosaics. The deposits are marked by geochemical heavy-metal (Pb, Zn, Ni, Mn, Cu, and Co) anomalies reported by Moxham (1972) in overlying soils. Similar heavy-metal anomalies associated with radar lineaments of the same northwest-trending suite may indicate undiscovered mineralized bodies at depth.

Preliminary geochemical analyses of the ore samples show as much as 220,000 ppb Hg content in Ellenville sphalerite and generally higher Ag, Fe,

[1]Eastern Washington University, Cheney, WA.

Hg, Ti, and Nb and lower Cd content than other Appalachian and MVT deposits.

Sulfide isotope statistics indicate that the sphalerite, chalcopyrite, and galena values are grouped closely around a mean of +24.37 $\delta^{34}S$ in relation to Cañon Diablo troilite and provide significant information for our genetic model.

The Shawangunk deposits have many similarities to other Appalachian and MVT ZnS-PbS deposits. All probably were emplaced by the migration along structural paths of connate brines from the interior of sedimentary basins to basin margins, but the Shawangunk deposits were formed at higher temperatures by lower salinity fluids as indicated by recent fluid-inclusion studies (J. S. Wilbur, Eastern Washington University, written comm., 1986) that suggest temperatures of ore deposition in the range of 150–265 °C in the Shawangunk district.

In most MVT and Appalachian base-metal districts, the bulk of the ore is hosted by carbonate rock units. The Shawangunk deposits are hosted by orthoquartzite. A 400-m-thick, largely carbonate sequence of Silurian to Devonian age overlies the Shawangunk Formation. This sequence is covered by Quaternary deposits in the Rondout-Mamakating Valley on the western side of the Shawangunk ridge and could represent a host for related, but yet undiscovered, sulfide deposits in this area.

Reference Cited

Moxham, R. L., 1972, Geochemical reconnaissance of surficial materials in the vicinity of Shawangunk Mountain, New York: New York State Museum and Science Service Geological Survey Map and Chart Series, no. 21, 20 p.

Appalachian Metallogenic Map

Jacob E. Gair, William F. Cannon, John D. Peper, Sallie I. Whitlow, Suzanne S. Cannon, and Beth D. Martin

The Appalachian Metallogenic Map and accompanying information provide a systematic compendium of metallic mineral deposits on a new geologic base. The map illustrates major metallogenic-geologic relations and is expected to aid in making mineral-resource assessments and in identifying geologic features favorable for exploration. The map is a companion to maps being prepared with the same format and at the same scale, 1:1,000,000, by cooperating groups in the Canadian Appalachian provinces. All known deposits that have been mined are shown, as well as numerous prospects of record. Deposits are represented by symbols depicting the geologic class, scaled to three ranges (large, moderate, small) of deposit size. Nine geologic classes of deposit and one "uncertain" category are shown, including stratabound concordant, stratabound discordant, vein, supergene residual, layered igneous, stockwork (pipe), placer, skarn, and pegmatite. Eighteen metallic commodities and two nonmetallic commodities, sulfur and fluorine, where these are associated closely with metallic commodities, are shown. The commodities are identified by color within deposit symbols. Deposits, which are numbered by State, are listed in an accompanying pamphlet along with the name of the deposit, if any, and additional information, including (1) chemical class of deposit, such as native metal, oxide, sulfide, and so forth, (2) ore characteristics, such as disseminated or massive, (3) genesis of the deposit, such as marine sedimentary or hydrothermal, and (4) host rock for mineralization, such as felsic volcanic or carbonate. Because crowding and overlapping of deposit symbols in many parts of the map would have resulted in obscuring one symbol by another, we could not include this additional information on the map. Some local areas of the map with excessive deposit "congestion" have been enlarged to a scale of 1:500,000 to clarify deposit numbers. Much of the map and pamphlet information and references to literature is available in the U.S. Geological Survey Mineral Resources Data System (formerly the Computerized Resources Information Bank).

The geologic map is modeled closely on the geologic base for the Metallogenic Map of Nova Scotia by Chatterjee (1983) and incorporates much new information from detailed mapping done during the last dozen years or so. The geologic features shown are those considered particularly significant for the formation (occurrence) of metallic mineral deposits. The principal feature is lithology, grouped according to volcanic or sedimentary, corresponding metamorphic, or igneous plutonic origin and as mafic-ultramafic bodies. Examples of some of these lithologies are dominantly felsic volcanic; dominantly coarse clastic sedimentary; dominantly carbonate sedimentary, granite, tonalite, gabbro (that is, igneous plutonic); and felsic (or mafic) paragneiss. The significant geologic features of the map also include a division of the stratified volcanic and sedimentary rocks into the following age units: Middle Proterozoic, Late Proterozoic and (or) Cambrian, Lower and Middle Cambrian, Cambro-Ordovician, Middle Ordovician-Devonian, Carboniferous, and Triassic-Jurassic. The plutonic rocks likewise are separated

chronologically, in millions of years, into four groups—greater than 520, 520–440, 440–310, and less than 310. Specific radiometric ages of the larger plutons are shown on the map. Selected major unconformities, anticlinoria, synclinoria, domes, basins, and faults also are significant features of the map.

Note. The map to be published will display geologic information by combinations of lines, patterns (for lithology), and colors (for age). In the preliminary version shown at the McKelvey Forum, lithologies and ages are shown by color on separate sheets.

Reference Cited

Chatterjee, A. K., 1983, Metallogenic map of the Province of Nova Scotia: Department of Mines and Energy, Nova Scotia, scale, 1:500,000.

Gold Veins of the Seward Peninsula, Alaska

Bruce M. Gamble

Gold-bearing veins of the Seward Peninsula, AK, occur along high-angle faults in the Nome Group metamorphic rocks. The veins can be divided into two types—low and high sulfide. The low-sulfide type is more common and generally contains less than 3 percent arsenopyrite and (or) pyrite; galena, sphalerite, and scheelite occur locally. Quartz is the dominant gangue mineral, but plagioclase (albite-oligoclase) and (or) carbonate minerals (calcite, dolomite, ankerite) locally make up as much as 50 percent of the veins. Minor amounts of chlorite, sericite, and clay minerals also may be present. The high-sulfide veins contain 20–80 percent stibnite and minor amounts of pyrite and arsenopyrite. Quartz is the dominant gangue mineral, but some sericite, calcite, and clay minerals are usually present. Veins at Bluff (83 km east of Nome) are unusual in that they contain as much as 60 percent arsenopyrite and lesser pyrite and stibnite. Again, quartz is the dominant gangue mineral; sericite and clay minerals are present in small amounts.

Free gold (visible and microscopic) is rare in both vein types, which suggests that much of the Au may occur in sulfides. Au content of the veins varies widely. Grab samples from the low-sulfide veins show Au values ranging from 0 to 120 ppm. Those from the high-sulfide veins show values ranging from 0.5 to 40 ppm. Significant, but highly variable, amounts of As, Sb, Bi, Ag, W, Hg, Cu, Pb, and Zn are also present in the veins.

Veins range from 2 cm to 4 m wide, but most are less than 50 cm. More than one vein may be present in a single fault zone, and the wallrocks between the veins may carry low Au values. The veins at Big Hurrah (58 km northeast of Nome) are the largest on the Seward Peninsula. They range from 0.5 to 4 m wide, and as many as four veins are present in a single fault zone. Approximately 810 kg (26,000 oz) of gold was produced at the Big Hurrah Mine, primarily between 1903 and and 1907.

Fluid inclusions in vein quartz from Big Hurrah contain CO_2 and CH_4 (Read, 1985). A pressure estimate of 0.8 kbar, and temperature estimates ranging from 300 to 400°C indicate emplacement after peak blueschist facies metamorphic conditions in Late Jurassic to Early Cretaceous time. Quartz from several veins on the Seward Peninsula yield δO^{18} isotope values that range from +10.2 to +19.2 (Gamble and others, 1985); these values are consistent with a metamorphic origin for the veins.

Results obtained so far represent part of a ongoing study. Future work includes (1) obtaining additional measurements of fluid-inclusion compositions and homogenization temperatures, (2) K-Ar age determinations of suitable phases from several veins, (3) identification by X-ray of unknown phases, (4) assay of mineral separates, and (5) obtaining additional δO^{18} isotope data.

References Cited

Gamble, B. M., Ashley, R. P., and Pickthorn, W. K., 1985, Preliminary study of lode gold deposits, Seward Peninsula, Alaska, *in* Bartsch-Winkler, Susan, ed., 1985, The United States Geological Survey in Alaska—Accomplishments in 1985: U.S. Geological Survey Circular 967, p. 27–29.

Read, J. J., 1985, Gold-quartz vein deposition in an uplifted blueschist terrane, Seward Peninsula, Alaska [abs.]: Geological Society of America Abstracts with Programs, v. 17, no. 7, p. 696.

Spark-Aerosol Generation—A New Technique for the Direct Analysis of Geologic Solids by Inductively Coupled Plasma Spectrometry

D. W. Golightly, A. Montaser,[1] B. L. Smith, and A. F. Dorrzapf, Jr.

Aerosols generated by a unidirectional high-voltage spark are injected by flowing Ar into an Ar inductively coupled plasma (ICP). The particulates

[1]Department of Chemistry, George Washington University, Washington, DC 20052.

(size range: 0.1–100 μm) produced by the spark are efficiently atomized, ionized, and excited to emit subsequently the characteristic radiations measured by a direct-reading polychromator. Nonconductive geologic materials are presented to the 4-mm point-to-plane spark gap, which requires electrical conductivity of both electrodes, in the form of a disk (25 mm diameter, 3 mm thick) that is formed in a die of a hydraulic press (39.5 MPa for 60 s) from a 1:4 mixture of pulverized sample (–100 mesh) and Cu powder (–22 mesh).

Spark erosion of material from the surface of the composite Cu disk is an erratic process. However, spectral line signals from analytes and matrix elements indicate that a pseudosteadystate condition is reached after 70–80 s of sparking. This situation, which persists for 10–20 s, provides an interval suitable for the necessary 5- to 10-s integrations of spectral line signals. Operating conditions, including the spark current (4.3 A) and break frequency (2 breaks per half cycle), delay interval (70 s), plasma power (1.3 kW), observation height (20 mm), and injector gas flow rate (1 L/min) were optimized by multiple-element sequential simplex optimization.

The capabilities of this new technique for the generation of aerosols directly from the solid phase are illustrated by recent applications of the technique to the determinations of Ce, Co, Fe, Ni, P, and Pb in Co-rich ferromanganese nodules. The line-rich spectra of Fe and Mn, which produced many spectral interferences, limited the number of elements that could be determined. For measurements that were feasible, the precision, based on six replicate determinations, ranged from 7 (Ce) to 14 percent (Fe) relative standard deviation. Because only two nodule standards (USGS–Nod–A–1, USGS–Nod–P–1) are available, the method of standard additions was used for these determinations. Also, the erratic sampling by the spark made necessary the use of the Mn(II) 257.6-nm line as an internal reference for all spectral measurements. Unlike conventional approaches, which require fusions or mixed-acid dissolutions of materials followed by pneumatic or ultrasonic nebulization of a solution

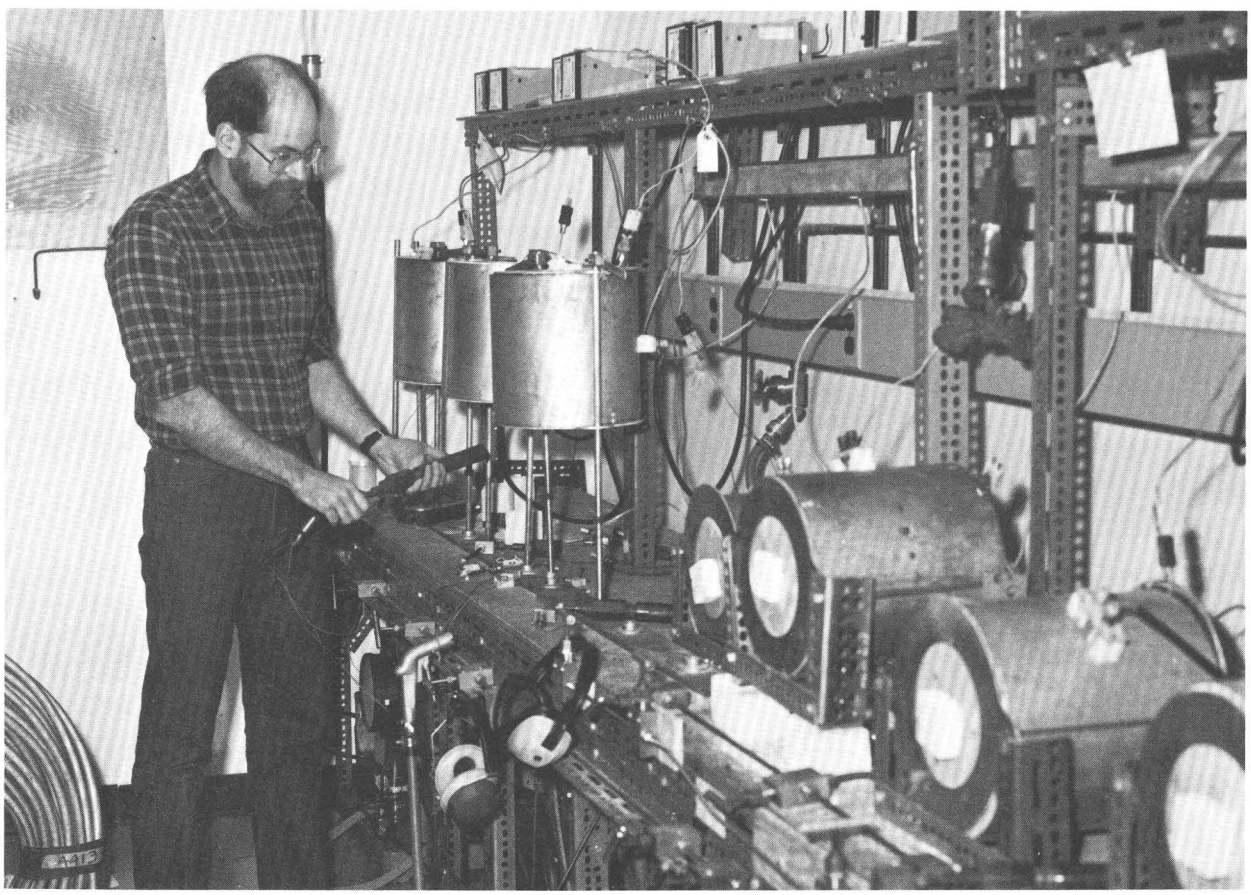

Laboratory furnaces (cylindrical objects on laboratory bench) used to heat samples to estimate pressure and temperature conditions when mineral deposits formed. Here, a U.S. Geological Survey geologist places a sample in a cold-seal hydrothermal vessel that will be heated in one of the furnaces.

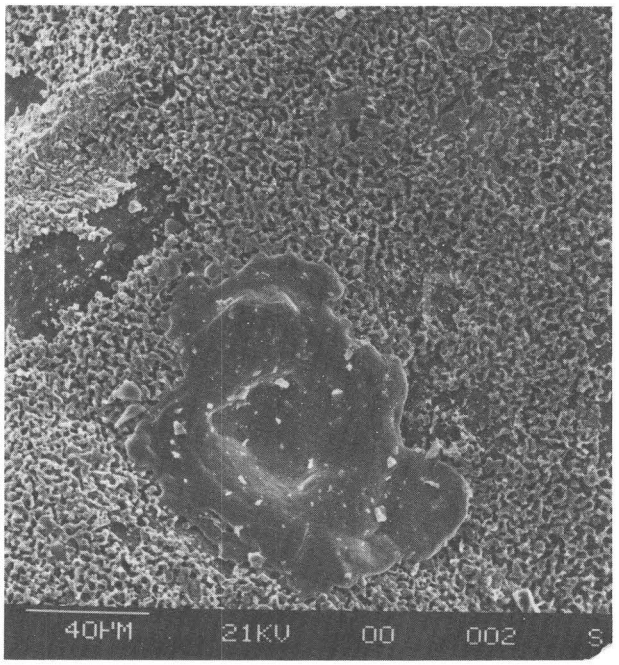

Scanning electron microscope photomicrograph of AgCl (cauliflower shape) developing from AgS (mottled) that is coating and impregnating a pyrite crystal. This crystal is from a pyrite-rich vein on St. Thomas, U.S. Virgin Islands. The vein also contains Au-Ag tellurides, Ag tellurides, Fe tellurides, native gold, and electrum.

into the plasma, the spark aerosol generator provides a means for the direct introduction of sample into the ICP. This capability is expected to be particularly valuable in the analysis of mineral phases that are difficult to dissolve, such as beryl, cassiterite, chromite, rutile, and zircon.

Petrology and Platinum-Group Element Variation in Zoned Ultramafic Complexes, Klamath Mountains, Oregon and Northern California

Floyd Gray, Norman J Page, and Barry C. Moring

Alaskan-type ultramafic-mafic complexes contain platinum-group element (PGE) resources, principally platinum, palladium, and minor rhodium. Some of the better known examples of these ultramafic-mafic complexes occur in southeastern Alaska and British Columbia. Others are found in the Klamath Mountains of Oregon and northern California and the western Sierra Nevada in California. A detailed investigation of three postorogenic, Alaskan-type ultramafic-mafic complexes in the Klamath Mountains was undertaken to develop a detailed understanding of the petrogenesis of the complexes and to characterize the PGE occurrences.

Alaskan-type ultramafic-mafic complexes in the Klamath Mountains include the Lower Coon Mountain pluton and the intrusive suites at Tincup Peak and at Chanchelulla Peak. These rocks range in age from 142 to 163 Ma and intrude metasedimentary, metavolcanic, and ophiolitic cumulate ultramafic to gabbroic rocks that form part of the accreted oceanic terrane of the Klamath Mountain province.

The Lower Coon Mountain pluton consists of layered clinopyroxene-rich lithologies occurring in chronological sequence, and the intrusive suite at Tincup Peak consists of a cogenetic sequence of wehrlite, clinopyroxenite, magnetite clinopyroxenite, feldspathic hornblende-magnetite clinopyroxenite, and dunite-olivine clinopyroxenite and a large component of pegmatitic hornblende gabbro. The ultramafic-mafic intrusive suite at Chanchelulla Peak, part of the Wildwood pluton, consists predominantly of clinopyroxenite, minor interlayered dunite, and wehrlite with minor hypabyssal gabbroic rocks.

Clinopyroxene compositions in the three intrusive suites are calcium rich, range from $Wo_{54.7}$-$En_{45.1}$-$Fs_{0.19}$ to $Wo_{44.9}$-$En_{43.8}$-$Fs_{11.3}$, and resemble clinopyroxene with alkalic affinities. Olivine ranges from Fo_{72} to Fo_{83}, and plagioclase ranges from An_{68} to An_{96}. Cyclic units of layered cumulus magnetite + spinel (± ilmenite) and coarse interstitial magnetite occur at Tincup Peak and Lower Coon Mountain.

Characteristics of the rocks include (1) Rh contents up to nearly 1 ppb, (2) Ir and Ru contents of less than 100 and 20 ppb, respectively, (3) Pd contents that vary between rock units within intrusive suites and between the suites, and (4) relatively similar Pt contents among all units. Concentrations of Pd average 6.3 ppb at Lower Coon Mountain, 13.7 ppb at Chanchelulla Peak, and 36.4 ppb at Tincup Peak. Individual rock units within each intrusive suite yield a Pt:(Pt+Pd) (Cohen-corrected abundance) that is greater in olivine-rich rocks than in clinopyroxenite and significantly greater than in gabbro, which suggests chemical fractionation of Pd within intrusive suites.

All three intrusive suites contain disseminated sulfides, mainly pyrrhotite + pentlandite + chalcopyrite. Chalcopyrite and bornite at Tincup Peak are associated with disseminated nickel sulfides. The Chanchelulla Peak pluton also contains lenticular zones of disseminated to interstitial sulfides, mainly pyrrhotite, near its contact with sulfide-bearing hornfelsic rocks.

Sulfide minerals, the most significant collectors of PGE, exhibit similarities in occurrence, mineralogy, and chemistry; however, differences in their distribution and in the importance of chemical and physical processes that may have produced the sulfide occurrences are significant.

Revision of the Stability Field of Wüstite and Recommended Standard Oxygen Potentials for the Solid Oxide Buffers

John L. Haas, Jr.

From a detailed review of the published data for selected oxygen buffer assemblages, the composition $Fe_{0.947}O$ commonly associated with wüstite was found to be metastable below 825°C. The composition of wüstite at the isobaric invariant temperature, 566(±10)°C, is close to $Fe_{0.915(\pm 0.005)}O$. The revised composition is consistent with the best observations of the phase stabilities in the stable region above and in the metastable region below 566°C. The results are consistent with the experimental data in the much-cited classic study of Darken and Gurry (1945). The results are inconsistent with the extrapolations made by Darken and Gurry to temperatures below 1,100°C. Most phase diagrams for the system Fe-O are based on Darken and Gurry's (1945) extrapolation of the stability limits of wüstite. The revised stability field is shifted systematically to higher excess O contents (more Fe vacancies) between 1,100 and 566°C.

The standard O_2 potentials of the O_2 buffer assemblages, Fe-wüstite, wüstite-magnetite, Fe-magnetite, magnetite-hematite, quartz-fayalite-Fe, quartz-fayalite-magnetite, Ni-bunsenite, Cu-cuprite, and cuprite-tenorite were developed in the same review. The revised potentials are consistent with direct observations, indirect observations where

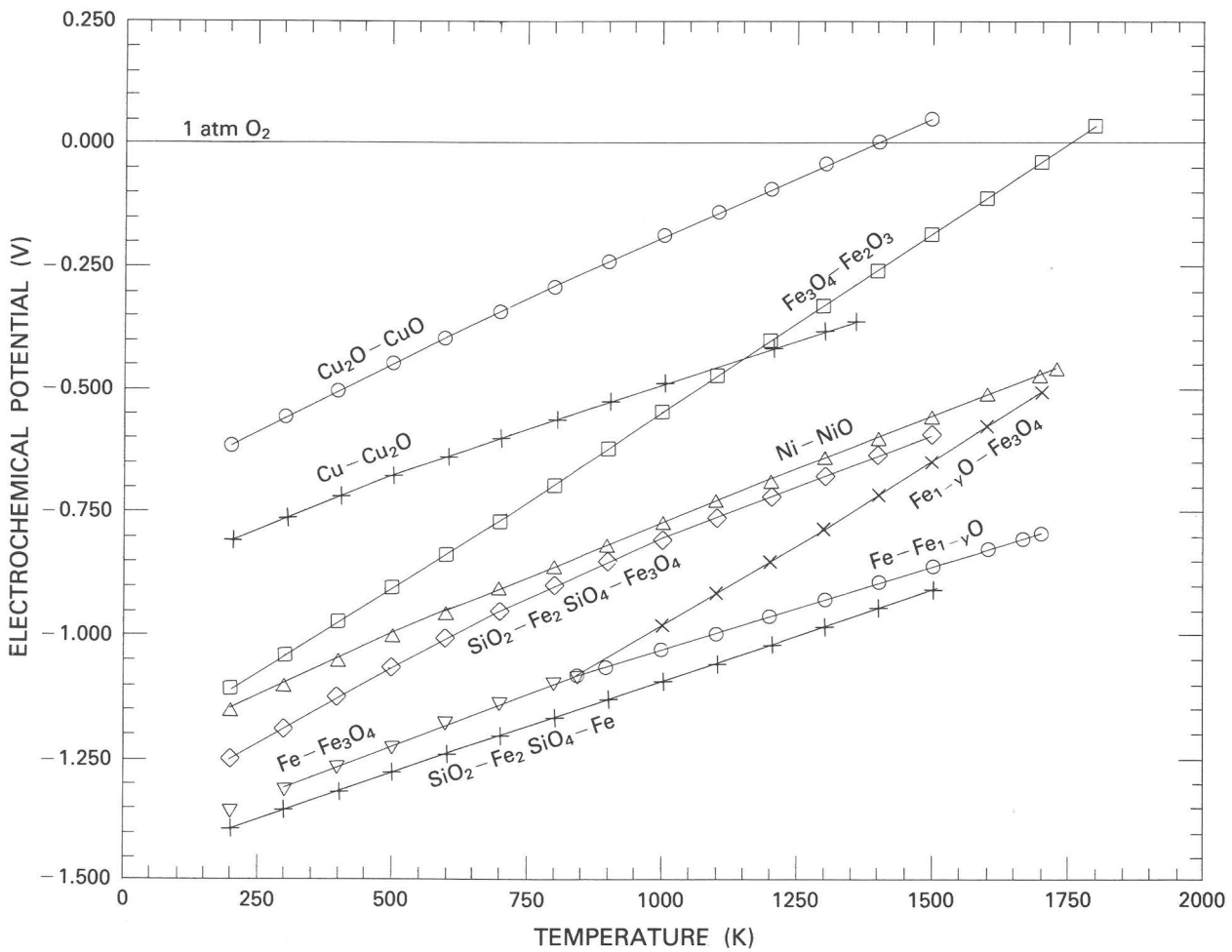

Figure 1. Plots of the recommended standard O_2 potentials relative to the ideal diatomic gas at 1 atm as a function of the absolute temperature.

one buffer assemblage is compared against another, indirect observations where H_2O:H_2 or CO_2:CO were used to fix O_2 potentials and volumes, densities, heat capacities, and entropies for each of the phases within the precisions for the observations. The recommended potentials relative to the ideal gas O_2 at 1 atm, are shown in figure 1. Most of the buffer curves are nearly linear. However, the quartz-fayalite-magnetite and the magnetite-hematite curves show pronounced curvature due to the heat effects associated with the magnetic anomalies in magnetite at 575°C and in hematite at 682°C. The curvature in the other curves that include magnetite is not evident because wüstite becomes unstable at nearly the same temperature as the magnetic anomaly in magnetite.

Reference Cited

Darken, L. S., and Gurry, R. W., 1945, The system iron-oxygen, I, The wüstite field and related equilibria: American Chemical Society Journal, v. 67, p. 1398–1412.

Tectonic Setting of Some Cretaceous and Cenozoic Structural and Magmatic Systems of the Western United States

Warren B. Hamilton

Convergence of North American and eastern Pacific plates was slow during most of Cretaceous time; the subducting slab sank steeply below the advancing continent, and the magmatic arc was near the coast. Convergence was rapid during latest Cretaceous and early Paleogene time; the continent overrode the slab and was eroded against it, and the magmatic arc migrated far inland. Convergence slowed in late Paleogene time, and the slab again sank steeply. A strike-slip continental margin has evolved during the Neogene.

Obliquely eroded crustal sections in arc batholiths show this crustal column to be typical—about 30 km depth, migmatites and granitic rocks of garnet-amphibolite or low-pressure granulite facies; 25–15 km, upper amphibolite facies migmatites and granitic rocks, many of them peraluminous, that crystallized from melts cooler and wetter than those either deeper or shallower; 15–4 km, crosscutting plutons of hornblende-biotite granitic rocks; 4–0 km, calc-alkalic volcanic rocks, mostly as caldera complexes, ignimbrites, and voluminous ash dispersed to mudstones and shales.

Foreland thrusting of preexisting stratal wedges was synchronous with middle and Late Cretaceous arc magmatism. Gravitational spreading from the magmatically thickened zone may have driven the thrusting.

When convergence was slow, accreted materials were metamorphosed at high pressure and low temperature beneath the leading part of the overriding continental plate, and some metamorphic rocks were cycled into melange above the sinking slab. During subsequent rapid convergence, accreted materials were underplated against tectonically eroded continental crust, beneath which they are now exposed.

The western part of the continent was slowed by drag on the subducted slab during rapid convergence, and rotation of the Colorado Plateau relatively clockwise toward the continental interior produced Laramide Rocky Mountain crustal shortening. Laramide basement thrusts flatten downward into anastomosing zones of ductile shear that outline midcrust lenses. Midcrust shear zones of the same age outline analogous lenses exposed in south-central California.

Severe intra-arc extension, orthogonal to the continental margin, affected magmatically heated Basin and Range crust during middle Tertiary slow convergence. Late Cenozoic oblique extension developed as the strike-slip continental margin evolved. Both regimes produced similar deformation. The middle crust was extended as lenses slid apart along ductile shear zones. The aggregate top—"detachment faults"—of these lenses increased in area as deep lenses emerged from beneath shallow ones. The brittle upper crust responded by block rotations. Range-sized fault blocks are allochthonous above the detachments, against which steeply rotated basin fills are truncated and new fill is deposited directly. Although some detachments surface as range-front faults, most originate at midcrustal depths. Some detachments remain active even after tectonic denudation has brought them to the surface, whereas others are broken by new steep faults related to deeper detachments. The lower crust is extended by more pervasive ductile flow. The Basin and Range Mohorovičić discontinuity has been remade magmatically. Similar extension affected Idaho and northeastern Washington during Eocene time. Neogene uplift of the Western United States largely records mantle heating, inferred to be due, in part, to asthenosphere diapirism consequent on extension and in part to conductive heating of subducted lithosphere.

Authigenic K-Feldspar—An Indicator of the Geochronology and Chemical Evolution of Mineralizing Fluids in Carbonate-Hosted Lead-Zinc Deposits

Paul P. Hearn, Jr., John F. Sutter, and Harvey E. Belkin

Rocks containing abundant authigenic K-feldspar are now known to occur in clastic-rich zones of lower Paleozoic carbonate rocks throughout the Valley and Ridge province of the central and southern Appalachians, in correlative lithologies in western New England, and in the midcontinent area. Recent $^{40}Ar/^{39}Ar$ analyses, petrographic and fluid-inclusion studies, and geologic setting strongly suggest that the authigenic K-feldspar formed during the migration of basinal brines mobilized by orogenic activity and, thus, may provide useful information regarding the origin of nearby carbonate-hosted Pb-Zn mineralization.

The authigenic K-feldspar in these rocks occurs most conspicuously as overgrowths on detrital K-feldspar but is present in much larger quantities as a fine-grained matrix, which apparently is derived from the metasomatism of precursor clay minerals. Even assuming extensive volume reduction by compaction, mass-balance calculations indicate that the authigenic K-feldspar could not have formed by the diagenetic redistribution of components in an initial volume of sediment and pore water, but must have involved the movement of multiple pore volumes of fluid through these rocks. For four K-feldspar separates from Cambrian rocks in the central and southern Appalachians, synthetic $^{40}Ar/^{39}Ar$ age spectra of authigenic K-feldspar overgrowths (made by subtracting a spectrum of detrital cores with overgrowths from a spectrum of cores chemically stripped of their overgrowths) yield Late Carboniferous to Early Permian ages (278–322 Ma). A single K-feldspar separate from the Bonneterre Dolomite (southeastern Missouri) also yields a late Paleozoic age (300 Ma). Fluid inclusions in quartz and K-feldspar overgrowths on detrital grains in unmineralized rocks from the central and southern Appalachians have homogenization temperatures from 100 to 200°C and freezing-point depressions from –14 to –18.5°C (18–21 weight percent NaCl equivalent). The similarity of these fluid inclusions to those in nearby Mississippi Valley-type (MVT) ore deposits (Mascot-Jefferson City, Austinville-Ivanhoe, Friedensville) suggests that the authigenic K-feldspar and the ore deposits may be related genetically. This hypothesis is supported by the recent discovery of authigenic K-feldspar intergrown with sulfide minerals in siliceous zones of MVT ore deposits in eastern Tennessee (Mascot-Jefferson City) and eastern Pennsylvania (Friedensville), and at four smaller stratabound Pb-Zn deposits of indeterminate origin in New York, Vermont, and Quebec.

These findings agree with the conclusions of other workers that MVT mineralization in the central and southern Appalachians and the midcontinent region is related to the movement of basinal brines mobilized during late Paleozoic deformation along the Ouachita-Appalachian fold belt. Also, the apparent stability of K-feldspar in these ore fluids supports the contention that such fluids were not strongly acidic and implies that the metasomatism of clays may have been a more important source of metals than the dissolution of detrital K-feldspar.

The results of this work suggest that the association of authigenic K-feldspar with sediment-hosted ore deposits may be more common than had been realized. Accordingly, this mineral phase promises to provide useful information regarding the time of migration and the chemical evolution of ore-forming fluids in a variety of geologic environments.

Composition and Distribution of Cobalt-Rich Ferromanganese Crusts From the Pacific

James R. Hein, Lisa A. Morgenson, Charlaine Fleishman, William C. Schwab, and David A. Clague

We compiled data from the published literature and from unpublished U.S. Geological Survey files on the chemistry and distribution of Co-rich ferromanganese crusts in the Pacific. The U.S. Geological Survey collected samples from the Exclusive Economic Zone of the Hawaiian, Johnston, Palmyra, and Marshall Islands, as well as from the Gulf of Alaska Seamount province and the Lau Basin–Tonga Ridge area (table 1).

Ferromanganese crusts coat most hard substrates on the flanks of seamounts, ridges, and plateaus. Crusts commonly average 2–4 cm in thickness, are laminated, and may have well-defined outer and inner layers separated by a paper-thin layer of phosphorite. Growth rates vary between 2.5 and 5 mm/m.y. Crusts generally are significantly younger than the substrates upon which they rest because the flanks of the seamounts and the ridges do not provide a mechanically stable environment

Table 1. Average chemical composition for various elements of crusts from water depths less than 2,500 m from the Exclusive Economic Zone of the United States and other Pacific nations

[All data are in weight percent. n, number of analyses for various elements. –, no data.]

Areas	n	Mn	Fe	Co	Ni	Cu	Pb	Ti	SiO_2	P_2O_5	Fe/Mn
Hawaii and Midway (on axis)	2–38	24	16	0.91	0.45	0.05	–	1.1	7.9	–	0.73
Hawaii and Midway (off axis)	4–15	21	18	.60	.37	.10	0.18	1.3	16	1.0	.88
Johnston Island	12–40	22	17	.70	.43	.11	.17	1.3	12	1.2	.81
Palmyra Atoll-Kingman Reef	7–8	27	16	1.1	.51	.06	.17	1.1	5.5	1.9	.61
Howland-Baker Islands[1]	3	29	18	.99	.63	.08	.14	1.2	6.2	1.7	.64
Marshall Islands	55–63	21	13	.74	.45	.08	.14	.9	4.4	1.5	.61
Average central Pacific crusts	34–167	22	15	.78	.44	.08	.16	1.1	6.3	1.5	.71
Northern Mariana Islands (and Guam)	6–7	12	16	.09	.13	.05	.07	–	–	–	1.41
Western U.S. borderland	2–5	19	16	.30	.30	.04	.15	.31	17	–	.95
Gulf of Alaska Seamount Provinces	3–6	26	18	.47	.44	.15	.17	.57	–	.98	.72
Lau Basin (hydrothermal)	2	46	.60	.007	.005	.02	.006	.005	–	.05	.01
Tonga Ridge and Lau Basin (hydrogenous)	6–9	16	20	.33	.22	.05	.16	1.0	–	1.0	1.26
South China Sea[2]	14	13	13	.13	.34	.04	.08	–	14	–	1.07
Bonin Island area (Japan)	1–10	21	13	.41	.55	.06	.12	.67	4.9	.82	.70
French Polynesia	2–9	23	12	1.2	.60	.11	.26	1.0	6.5	.34	.56
Average for Pacific hydrogenous crusts, all data	56–319	22	15	.63	.44	.08	.16	.98	11	1.1	.81

[1]Data provided by P. Halbach, Technical University of Clausthal.
[2]Data provided by H. R Kudrass, Bundesanstalt fur Geowissenschaften und Rohstoffe.

for crust growth. Talus is coated with crusts about one-half as thick as crusts on rocks recovered from nearby outcrops.

Cobalt contents of up to 2.5 weight percent have been measured, but average contents range up to 1.1 percent. In addition, crusts are rich in Pt (to 1.3 ppm), Ni (to 1.0 percent), and Pb, Ti, and Ce. Crusts are composed predominantly of δ-MnO_2 and $FeOOH||\cdot H_2O$. Co, Ni, Pb, Pt, Ce, As, Mo, Cd, and Zn are correlated positively with the Mn phase, and Cu and Be, with the Fe phase. Fe, Cu, Be, K, Ce, Al, Ti, Si, and Ba increase in crusts with increasing depth of water, whereas Mn, Co, Ni, Pb, Mo, Cd, As, and Sr show the inverse relation. Many of these elements also show regional variations, including apparent changes with latitude.

The metals in the crusts are derived from seawater. Once the first layer of ferromanganese oxide is deposited, the addition of metals to the oxide surface becomes autocatalytic. The relative amounts of oxide phases in the crusts may be determined by their ratios in colloidal flocs in the surrounding seawater. The crusts rich in the strategic and economically important metals Co, Ni, Mn, and Pt occur in water depths of less than 2,500 m and lie beneath the O-minimum zone where the Fe:Mn is small. Co and other metals are fixed in the crusts

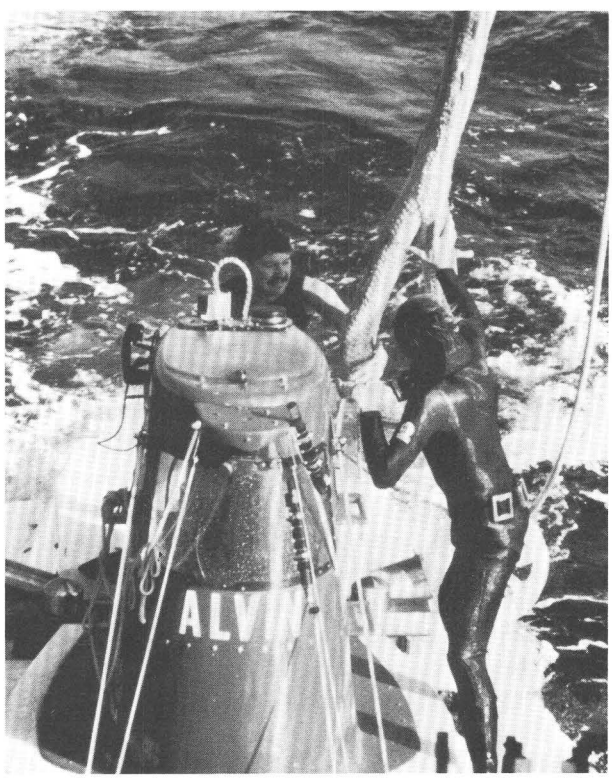

Crew members securing lines on the submersible vessel *Alvin* after it surfaced following a U.S. Geological Survey research dive on the metal-sulfide deposits of the Juan de Fuca Ridge near Washington.

by lattice substitution for Mn^{4+} in the MnO_2 or by coprecipitation of Co oxide with Mn oxide.

Important criteria that may characterize areas of thick Co-rich crusts include volcanoes and ridges shallower than 1,500–1,000 m, substrates older than about 20 Ma, areas of strong current activity, volcanic structures not capped by large modern atolls or reefs, a shallow and well-developed O-minimum zone, and slope stability and absence of local volcanism.

Based on these criteria and high concentrations of Co, Ni, and Pt, areas of high economic potential can be outlined and include the Kiribati, Marshall, and Micronesia Island groups and Johnston and Kingman-Palmyra Islands. Seamounts in the continental borderlands and island arcs of the south and west Pacific have lower potential for Co-rich crusts.

Sulfide Solubilities in Buffered Systems at Elevated Pressures and Temperatures and Their Depositional Implications

J. J. Hemley, G. L. Cygan, and W. M. d'Angelo

Experimental studies have been conducted on the solubility of Fe, Zn, Pb, and Cu sulfides in chloride solutions at elevated pressures and temperatures. The solutions were buffered in pH by quartz monzonite (that is, the assemblage K-feldspar–muscovite-quartz) and in O and S activities by assemblages in the Fe-S-O or Fe-Cu-S-O systems. Most experimentation was on the pyrite-pyrrhotite-magnetite buffer point. Temperature ranged from 300 to 700°C, and pressure, from 0.5 to 2 kb.

As expected, temperature and total chloride exhibit strong control on solubility, but total pressure proves to be of equal importance. At 400, 500, and 600°C, Fe solubilities in a system at 1 kb total pressure and 1 m Cl and on the pyrrhotite-pyrite-magnetite point were 1,000,150, 7,000,700, and 12,4001,000 ppm, respectively. At 500°C, 1 kb, and 2 m Cl, Fe was increased to about 20,000 ppm. At 500°C, 1 kb, 1 m Cl, and with sphalerite and galena also present, Zn and Pb solubilities were 2,300 and 2,600 ppm, respectively, and Fe was reduced to 4,200 ppm. For the same system at 0.5 kb, Fe, Zn, and Pb values were increased to 8,500, 4,300, and 8,700 ppm, respectively, and, at 2 kb, they were decreased to 1,700, 800, and 1,200 ppm, respectively. Mo and Ag sulfides were also present in some of the runs, but concentrations were typically low, on the order of 10–100 ppm.

Although the solubility characteristics of only Fe, Zn, Pb, and Cu were dealt with to date in our study, the experimental results appear to have important applications to ore genesis in general. The changes with pressure are particularly important to ore-mineral transport. Metals could be transported without deposition over long distances on a decreasing pressure gradient so long as the decrease in temperature was not sufficient to significantly offset the pressure effect. Such a control would be approximated by a near-adiabatic cooling path, a condition probably fairly common geologically, especially in the more deep-seated hydrothermal systems. Deposition then could occur by way of several possible physical-chemical changes, such as an increase in pH, dilution of a brine, or a more extreme and abrupt drop in pressure or temperature. Competition between Fe and other base metals for chloride ligands is also important. On passing through Fe sulfide or Fe oxide-bearing rocks, mineralizing solutions carrying relatively high base metals and low Fe would dissolve Fe and deposit base metals, which would produce sulfide replacement and zoning relations that are characteristics of many sulfide ore bodies.

The data also bear on the problem of original dissolution and entrainment of metals into the mineralizing fluid. In the adiabatic decompression path described, extensive leaching tends to occur in the beginning portion of the path; that is, close to the intrusive heat source. Maximum acquisition of metals, therefore, would tend to occur in a diffuse root zone of metasomatism well removed from the ore-body site, with maximum deposition high in the system where major perturbations in temperature, pressure, and chemistry are more likely to develop. The relative importance of orthomagmatic processes versus leaching at a heat source by externally derived fluids as the source of metals is yet to be established for most hydrothermal deposit types, but the processes delineated by the study apply regardless of the ultimate source of fluids or metals.

Petrogenesis of Gabbronorite at Yakobi and Northwest Chichagof Islands, Alaska

Glen R. Himmelberg,[1] Robert A. Loney, and Peter I. Nabelek[2]

On Yakobi Island and at Mirror Harbor on the northwestern coast of Chichagof Island, gabbronorite

[1]U.S. Geological Survey and Department of Geology, University of Missouri, Columbia, MO.
[2]Department of Geology, University of Missouri, Columbia, MO.

occurs as irregular bodies, as much as 5.5 km in maximum dimension, mostly within a 40- to 43-Ma composite pluton consisting largely of tonalite. The gabbronorite is the host rock for a magmatic Ni-Cu sulfide deposit consisting dominantly of pyrrhotite, pentlandite, and chalcopyrite. The gabbronorite characteristically contains more orthopyroxene than augite, as well as a significant amount of hornblende. Rock types mapped as gabbronorite range from hornblende pyroxenite, through hornblende-pyroxene gabbronorite, to quartz-bearing norite and gabbronorite. The tonalite pluton is composed of hornblende diorite, biotite-hornblende diorite, hornblende-quartz diorite, biotite-hornblende tonalite, and biotite granodiorite. Contacts between the types of gabbronorite are generally gradational on a scale of centimeters to meters, and those contacts between the gabbronorite and the tonalite pluton are gradational on a scale of meters to tens of meters. Rock textures, pyroxene-hornblende relations, and rock and mineral chemistry of the gabbronorite change systematically as the gabbronorite grades into the tonalite. The field, petrographic, and chemical data, including trace element abundances, of the gabbronoritic and tonalitic plutonic rocks can best be explained either by crystallization of gabbronorite from a tholeiitic magma with subsequent assimilation of tonalite that was simultaneously undergoing fractional crystallization or by fractional crystallization of a quartz diorite parent magma, which yielded the range of gabbronoritic and tonalitic plutonic rocks.

Regional Structure and Distribution of Hydrothermal Activity Within Escanaba Trough, Southern Gorda Ridge

Mark L. Holmes and Janet L. Morton

The Gorda Ridge is a 300-km-long segment of the Pacific midocean ridge system located 250 km off the coast of northern California and southern Oregon. It is bounded on the north by the Blanco Fracture Zone and on the south by the Mendocino Ridge. This slow- to medium-spreading rate axis exhibits numerous morphological similarities to the slow-spreading mid-Atlantic Ridge and is unique in this respect among Pacific ridge crests. The axis of the Gorda Ridge is characterized by a deep (3,200–3,800 m) axial valley flanked by steep ridges rising to depths of 2,000–2,500 m. The ridge is divided into three segments by right lateral offsets at lat 41°37′ N. and lat 42°26′ N.

Escanaba Trough, which is the southernmost ridge segment, contains more than 500 m of Pleistocene turbidite and hemipelagic sediment derived primarily from the Gorda Fan. Seismic reflection studies conducted in September 1985 delineated at least five discrete volcanic centers (3–6 km in diameter and spaced along the trough axis at intervals of 15–20 km) that dome and pierce the sediment fill of Escanaba Trough. On GLORIA long-range side-scan imagery, these volcanic edifices appear as approximately circular areas of higher seafloor reflectivity. Heat-flow values exceeding 1,200 mW/m^2 were measured over two of these intrusion zones. Dredge hauls and camera tows over two of these intrusive bodies at lat 40°45′ N. and lat 41° N. recovered or photographed mudstone slabs, fresh basaltic glass, and many occurrences of polymetallic sulfide consisting of pyrrhotite, marcasite, sphalerite, galena, chalcopyrite, and barite. The hydrothermal activity appears to be confined to the axial parts of the central graben in the vicinity of the the volcanic intrusive centers.

Geophysical Studies in the Vicinity of the Getchell Fault System, Humboldt County, Nevada

D. B. Hoover, B. D. Smith, V. J. S. Grauch, and M. Podwysocki

Interdisciplinary geophysical studies from regional to mine scale have been conducted along the Getchell trend of bulk-minable, disseminated Au deposits. This trend is defined by the Chimney, Getchell, Pinson, and Preble Au deposits, which generally are alined northeasterly for 20 mi along the eastern side of the Osgood Mountains, Humboldt County, NV. These deposits, related directly to the Getchell and associated faults, are presumed to have a common genesis. The Getchell trend and its Au deposits have been studied using gravity, magnetic, electromagnetic, induced polarization, radiometric, and remote sensing methods.

Regional gravity and aeromagnetic data have been useful for identifying the area's major lithologic units and structures, some of which may indicate features associated with the genesis of the Au deposits. Cretaceous granodiorite of the Osgood Mountains pluton is well defined by a regional north-south aeromagnetic high. There are also northwest magnetic trends within the pluton. Detailed ground magnetic surveys show local magnetic highs associated with Cretaceous dikes and with skarns developed at the contact between the pluton

and Paleozoic carbonate rocks. Regional gravity data define a northeast-trending high coincident with the Getchell Au trend that possibly reflects a deep crustal feature.

Shallow and deep penetrating electromagnetic methods have been used to map conductive features in the Getchell trend. Near-surface conductive fault zones have been detected by Slingram and very low frequency methods. The deeper conductive expression of the Getchell fault system has been detected in 12 traverses using telluric profiling data supplemented with audiomagnetotelluric sounding data. A previously unknown fault zone under alluvial cover east of the main Getchell fault was discovered using the telluric method.

Characterization of the electrical properties of rocks within the Getchell and Pinson areas has begun using spectral induced polarization methods. Results of in-situ and laboratory measurements indicate that the electrical signatures of mineralized rocks containing remobilized carbonaceous material are different from the signatures of unmineralized carbonaceous metasediments. Laboratory spectral reflectance measurements suggest that montmorillonite within the mineralized rock may be one source of the differences in electrical properties. These variations in electrical properties imply that complex resistivity surveys may be useful in detecting deposits within the Getchell trend.

Ground radiometric measurements were evaluated for applicability to exploration because reported K metasomatism associated with disseminated Au deposits could cause radiometric anomalies. The C-rich zones of the Getchall fault are distinctly higher in U and K than the host carbonates. However, wind-blown detritus from the granodiorite obscures radiometric signatures in routine ground surveys. On the other hand, detailed surveys in open pits indicate that mine and borehole radiometric measurements may be practical in deposit evaluation.

Remote sensing methods have been used to characterize various silica-bearing rocks, some of which are associated with disseminated Au deposits. Jasperoid replacements in carbonate rocks exhibit anomalous midinfrared reflectance spectra. X-ray analysis of these jasperoids shows that they are composed almost exclusively of quartz; however, they lack a characteristic double reflectance signature expected for quartz. The difference may be due to poor crystallinity of silica. With further study, jasperoids possibly might be detected unambiguously by midinfrared remote sensing methods. Identification of different silica-bearing rocks may lead to a rapid, cost-effective exploration tool for Au deposits.

Very Low Frequency Aerial Surveys Applied to Regional Mineral Assessment

Robert Horton and Carl Long

Combined aeromagnetic and very low frequency (VLF) aerial measurements were made as part of two U.S. Geological Survey Conterminous United States Mineral Assessment Program (CUSMAP) projects. The surveys, conducted from 1983 to 1986, include portions of the Glens Falls (Vermont and New Hampshire) and International Falls–Roseau (Minnesota) CUSMAPs. The aerial VLF method is an electromagnetic technique that responds to the electrical conductivity of near-surface geologic features; it is useful in mapping bedrock conductors, such as black slates, and in locating areas where conductive glacial overburden is thin or absent. In these two surveys, the primary objective of the VLF measurements was to contribute new structural, lithologic, and glacial deposit information that cannot be obtained from magnetic measurements.

The VLF technique is based on measurement of the local electric and magnetic fields of a vertical polarized groundwave transmitted at 20–25 kHz by one of several VLF communication transmitters located worldwide. The Geological Survey's VLF aerial system measures the in-phase and quadrature parts of three components of the magnetic field and the quadrature part of the horizontal electrical field using the vertical electric field as a reference. Anomalies observed in the in-phase and quadrature parts of the magnetic field indicate lateral changes in conductivity. By assuming that the ground is homogeneous, the inverse of conductivity, "apparent resistivity," may be calculated from the horizontal electric field.

The eastern one-half of the Glens Falls CUSMAP was surveyed with an 800-m flight line spacing. In general, the geology of the area is comprised of a thick series of steeply dipping Paleozoic metasediments interspersed with volcanic and small igneous intrusive rocks. The VLF data show asymmetric and symmetric anomalies in the magnetic field that are continuous across several flight lines, which indicate conductive lithologic boundaries and structural features. Ground follow-up investigations identified conductive carbonaceous, graphitic, and sulfide zones that are coincident with the VLF aerial magnetic anomalies. Several of the conductive anomaly locations identified by this VLF survey suggest favorable ground for the occurrence of massive sulfide deposits. Some high-resistivity anomalies

observed in the electric field data correlate with known intrusive units. Mineral deposits associated with intrusive bodies may occur in these resistive terrains.

The western one-half of the International Falls and the eastern one-half of the Roseau CUSMAPs were surveyed with a 400-m flight line spacing. Here Precambrian bedrock terrain is covered partially by glacial overburden that makes geologic mapping dependent upon sparse outcrops and exploration drilling. The glacial tills contain conductive lake sediments that inhibit VLF mapping of buried bedrock features. However, the calculated apparent resistivity is useful in identifying areas with thin or no glacial cover. Low-resistivity background levels (<100 ohm-m) generally were produced by the glacial overburden. High-resistivity anomalies (>1,000 ohm-m) usually correlate with high topographic areas that may contain outcrops or very thin overburden. However, high topographic areas that reflect low resistivities are caused by glacial moraines, filled valleys within bedrock outcrops, and possibly near-surface bedrock conductors. Low topographic areas that reflect high resistivities are caused by bedrock outcrops that have little or no surface expression or possibly sand and gravel deposits. The Minnesota VLF survey has identified possible sand and gravel deposits, new outcrops, and near-surface bedrock drilling targets that will benefit geologic mapping in the area.

Bentonite Resources, Cation-Exchange Capacity, Mineralogy, and Uses

John W. Hosterman

Bentonite is defined as any material composed chiefly of the clay mineral, smectite, and whose physical properties are controlled by it. Fuller's earth is defined as any naturally occurring material that has a high absorptive capacity for liquids or gases. Most fuller's earth is produced from palygorskite and from bentonite. Ground silica, diatomaceous earth, talc, pyrophyllite, and kaolinite also are used to make fuller's earth, but they are not included here.

The wide variety of physical properties of bentonite makes it suitable for many commercial utilizations and applications. The unique properties of bentonite make it an excellent ingredient in drilling muds where freshwater is present. Large amounts of bentonite are processed for bonding and pelletizing. The Na-bentonite is a swelling variety that is used for bonding foundry sand and pelletizing taconite iron ores. The Ca-bentonite is a nonswelling variety that is used in bonding foundry sand where a high green strength is required. Other utilizations of bentonite include adhesives, animal feed, clarifying oils, fertilizer and pesticide carrier, sealer, and waste disposal.

Most of the present commercial deposits of bentonite are from geologic units that are of Cretaceous or Tertiary age. The best grade Na-bentonite occurs in the Mowry Shale of Cretaceous age in Wyoming and Montana. The most abundant Ca-bentonite deposits are found in the Jackson and Claiborne Groups of Eocene age in Texas. No deposits of commercial bentonite have been found in rocks older than Mesozoic, and only one deposit of bentonite at Ash Meadows, NV, is believed to be Pleistocene in age.

Bentonite production in the United States was 2.9 million short tons in 1983. This is a major decrease from a production peak of 4.9 million short tons in 1981; 65 percent of the bentonite production came from Wyoming, and the balance of the production came from nine other States. The resources of all grades of bentonite in the United States are undoubtedly large. Probably 800 million tons of bentonite are in Wyoming, Montana, and Texas. However, because of the continuous demand for Na-bentonite over the last 75 yr, resources of this grade are rapidly declining.

Mineral-Resource Assessment of the Baird Mountains Quadrangle, Western Brooks Range, Alaska

Susan M. Karl, Jeanine M. Schmidt, Peter Folger, Bill Thompson, Carl Long, Richard Goldfarb, and Inyo Ellersieck

Studies conducted for the Alaska Mineral Resource Assessment Program in the Baird Mountians quadrangle in northwestern Alaska included reconnaissance and local detailed geologic mapping, systematic rock, stream sediment, and heavy-mineral concentrate geochemical sampling and subsequent statistical analysis, detailed investigations of known and newly discovered mineral occurrences, and synthesis of geologic and geochemical data with regional gravity and aeromagnetic data. Additional techniques applied to resource evaluation undertaken during this study included analyzing insoluble residues from carbonate rocks and stream sediments from carbonate-dominated catchment basins and audiomagnetotelluric (AMT) profiling in tundra-covered terrain.

The rocks in the Baird Mountains quadrangle, structurally complicated by regional folding and

thrusting, consist mainly of Paleozoic marine carbonate, pelitic, and clastic rocks with minor amounts of nonmarine clastic rocks. Mafic and felsic volcanic and volcaniclastic rocks are intercalated locally with the Paleozoic sequences. Mesozoic marine sedimentary and mafic volcanic rocks overlie the Paleozoic rocks in the northwestern part of the quadrangle. Mixed metamorphic rocks and intermediate intrusive rocks of Precambrian age are tectonically interleaved with Paleozoic sedimentary and volcanic rocks in the northeastern part of the quadrangle. Polymetamorphosed pelitic schists dominate the southern part of the quadrangle.

Previously known mineral occurrences in the Baird Mountains quadrangle include the carbonate-hosted Omar Cu prospect, the Frost Pb-Zn-Ba occurrence, and placer Au from the Timber Creek-Klery Creek area. During the course of this study, two new mineral occurrences were discovered—the Ahua, in the Kilyaktalik Peaks area, which consists of Ag mineralization hosted in silica-pyrite altered carbonaceous black shales, and the Powdermilk, in the Omar River area, which consists of stratabound Zn-Pb sulfide mineralization in bedded dolostones of possible Ordovician age.

Profiles from modeled AMT data identified major structures and lithologic trends in poorly exposed areas and in the subsurface. Low resistivities in the Kilyaktalik Peaks area indicate potential for mineralization.

Analyses of insoluble residues recovered from acid leaching of stream sediments broadened dispersion halos for base-metal elements in carbonate rocks by enhancing geochemical anomalies without affecting background concentrations and may prove to be an important exploration tool in areas of the Brooks Range underlain by carbonate rocks.

Seven potential resource areas were defined by stream sediment values, bedrock geochemistry, and interpretation of R-mode factor analysis of heavy-mineral concentrate data—the Agashoshok-Eli River area with high Ag-Pb-Zn values (clastic rocks) and high Fe-Co-Cu-Ni values (carbonate and mafic rocks), the Squirrel and Omar Rivers area with high Ag, Pb, Zn, and Mo values (carbonate rocks), the Nakolikurok Creek area with high Fe-Co-Cu-Ni-Mn values (mixed carbonate and clastic rocks), the upper Tukpahlearik and Anaktok Creek area with high Fe-Co-Ni-Cu-Mo-Ag-Mn values (mixed metapelitic rocks, carbonate rocks, and carbonaceous slates), the Kilyaktalik Peaks area with very high values in Ag-Pb-Zn-Ba-Mo (carbonaceous shale, pelitic, and mixed clastic rocks), the Nanielik Creek area with high Ag and base-metal values (pelitic, clastic, volcanic, carbonaceous, and carbonate rocks), and, finally, concentrate samples containing abundant scheelite plus occasional Au and (or) Ag may extend the known Klery Creek placer resource roughly 30 km to the northeast.

Effect of Topography on Gas Flow in Unsaturated Fractured Rock—Numerical Simulation

K. L. Kipp, Jr.

Air flow in certain bore holes open to the unsaturated zone at Yucca Mountain, NV, cannot be accounted for completely by diurnal barometric pressure variations. This observation led to the hypothesis of thermally driven air circulation within the mountain that is affected by the topographic relief. An idealized numerical model was formulated to test the hypothesis that the seasonal variation of air temperature at the mountain surface coupled with the topographic relief causes a natural periodic air circulation through the unsaturated zone in the mountain. The model was based on the solution of finite-difference approximations to the coupled equations of flow of air saturated with water vapor, transport of heat, and transport of a solute tracer. The coupling occurs through the density, viscosity, and interstitial velocity terms. The vapor-saturated air was treated as an ideal gas, and the presence of water vapor was accounted for by use of a virtual temperature. The mountain is comprised of porous- and fractured-rock layers with a soil layer at the land surface and was approximated by two zones of porous media, one representing the rock and the other representing the soil. The simulation region was a two-dimensional vertical slice of rectangular shape, representing a slice part way through the mountain. The boundary conditions used were as follows: (1) along the upper part of the left side and along the top (mountainside and crest), specified pressure and temperature based on atmospheric conditions, (2) along the lower part of left side (below the mountainside), zero air flux and zero heat flux, (3) along the bottom (below the mountain base), no air flux and specified geothermal-heat flux, and (4) along the right side (symmetry plane), zero air flux and zero heat flux. The solute tracer was introduced by a steady flux along the mountainside. The initial conditions were the result of a steady state simulation of typical spring conditions. Then, the temperatures and pressures at land surface were

varied seasonally. Simulations were advanced in time, until a periodic steady state was achieved for the air circulation and heat transport.

The resulting air-velocity fields, temperature fields, tracer-plume configurations, and boundary fluxes indicated that the seasonal temperature variation at the land surface coupled with the topography indeed can induce atmospheric circulation through the mountain. In summer, air enters the mountain along the crest and leaves along the lower one-half of the mountainside. In winter, flow is reversed, but with a slightly slower rate. The temperature field is affected by the seasonal variations within 20 m of the land surface. The solute-tracer plume responds to the air-circulation pattern most markedly within 40 m of the mountainside. In view of the feasibility of topographically affected air circulation through a mountain and the resulting potential for transport of consitituents in the vapor phase from within the mountain to the atmosphere, additional field and numerical simulation studies are in progress.

Mineralogy and Chemistry of Hydrothermal Sulfide and Petroleum Deposits From Escanaba Trough, Gorda Ridge

Randolph A. Koski, Robert A. Zierenberg, Keith A. Kvenvolden, and Wayne C. Shanks III

In 1986, surveys with a towed camera system and the deep-ocean submersible *Sea Cliff* revealed that small conical chimneys and low semicontinuous mounds are widespread over the sediment surface at the SESCA (lat 40°45′ N.; long 127°30′ W.) and NESCA (lat 41° N.; long 127°30′ W.) sites in Escanaba Trough on the southern Gorda Ridge. Although active venting has not been observed, the recovery of hydrothermal deposits by dredge and submersible indicate recent hydrothermal discharge onto the seafloor. Samples dredged from Escanaba Trough include texturally homogeneous pyrrhotite-rich massive sulfide with generally low base- and precious-metal content (Cu to 4 percent in some samples) and zoned polymetallic sulfide with high Zn (to 43 percent), Pb (to 8 percent), and Ag (to 700 ppm) contents. The massive sulfide samples consist predominantly of pyrrhotite, sphalerite, galena, barite, cubic cubanite, chalcopyrite, tetrahedrite, and loellingite. Minor phases, identified by scanning electron microscopy, include argentite and native bismuth. The association of loellingite ($FeAs_2$) and pyrrhotite indicates deposition from a metal-poor and sulfur-deficient fluid that percolated through the underlying sediment. Barite-rich crusts on some pyrrhotitic massive sulfide samples have high Zn (to 17 percent), Pb (to 4 percent), Ag (to 400 ppm), and Au (to 2 ppm). Massive talc deposits mantle some of the pyrrhotite-rich sulfide deposits at the SESCA site.

Subsurface fluid flow and deposition is indicated by sulfide veinlets and the presence of abundant disseminated chlorite, talc, pyrite, and chalcopyrite in sediment cores. Samples of sediment with interlayered sulfide and mudstone breccia enclosed in a pyrrhotite-rich sulfide matrix have been dredged from the SESCA site. An altered sediment sample with interstitial sulfide contains high Pb (13.7 percent), as well as high Zn (7 percent), and Ag (340 ppm). The abundance of Pb in Escanaba Trough samples implies extensive interaction between hydrothermal fluids and the sediment at depth.

A sample of sulfide-bearing turbiditic sediment also contains 5.6 percent interstitial asphaltic petroleum. This petroleum is composed of 44 percent polycyclic aromatic hydrocarbons, 2 percent aliphatic hydrocarbons, and 54 percent nonhydrocarbons. The extent of hydrocarbon aromatization and isomerization suggests rapid and intense thermal maturation due to interaction with hydrothermal fluid. Molecular markers, such as the dominance of odd-carbon-number alkanes, indicate that the petroleum source probably is continentally derived terrigenous plant matter in the Pleistocene and Holocene sediment that fills Escanaba Trough.

New Uses of Ammonium Minerals in Geochemistry

M. Dennis Krohn

The ammonium ion (NH_4) is known to replace K or other cations in several aluminosilicate and sulfate minerals, including feldspar (buddingtonite), mica (tobellite), illite, and jarosite. Recent discoveries have added ammonioalunite and ammonioleucite to the list of natural ammonium minerals. Previously, ammonium minerals could not be identified in the field because they have no diagnostic optical properties and generally are recognized in X-ray diffraction by slight shifts in peak intensity and position from K-bearing analogs. Recent work at the U.S. Geological Survey has shown that ammonium minerals have diagnostic spectral properties in the near-infrared wavelength

region and can be mapped readily in the field using ground-based or aerial sensors. Unlike chemical techniques, the specific mineralogy of the ammonium cation can be distinguished using the near-infrared spectral techniques.

Research is underway to determine whether ammonium minerals have sufficiently specific geochemical affinities to be useful as an indicator of paleogeochemical conditions. Ammonium minerals occur in several economically important geologic environments including disseminated Au deposits, Hg-bearing hot springs deposits, sedimentary exhalative Pb-Zn-Ag deposits, oil shales, and anthracite coal beds. Based on field studies, the present working hypothesis is that the formation of ammonium minerals indicates the interaction of hydrothermal fluids and brines with organic matter within a restricted range of acidity and redox conditions. Such a hypothesis may be considered as a type of organic aureole. Near-infrared reflectance techniques have been particularly successful in identifying ammonium-bearing minerals at hot springs deposits; such minerals generally show an enrichment of 10–100 times background values for ammonium. Distribution of ammonium-bearing minerals at these sites appears to be concentrated along fracture surfaces within hydrothermally altered rocks, which suggests some type of localization by hydrothermal fluids. The presence of pitted ammonio-alunite crystals and euhedral buddingtonite crystals at one site suggests at least two stages of crystallization.

Several factors must be considered in applications using ammonium minerals. Lack of a host cation site for substitution limits the potential rock types where ammonium minerals can occur. Common minerals such as quartz, kaolinite, and calcite have no substitution site and cannot be considered. Opaque minerals in the rock may quench the spectral features and reduce the near-infrared detectability of ammonium-bearing minerals. Although concern has been expressed that ammonium minerals are not theoretically stable in an oxidizing environment, near-infrared studies have documented clearly ammonium-bearing minerals at the surface in rocks of Tertiary age in semiarid to temperate climates. In summary, the demonstrated detectability and relative stability of ammonium-bearing minerals combined with their occurrence in several economically important ore

U.S. Geological Survey scientists performing induced polarization geophysical tests on sediment core (tube at left bottom) during a June 1985 cruise of the eastern U.S. seaboard.

U.S. Geological Survey mineralogist operating a calorimeter for measuring heat capacities of minerals at very low temperatures. These measurements are essential for calculating thermal stability of minerals of very high temperatures, thus increasing our understanding of how deposits of strategic minerals formed.

deposit settings suggest that detection of ammonium minerals should be included in appropriate geochemical exploration programs.

Ion-Exchange Fertilizer for the Utilization of Low-Grade Phosphate Ores

Tung-Ming Lai and Dennis D. Eberl

Nutrients are released to plants from phosphate rock when ammonium-saturated ion exchangers are present. The generalized reaction is

Phosphate rock + NH_4 exchanger
= Ca exchanger + NH_4^+ + $H_2PO_4^-$.

The ion exchanger is a sink for Ca ions, thereby decreasing Ca activity in the soil solution and permitting further dissolution of the phosphate rock. This system offers the possibility of using low-grade phosphate ore as fertilizer, particularly if an ion exchanger, such as smectite, is present in the ore and if the ion exchanger can be ammonium saturated. The system also makes N and Ca available to plants and can be regenerated by adding additional NH_4 exchanger to soil-phosphate rock mixtures or by resaturating the ion exchanger with NH_4^+. Only the NH_4 exchanger needs to be added to soils that already contain phosphate compounds; by this method, phosphate that has been fixed as apatite in soils by the reaction of soluble phosphate fertilizer with the soil can be made available for uptake by plants.

The rate of nutrient release can be adjusted by varying the ratio of exchanger to phosphate rock. Seedling uptake experiments indicate that the ion-exchange fertilization system surpasses a soluble P system in P uptake by barley after several cuttings from the same pots. Preliminary results from greenhouse pot trials using sudangrass indicate that dry yields from the ion-exchange system are larger than those from a soluble P system. A new method

that uses mixtures of OH- and H-saturated exchange resins has been developed for measuring P availability in soils that have been treated with the ion-exchange system.

Fertilization by ion exchange offers an alternative technology to the application of readily soluble and concentrated plant nutrients and may circumvent some of the problems associated with soluble fertilizers.

Quantitative Analysis of Fluid-Inclusion Gases—Applications to Studies of Ore Deposits

G. P. Landis, A. H. Hofstra, D. L. Leach, and R. O. Rye

Quantitative methods of fluid-inclusion gas analysis using a quadrupole mass spectrometer have been applied to the study of ores from the Coeur d'Alene district, Idaho; Mississippi Valley-type (MVT) deposits, Missouri, Arkansas, and Kansas; the Creede district, southern Colorado; and wood tin deposits, southern New Mexico. The chemistry of volatiles in ore and gangue mineral fluid inclusions helps characterize ore-forming fluids. Trends in volatile content and gas speciation, determined throughout the mineral parageneses, can be used to interpret the geochemical processes leading to ore formation.

Analyses are obtained from samples previously studied by fluid-inclusion petrographic and microthermometric methods and constrained by a geologic framework. While under vacuum, inclusion gases are released either by mechanical crushing of host material or by thermal decrepitation. Controlled thermal ramp heating coupled with real-time multiple ion monitoring are used to profile gas release as a function of temperature. These profiles define discrete fluid-inclusion populations that can be distinguished from adsorbed-desorbed gas release, "matrix" gas, and the thermal decomposition of host minerals. Matrix gas collectively refers to the following sites of gas entrapment in the host mineral: submicrometer-sized fluid inclusions, domain boundaries, microstructures, crystal defects, and gas dissolved in the crystal. Chemical reactions of gases due to heating are evaluated easily. Sharply defined spikes representing sudden release of gas from single or multiple fluid inclusions are superimposed upon the thermal profiles. Quantitative analysis of these "bursts" permits detailed study of ore fluid chemistry at the level of individual fluid inclusions. Analyses of gas mixtures from discrete fluid-inclusion populations tightly constrain ore genesis models.

Gas data are quantified from the partial pressure of each gas determined in the mass spectrometer and the pressure-volume-temperature relations of the gas mixture in the inlet system. The following parameters are applied for each gas in a M x N matrix solution: ionization fragmentation, gas sensitivity, and kinetic adsorption-desorption on vacuum surfaces. Rapid, highly sensitive, and precise analyses are possible with a minimum detectable partial pressure of 8×10^{-15} mbar, a partial pressure sensitivity of 8×10^{-9} (that is, 8 ppb), a maximum scan rate of 100 μs per atomic mass unit (AMU), over a range of 0–255 AMU, and an electrometer dynamic range of five orders of magnitude. All instrument control is enabled by assembly and FORTRAN codes on a PDP 11/73 computer with 4 MByte memory and 110 MByte Winchester disk capacity. Any gas species with major atomic mass unit peaks within the range of the instrument can be detected. The present system is calibrated for 32 primary gases and light hydrocarbons, including H_2O, CO_2, N_2, O_2, H_2, He, Ar, CH_4, H_2S, SO_2, N-O gases, NH^3, HF, and HCl, and common organics up to C_6. Total relative analytical precision of 1–3 percent is typical. A separate gas chromatograph-mass spectrometer is used to identify more complex organic spectra.

The following results are obtained from the above studies of ore systems: (1) Coeur d'Alene vein samples document the generation and evolution of ore fluids during metamorphism of the Belt basin. Fluid inclusions in Zn-rich veins contain greater concentrations of CH_4, short chain hydrocarbons, and N_2 than in younger Ag-rich veins in which CO_2 is dominant. Reduced fluids in Zn-rich veins probably were derived from devolitalization reactions of sediments containing organic matter and NH_4-bearing phyllosilicates. Changes in P-T, fO_2, and loss of volatiles by gas phase separation may have generated a more oxidized CO_2-rich fluid for the younger Ag veins. (2) The most abundant gases determined in samples from studied MVT's are CO_2, N_2, and CH_4. The hydrocarbon content of these fluids is low (<0.1 mole percent) and consists largely of CH_4 with traces of C_2H_6. Water- and CO_2-rich inclusions combine to yield bulk analyses of several mole percent CO_2. The CO_2-rich (>20 mole percent) individual inclusions represent a period of local CO_2 effervescence during host rock dissolution and sulfide deposition. The thermal maturity and low concentration of hydrocarbons together with the high CO_2 content suggest that these

ore-forming fluids are highly evolved basinal brines. (3) The gas studies of epithermal ores from the Creede district, combined with existing extensive detailed geologic and geochemical data, provide strong constraints on the sources of fluids and the role of mixing and boiling during ore deposition. The presence of variable amounts of organic gas species throughout the paragenesis points to a significant input from caldera moat sediments in the hydrothermal process. (4) The data from the Black Range tin occurrences confirm a magmatic origin for the ore fluids and permit study of the evolution of magmatic fluids during the period of ore deposition.

Genesis and Tectonic Setting of Volcanogenic Massive Sulfide Deposits, Eastern Alaska Range, Alaska

Ian M. Lange, Warren J. Nokleberg, John N. Aleinikoff, and Stanley E. Church

A belt of volcanogenic massive sulfide deposits and occurrences extends for over 200 km along the northern flank of the eastern Alaska Range. The deposits occur in the Jarvis Creek Glacier subterrane, which forms the southern margin, and in the highest structural level of the Devonian and Mississippian Yukon-Tanana terrane. The deposits and enclosing metavolcanic and metasedimentary schists exhibit two periods of regional metamorphism and penetrative deformation—an older amphibolite facies event and a younger lower greenschist facies event. From west to east, the major districts are at Hayes Glacier, McGinnis Glacier, and Robertson River.

The Hayes Glacier district contains the Miyaoka occurrence west of the glacier and several other occurrences east of the glacier. The occurrences strike west-northwest for about 10 km and consist of massive pyrite and pyrrhotite and minor chalcopyrite, sphalerite, and galena in south-dipping sulfide pods, lenses, and stringers that parallel the enclosing schists. Protoliths for the host rocks are mainly andesite and dacite tuffs and flows, shale, and marble, with lesser quartz-rich keratophyre flows and tuffs, volcanic graywacke, and siltstone. Selected samples contain up to 0.7 percent Pb, 0.5 percent Zn, 0.9 percent Cu, 0.5 percent As, 0.5 percent Sn, 0.2 ppm Au, and 10 ppm Ag.

To the east-southeast, the McGinnis Glacier district contains two occurrences about 1 km apart. The occurrences consist mainly of massive pyrite and pyrrhotite with lesser sphalerite, chalcopyrite, and galena in highly deformed lenses and pods. Protoliths for the host rocks are mainly andesite flows and tuffs, shale, marl, and marble. Selected samples contain up to 0.3 percent Pb, 2.3 percent Zn, 0.3 percent Cu, 0.1 ppm Au, and 50 ppm Ag.

Farther southeast, the Robertson River district contains about 10 or more occurrences in a 200-km^2 area. The occurrences consist of layers and zones of varying amounts of massive to disseminated pyrite, chalcopyrite, galena, sphalerite, and bornite. The layers and zones are generally conformable to layering in west-northwest-striking schists. Protoliths for the host rocks vary widely and include andesite, dacite, quartz keratophyre tuffs and flows, shale, quartzite, marl, and sparse marble. The occurrences are associated spatially with diorite or gabbro sills that exhibit only the younger lower greenschist facies metamorphism and deformation. Selected samples contain up to 1.5 percent Pb, 11 percent Zn, 1.3 percent Cu, 0.5 percent As, 6 ppm Au, and 300 ppm Ag.

Regionally, the sulfide occurrences are interpreted as Kuroko-type deposits that formed along the submarine volcanic part of a Devonian continental margin igneous arc. Deeper level portions of the arc are exposed in structurally lower levels of the Yukon-Tanana terrane to the north and contain Devonian to Mississippian metamorphosed granodiorite and

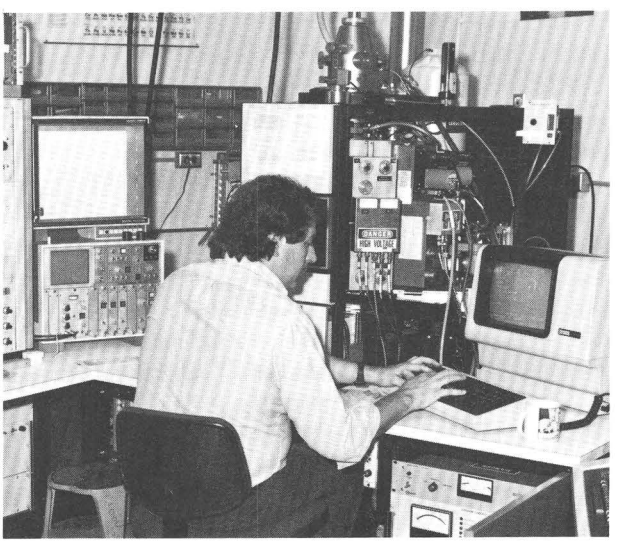

A U.S. Geological Survey geologist selecting analysis options of a cobalt-bearing mineral sample in this electron microprobe X-ray analyzer at the Survey laboratory in Reston, VA. Detailed quantitative studies of elemental composition of polished rock surfaces are performed with a resolution of 4 μm^2 (about 800,000 areas of that size would fit on a 2-mm-sized pinhead).

granite. U-Pb isotopic data on zircons from metavolcanic rocks hosting the sulfide occurrences indicate a 375-m.y. extrusive age. $^{207}Pb/^{204}Pb$ for sulfides from the three districts are similar and indicate Pb was derived, in part, from first cycle sediments eroded largely from Precambrian crystalline rocks. Radiogenic $^{207}Pb/^{204}Pb$ for feldspars in Devonian metavolcanic rocks are similar to those in sulfides and indicate incorporation of Precambrian (2.0–2.3 b.y., based on zircons) Pb into the Devonian magmas. A Precambrian crystalline source for quartz in metasedimentary rocks is indicated by locally abundant quartzite containing 2.3-b.y. zircons. Pb isotope ratios from sulfides and igneous feldspars also suggest arc formation outside of Alaska. Intense Cretaceous greenschist facies metamorphism and penetrative deformation is indicated by reequilibration of U-Pb isotopic ratios and by metamorphic K-Ar hornblende, biotite, and muscovite ages of 110–115 m.y. The Cretaceous metamorphism and deformation is interpreted as representing the tectonic emplacement of the Yukon-Tanana terrane into proto-Alaska.

A Worldwide Paleoclimatic Model for Quaternary Shoreline Placer Deposits of Titanium Minerals

Curtis E. Larsen and Eric R. Force

Titanium is extracted from marine placer deposits dominated by the mineral suite ilmenite-rutile-zircon-monazite. The occurrence of this suite is dependent on a source terrane containing pelitic rocks of sillimanite or higher metamorphic grade. Through weathering and erosion, detrital grains of these heavy minerals are transported along fluvial systems to coastal regions. Wave action and longshore transport sort and concentrate them along active shorelines where they are deposited on the upper beach face by swash-backwash action. Later, heavy minerals may be moved inland by eolian transport to be stockpiled in coastal dunes.

A warm, humid climate enriches this suite, as weathering removes unstable minerals, disaggregates composite grains, and upgrades the TiO_2 content of ilmenite by leaching of Fe. Detrital mineral grains inherit weathering from the regolith and older sedimentary hosts, and the in-situ weathering of Quaternary shoreline deposits is an important factor in determining the economic suitability of ilmenite from coastal placers. This is shown by mineralogic zonation within single deposits and by variation among coastal deposits of different ages within a single area. Removal of Fe from $FeTiO_3$ through leaching reflects cumulative weathering of the placers. This, in turn, varies systematically with the age and latitude of the deposits in some well-known districts.

In the Southeastern United States, for example, the southernmost sands from the oldest Quaternary shoreline deposits are the most weathered. These display a low percentage of unstable heavy minerals and a higher TiO_2 content in altered ilmenite. The inverse condition holds for the southern hemisphere where the highest TiO_2 contents are found in the more northerly of the older deposits of western Australia. On a worldwide basis, climate zones presently found between 35° N. and 35° S. appear to have been the most efficient in producing mineral assemblages beneficiated through weathering processes. Favorable source areas and coastal placers of the key mineral suite are present outside this zone, but the most valuable Quaternary coastal placers have weathered mineral suites and occur only within these latitudes.

Source terrane determines the location of minerals of this suite, but the weathering history and latitudinal distribution define its economic significance. Thus, new resource areas may be highlighted along coastal zones with similar Quaternary sea-level histories and subtropical weathering regimes.

The eastern coasts of South Africa and Mozambique, including the Richards Bay deposits, are analogs within this model, as is the southern coast of Brazil. The eastern coast of equatorial Africa shows source terranes and climatic regimes that suggest a favorable economic potential; however, Mauritania, on the arid northwestern African coast, has proper source terranes but lacks subtropical weathering. Its economic potential is demonstrably lower. The worldwide distribution of Quaternary placers containing titanium minerals indicates that studies of paleoclimate and contemporaneous weathering may provide models for pre-Quaternary deposits as well.

Central San Juan Caldera Cluster, Colorado—New Stratigraphic and Structural Interpretations and Implications for Mineralization

P. W. Lipman, M. A. Lanphere, R. L. Reynolds, J. G. Rosenbaum, and D. A. Sawyer

In the 1950's, T. A. Steven and J. C. Ratte recognized calderas in the central San Juan Mountains of Colorado; known relations were summarized by

Steven and Lipman (1976). New stratigraphic, structural, and petrologic data, supplemented by $^{40}/^{39}$Ar dating and paleomagnetic data gathered in 1985–86 now require several important reinterpretations.

The outline and stratigraphy of the Bachelor caldera and related rocks have been refined (fig. 1); the caldera is more equant than previously recognized, and its core is farther south. A partly buried ridge of precaldera lavas, 20 km long, defines the composite west wall of the Bachelor and the LaGarita calderas. The northeastern topographic wall of the Bachelor caldera is defined by contacts between autochthonous Fish Canyon Tuff and rockslide debris of the same material. Other rocks, previously interpreted as lavas and ash-flow tuff interlayered with Bachelor caldera fill, are slide breccias from the caldera walls. Compositionally zoned Mammoth Mountain Tuff, previously considered to be a discrete ash-flow unit of uncertain source, is an upper part of the intracaldera Carpenter Ridge Tuff. The distribution of Mammoth Mountain indicates that early subsidence of the Bachelor caldera was greater near the margins than in the core, imparting a domical structure to the caldera floor during subsidence.

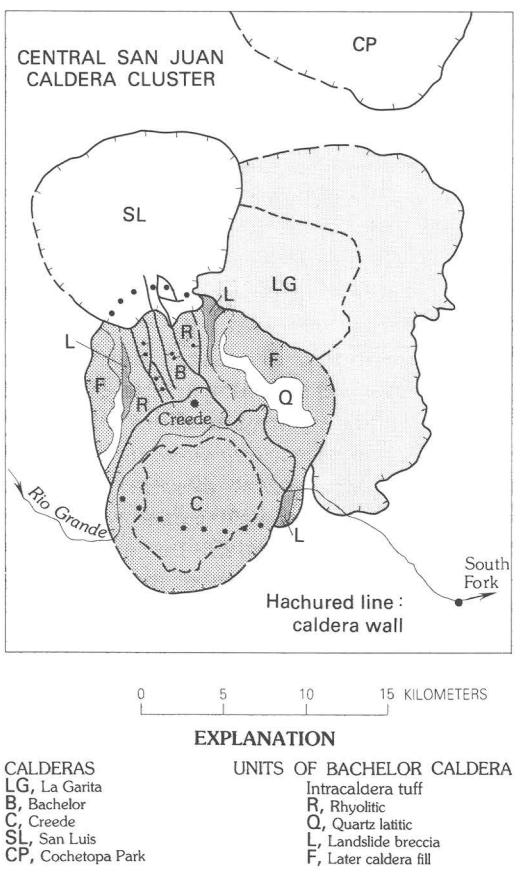

Figure 1. Geology of the central San Juan caldera cluster, showing details of the Bachelor caldera fill.

$^{40}/^{39}$Ar dating has been crucial in showing that the Creede caldera (26.5 Ma) predates the San Luis caldera (26.0 Ma) (table 1), reversing the previously interpreted age sequence based largely on the more eroded form of the San Luis caldera. The San Luis caldera is probably more eroded than the Creede caldera simply because it is topographically higher. Stratigraphic relations locally confirm this relation where tuffs from the San Luis caldera overlie ring-dome lavas (McKenzie Mountain flow) of the Creede caldera. Any tuffs from the San Luis caldera that once overlay sedimentary fill in the moat of the resurgent Creede caldera have been eroded completely.

Fill of the San Luis caldera (Nelson Mountain Tuff) includes, in addition to a thick upper quartz latite, collapse breccias interleaved with altered and mineralized rhyolitic tuffs that previously were correlated with texturally and compositionally similar Carpenter Ridge Tuff within the Bachelor caldera. Postsubsidence lavas near the San Luis caldera are the youngest in the region, some perhaps as young as mineralization in the Creede district (about 25 Ma). Some age and stratigraphic inconsistencies between the San Luis and the Cochetopa Park calderas require additional study.

These in-progress interpretations have far-reaching implications for the environment of associated ore deposition; for example, host rocks for precious-metal veins are not confined to fill of the Bachelor cadlera, as previously thought, but include fill of the younger San Luis caldera.

Table 1. Calderas and ash-flow units

Caldera	Tuff unit	Age (Ma)
San Luis	Nelson Mountain	25.9
	Rat Creek	26.1
Creede	Snowshoe Mountain	26.6
	Wason Park	26.8
Bachelor (includes Mammoth Mountain)	Carpenter Ridge	27.3
LaGarita	Fish Canyon	27.8

Reference Cited

Steven, T. A., and Lipman, P. W., 1976, Calderas of the San Juan volcanic field, southwestern Colorado: U.S. Geological Survey Professional Paper 958, 35 p.

Microbial Transformations of Iron Minerals

D. R. Lovley

Microbially catalyzed reduction of Fe(III) was studied in sediments and, under more controlled conditions, in cultures. When Fe(III) was in the form of amorphic Fe(III) oxyhydroxide, Fe(III)-reducing microorganisms could oxidize completely nonrecalcitrant organic matter to CO_2. These results demonstrated that the capacity for microorganisms to couple the oxidation of organic matter to Fe(III) reduction is much greater than generally considered. Fe(III)-reducing microorganisms in sediments and in culture readily reduced amorphic Fe(III) oxyhydroxide, even when the Fe(III) was adsorbed onto clay or when the Fe(III) was saturated with adsorbed organic matter or phosphate. Crystalline Fe(III) oxides were reduced slowly, if at all. Most of the Fe(III) in fresh and brackish water sediments was also resistant to microbial reduction. These results may explain the preservation of Fe(III) in many deposits. In cultures of Fe(III)-reducing organisms, the reduction of amorphic Fe(III) oxyhydroxide resulted in the production of magnetite and siderite. This is the first report of biological magnetite production under strict anaerobic conditions. Surprisingly, Fe(III)-reducing organisms were unable to further reduce magnetite. These results suggest a potential mechanism for the accumulation and persistance of magnetite in some mineral formations. Studies on the interactions between Fe(III) reduction and sulfate reduction demonstrated that, when reactive Fe(III) forms, such as amorphic Fe(III) oxyhydroxide, are available, Fe(III)-reducing organisms prevent sulfate reduction by outcompeting sulfate-reducing organisms for organic matter. This result suggests that chemical reduction of reactive Fe(III) by sulfide may not be an important mechanism in the formation of iron-sulfur minerals in sediments because sulfide is produced after the production of Fe(II). These studies have demonstrated how an understanding of the factors that control the rate and extent of microbial processes can aid in evaluating the factors that influence the formation and dissolution of minerals.

Steam emanating from a crack in the Main Terrace of the Steamboat Springs geothermal area near Reno, NV. This well-studied hot spring system contains significant concentrations of Au, Hg, As, Sb, Tl, and B.

Transport and Flood-Plain Storage of Metals Associated With Sediment Downstream From Lead, South Dakota

Donna C. Marron

Between 1880 and 1977, about 90 million metric tons of finely milled mine tailings containing arsenopyrite and other metallic sulfides were discharged into Whitewood Creek near Lead, SD. Overbank deposition and meander migration have caused much of the sediment to be stored in the flood plain and on terraces along Whitewood Creek and downstream along the Belle Fourche River. This stored sediment contains greater than background concentrations of a variety of metals, particularly arsenic.

The metal-contaminated sediments in the flood plains of Whitewood Creek and the Belle Fourche River contain as much as 0.6 percent arsenic; the arsenic concentrations of these sediments do not show a statistically significant decrease with increasing distance downstream from Lead. This lack of pattern apparently is caused by the overwhelming quantity of mine tailings that were discharged

into the stream system yearly in relation to the quantity of "clean" sediment that was available in the stream system to dilute the contaminated sediments. In contrast, arsenic concentrations of stream-bed sediments collected in Whitewood Creek and the Belle Fourche River in 1985, 8 yr after the cessation of mine-tailings discharge, decrease systematically with increasing distance downstream from Lead (K. E. Goddard, U.S. Geological Survey, written commun., 1986).

Metals analyses of different size fractions of contaminated flood-plain sediments show greater concentrations of metals in the finer sized fractions. In two samples from the flood plain of Whitewood Creek and two samples from the flood plain of the Belle Fourche River, arsenic concentrations in the greater than 64-μm fraction range from 60 to 95 percent of the arsenic concentrations of the 16- to 64-μm fraction and from 17 to 41 percent of the arsenic concentrations of the less than 4-μm fraction. Arsenic concentrations obtained by a partial digestion procedure that is not effective for sulfide minerals were more than 70 percent of the arsenic concentrations obtained by using a total digestion procedure for 13 flood-plain sediment samples for which both types of data were obtained. This result indicates that much of the arsenic that is presently (1986) in the contaminated flood-plain sediments no longer occurs in association with the primary sulfide minerals that were the original source of the arsenic.

Metal-contaminated sediment is stored in the flood plains of Whitewood Creek and the Belle Fourche River as point-bar deposits, overbank deposits, and deposits filling abandoned channels. Preliminary calculations of the quantity of metal-contaminated sediment stored on flood plains indicate that at least one-third of the mine tailings discharged into the river system presently are stored along about 120 km of the Belle Fourche River flood plain downstream of Lead. Measurements of meander-migration rates of channels in contaminated flood-plain areas indicate that the metal contaminated flood-plain deposits will continue to be a source of metals to adjacent streams for centuries.

PROSPECTOR II—Towards a Newer Geo-logic

Richard B. McCammon

One of the accomplishments of PROSPECTOR, a computer program developed in the mid–1970's, was to demonstrate the feasibility of encoding expert knowledge in a way that would allow nonexperts to evaluate the mineral potential of an area. In experiments, nonexperts using PROSPECTOR performed at or near the level of expert economic geologists. Despite this success, PROSPECTOR has had little use in mineral-resource studies; mainly, this failure is attributed to (1) the high cost of maintaining and providing easy access to a complex computer program, (2) the feeling that the system was vulnerable to misapplication in the hands of an inexperienced operator, (3) the limited number of models in its repertory, and (4) its inability to deal with spatial relations. PROSPECTOR II, patterned after INTERNIST I, is designed to overcome these problems.

The building block for PROSPECTOR II is the individual deposit model. For each model entered into the system, a model profile is constructed. The model profile consists of findings (observations), such as rock types, age, tectonic setting, mineralogy, alteration, and so forth, that have been reported to occur in association with known deposits considered to be instances of the model. Three variables are associated with each finding—an evoking strength, a frequency, and an import. The evoking strength answers the question, Given this finding, how strongly should I consider it to be specific to the ore-forming process attributed to the model? The frequency is an estimate of how often the finding is encountered in known deposits of the type represented by the model. The import, independent of the model, is the extent to which one is compelled to explain it at all. The evoking strengths, frequencies, and imports are expressed as numbers that represent a shorthand for judgmental information, inasmuch as the true quantitative information is unknown. Findings in the knowledge base are represented as numbers, such as age range; lists, such as mineralogy; or maps, such as anomaly patterns. In addition to model profiles, links between the models can be specified that express a predisposition of findings for one model with that of another.

Solving problems in PROSPECTOR II results primarily from the application of two heuristic principles—the generation of hypotheses through a partitioning algorithm and the formation of conclusions about hypotheses, using such strategies as reasoning by exclusion. Initial positive and negative findings are entered by the user. The program retrieves the complete differential diagnosis from the knowledge base. For each model hypothesis, the following lists are maintained: (1) all positive findings explained by the model, (2) findings that might be associated with a model but are absent in the

present instance, (3) findings not explained by the model, and (4) findings about which nothing is known in the present instance. A scoring system is used to rank the hypotheses in the differential diagnosis list. Hypotheses whose scores fall below a threshold number of points are discarded as unattractive. The sorted master differential diagnosis is used to identify a set of competitors to the topmost hypothesis. If no competitors are found, then the topmost hypothesis is accepted. Otherwise, a questioning strategy is pursued in an effort to "rule out" or "discriminate" among the set of competing hypotheses. Through questioning, a reduced set of plausible hypotheses and their relative scores are generated. The program recycles, all findings explained by the hypotheses being removed, and continues until all useful lines of questioning are exhausted. The interpretation based on all findings is presented to the user, along with an explanation of the line of reasoning that was followed. It is intended that PROSPECTOR II eventually will run on a microcomputer at the geologist's desk.

Mineral Resources Data System—New Techniques and Applications for Mineral-Resources Research

Antoinette L. Medlin, Donald F. Huber, Paul G. Schruben, George T. Mason, and Melissa L. Stoltz

Changes in computer hardware and software available to the national Mineral Resources Data System (MRDS) are being used to extend and improve its capabilities to respond to U.S. Geological Survey, Federal, State, and public inquiries. Software developments in the field of spatial data handling and display have led to the integration of what are called Geographic Information System (GIS) techniques. These techniques provide the capability for a GIS user to select, summarize, and display, as maps or tables, the information associated with line and point features from data bases of spatial and attribute information. Currently, MRDS consists of over 84,000 spatially located data records with attributes for mineral deposits and occurrences in the United States and many foreign countries.

In the past, a standard product from MRDS was a point location map with symbols representing a particular attribute from data records selected by user criteria. A current example of this type of map is the Glens Falls 1° x 2° study (Schruben and others, 1987).

Recent advancements in MRDS include developments in available data and software techniques. A number of files of digital line data for political, administrative, and geologic boundaries, all in geographic coordinates that can be displayed along with the point locations, have been acquired. MRDS has assembled information about these files into a data base, which provides an inventory of the currently available digital files, and has developed a plotting procedure for combining this data with MRDS data for GIS-like display or analysis. An option is also available for users to create their own digital line data files in the specified format and to plot them with MRDS data. Some of the available digital line files include national forest boundaries, wilderness boundaries, and the map by King and Beikman (1974). Examples of MRDS GIS-type applications have been prepared for Nevada, and commercially available GIS software is being tested.

The MRDS data bases have been converted to a modern relational data base management system (DBMS) to take advantage of current software features. A compatible DBMS, Revelation, is available commercially for microcomputers, and a micro-based version of MRDS, called MRDS-REV, has been developed to allow users to take advantage of the increased availability of personal computers. MRDS-REV has been used to enter and summarize the status of data available for areas in Alaska and Costa Rica.

References Cited

King, P. B., and Beikman, H. M., 1974, Geologic map of the United States: U.S. Geological Survey, scale 1:2,500,000.

Schruben, P. G., McBean, A., Nyahay, R. E., and Slack, J. F., in press, Mineral occurrences of the Glens Falls 1 x 2 degree quadrangle, New York, Vermont, and New Hampshire: U.S. Geological Survey Miscellaneous Investigations Series Map.

Inductively Coupled Plasma Mass Spectrometry—Applications of a New Technique in the Study of Mineral Formation Processes

Allen L. Meier and Frederick E. Lichte

Inductively coupled plasma mass spectrometry (ICP-MS) is a relatively new analytical technique that is extremely useful in studies of mineral formation processes. The high sensitivity and the low limits of detection (0.02–0.1 ng mL^{-1}) of this technique are

providing previously unobtainable information for the investigation of transport mechanisms and mobility of many elements in hydrothermal systems.

We are investigating the use of ICP-MS to analyze geological samples of diverse types for a variety of geochemical applications. The analysis of fluids extracted from inclusions in galena, sphalerite, and hydrothermal dolomite from the midcontinent provides new information about the movement of the fluids that deposited the Mississippi Valley-type deposits. Investigations of fluid and vapor transport and the partitioning of base and precious metals between liquid and vapor phases in hydrothermal systems are being aided by the speed this technique provides in determining trace elements in water at the parts per billion level and below. The migration of metals through glacial overburden is being examined by simultaneously measuring trace concentrations of 20 or more elements in selective extracts of soil and till samples. The mobility of U through organic-rich material is being investigated by analyzing pore water and extracts from humic acids to determine U at the parts per billion level. The ability of the ICP-MS technique to determine individual isotopes rapidly, without the need for chemical separation, is permitting greater application of isotope ratio methods. Pb isotope measurements from galena and Fe- and Mn-oxide coatings of sediments are being used to assign buried mineralization to specific episodes of known mineralization having isotopically distinct Pb isotope signatures. The sensitivity of this technique to determine the Pt-group elements in Au beads following fire assay is aiding in the exploration for and understanding of the geochemistry of these important metals. The application of the isotope-dilution technique for determining Os and Re in molybdenite makes this technique extremely useful for studies concerning the distribution and abundance of these elements. A method developed to determine the rare earth elements in rocks and minerals, without the need for separation or preconcentration, is allowing greater use of these elements in petrogenetic studies.

Nuclear Borehole Logging for Critical Metals

Jon Mikesell and Frank Senftle

In recent years, the United States has become increasingly dependent on foreign countries for its supply of critical metals such as Mn, V, and Cr. Recent political instability overseas is jeopardizing our supply of these elements, and new methods must be investigated that will increase our potential to explore for deposits of these metals and to measure their concentrations at depth.

One of the few techniques that is capable of this task within the narrow confines of a borehole is high-resolution gamma-ray spectroscopy. The U.S. Geological Survey has developed a borehole spectroscopy system that can be a valuable tool in exploration for critical metals; for example, quantitative logging for Mn in a borehole at about 0.5 cm/s has been tested down to concentrations of 0.2 percent Mn, and similar tests are currently in progress for V and Cr. An evaluation of the technique as applied to the other metals of possible strategic importance is considered. Thermal neutron activation and capture reactions are the only reactions that have sufficient sensitivity to be considered for exploration purposes. For the metals of industrial interest, the fast-neutron reaction cross sections are simply too small to yield the sensitivity needed for a practical exploration method using current state-of-the-art techniques.

An Expert System for Sedimentary Basin Analysis for Assessment of Mineral and Energy Resources

Betty M. Miller

Most of the world's energy resources and many of its metals and mineral resources are derived from sedimentary rocks within the framework of a sedimentary basin. The exploration and assessment of such resources requires an understanding of their relation to the host strata, whether they are primary or postdepositional deposits. The most important product resulting from a "basin analysis" is the documentation of the paleogeographic evolution of a sedimentary basin. Basin analysis requires an understanding of many diverse geological specialties and an ability to assess the relation between varied types of evidence.

The U.S. Geological Survey currently is involved in a research program to explore the feasibility of applying Expert Systems and knowledge acquisition techniques (specialties in the field of Artificial Intelligence) to the design and construction of a global system of sedimentary basin analysis. The first phase of a comprehensive expert systems approach includes the design and integration of regional geologic basin models and detailed basin analysis techniques into a computer system capable of incorporating large data files and graphic input

and output. This basin analysis program also will access an integrated computer satellite system that will provide a suite of resource-assessment methods used to estimate the remaining undiscovered resources of a variety of energy and mineral commodities whose origins are within sedimentary basins. The primary objective in this first phase of the investigation is to design for the microcomputer a prototype expert system for basin analysis that will enable the geologist to understand and reconstruct the geologic evolution of a sedimentary basin and ultimately to assess its energy and mineral resources.

The basic strategy uses expert systems techniques to design and develop a basin analysis program that will emphasize the evolution of a sedimentary basin through the documentation of its major components, as expressed by its stratigraphy, structural geology, and sedimentology. Previous work by the author on the design of sedimentary basin models, as a part of the muPETROL program (Miller, 1986) that uses expert systems techniques to classify world basins, is incorporated into the Basin Analysis Expert Systems Program (BA/ESP). The concepts used in muPETROL were the first phase toward analyzing the regional geologic framework and tectonic history which is preliminary to the detailed sedimentary basin analysis used in the BA/ESP program.

Special efforts are being directed in the design of BA/ESP toward utilizing the capabilities of an expert system to access (1) a variety of available computer data bases (that is, well data bases, stratigraphic data files, log files, and so forth) and (2) satellite computer systems that perform various integrated tasks for geological interpretation and quantitative assessment of energy and mineral resources, such as the frequently noted "play-analysis system."

The expert system, BA/ESP, will be used on an IBM-PC-XT/AT personal computer and run with the Knowledge Engineering System II, better known as the KESII expert systems program (by Software Architecture & Engineering, Inc.). This system would be available to the basin geologist who has access to a personal computer.

Reference Cited

Miller, B. M., 1986, Building an expert system helps classify sedimentary basins and assess petroleum resources: American Association of Petroleum Geologists, GEOBYTE, v. 1, no. 2, p. 44–50, 83–84.

National Geologic Mapping Program

F. K. Miller

The decline in geologic mapping and publication of geologic maps over the last two decades now is recognized widely in the geologic community. This increasing dearth of modern geologic maps has impacted the earth sciences and land use fields at all levels, but few areas as heavily as mineral-resource exploration and research. Geologic maps are a primary data source for nearly all exploration programs and mineral-resource-related research. The immediate availability of a modern geologic map saves time and money and can be a significant factor in the success or failure of a project.

To reverse the current decline in geologic mapping and to increase the rate of publication and versatility of geologic maps, the U.S. Geological Survey is establishing a vigorous National Geologic Mapping Program. The program is designed to rebuild the primary geologic map data base of the Nation and to supply pure and applied science researchers with basic geologic data. The program will increase new geologic mapping, provide a focal point to coordinate increased Federal, State, and academic mapping activities, and augment development of new mapping and publication technology. It will be conducted under four major components: Federal geologic mapping, Federal-State cooperative geologic mapping (COGEOMAP), geochronology and geologic processes, and modernizing mapping and map production technology. A fifth component, a university grants program, will be initiated when funds are available for this purpose.

Geology and Mineral Resources of the Iditarod Quadrangle, West-Central Alaska

Marti L. Miller and Thomas K. Bundtzen[1]

In 1984, the U.S. Geological Survey and the Alaska Division of Geological and Geophysical Surveys [now the Alaska Division of Mining and Geology (ADMG)] began a 4-yr joint project to assess the mineral resources of the Iditarod Quadrangle. The ADMG had been conducting 1:63,360-scale geologic mapping and prospect evaluations within the quadrangle since 1977. In 1984, the Geological Survey began work on a more regional scale, and the two agencies merged their studies under the Alaska Mineral Resources Assessment Program.

[1]State of Alaska, Division of Geology and Geophysics, Fairbanks, AK.

The Iditarod Quadrangle is largely underlain by interbedded sandstone, shale, and conglomerate of the late Early to Late Cretaceous Kuskokwim Group. These rocks form the core of the Kuskokwim Mountains, a dissected upland of accordant rounded ridges and broad sediment-filled lowlands. The Kuskokwim Group was deposited in a southwest-trending elongate basin. Deep water turbidite facies rocks dominate, but shallow shoreline facies rocks are also present.

Late Cretaceous-early Tertiary volcanoplutonic complexes intrude and overlie the Kuskokwim Group. Five such complexes crop out within the quadrangle and form the highest and most rugged terrain. They consist of andesite and basalt that overlie or are in fault contact with monzonite plutons; locally, the plutons intrude and partially assimilate the comagmatic volcanic rocks. An extensive field of subaerial felsic to mafic volcanic rocks, coeval with the volcanoplutonic complexes, covers much of the western part of the quadrangle.

Pre-Cretaceous rocks are exposed poorly. Precambrian to late Paleozoic basement rocks that represent parts of the Innoko, Ruby, and, possibly, Kilbuck terranes occur in a narrow northeast-southwest-trending belt in the western one-half of the quadrangle. Radiometric data reveal that amphibolite-grade metamorphic rocks in the belt are some of the oldest rocks in Alaska. U-Pb age determinations indicate a protolith age of Early Proterozoic; Late Proterozoic and Cretaceous K-Ar age determinations suggest a complex metamorphic history for these amphibolite-grade lithologies. Ultramafic and gabbroic rocks correlative with Jurassic ophiolites of the Yukon-Koyukuk trend crop out in the northern part of the quadrangle.

The Kuskokwim Group rocks have been deformed into a series of northeast-trending synclines and anticlines. High-angle faults parallel this fold structure, and emplacement of the plutons and volcanic rocks appears to be controlled by these faults. The Nixon-Iditarod fault, a major strike-slip transcurrent structural boundary in Alaska, bisects the quadrangle on a northeast-southwest diagonal.

Mineral resources include Au, Ag, Hg, Sb, Sn, W, Cr, and Bi. A minimum of 1,600,000 oz of gold, 240,000 oz of silver, 1,534 flasks of mercury, and a few hundred units of tungsten have been produced mainly from placer deposits since 1906. The Late Cretaceous-early Tertiary volcanoplutonic complexes and related dikes are the major sources of the hard-rock and heavy-mineral placer deposits. The mineral deposits are controlled structurally and occur in monzonitic plutons and associated wallrocks.

Placer gold continues to be the most economically significant mineral resource. The general formation of the placer gold deposits is best explained by mechanical erosion of gold-bearing hard-rock deposits. The present distribution of the gold is a result of several specific factors that include (1) structural controls, such as regional tilting or uplift, (2) geomorphic evolution of stream drainages in a periglacial environment, and (3) stream piracy, often a result of late Pleistocene glacial processes. Applying these factors may lead to the discovery of unexploited placer deposits.

Origin of Platinum-Group Metals, Gold, and Rhenium in the Earth's Mantle and the Role of Sulfide in Mantle-Crust Partitioning

John W. Morgan

Trace-element analyses of highly siderophile elements, including platinum-group metals (PGM), Au, and Re, and chalocogens, including S, Se, and Te in spinel lherzolite xenoliths (SLX) of upper mantle origin suggest that these elements were introduced after formation of the core by an extraterrestrial influx during the first 600 m.y. of the Earth's history. The evidence is summarized as follows. Abundances of PGM in SLX are relatively constant worldwide, averaging 0.7 percent of those in Type I carbonaceous chondrite meteorites (C1). The PGM interelement ratios (for example, Os:Ir, Pd:Ir) are closely similar to those in C1. For Re and Au, absolute abundances are more variable, and both appear to be anticorrelated with the degree to which the SLX has been depleted by loss of a basaltic partial melt. In the least depleted SLX, however, Re:PGM and Au:PGM are close to C1, which implies that highly siderophile elements are present in undepleted upper mantle material in C1 (or "cosmic") proportions. This inference is confirmed by ^{187}Os isotopic evidence from osmiridium of known age, which indicates a chondritic Os:Re of 12 (by weight) in the mantle source. In SLX, S and Se correlate strongly with Re, and abundances of these chalocogenic elements in undepleted mantle averaging 0.3 percent x C1 may be deduced. Thus, the average composition is depleted more than C1 chondrites in S and Se (and Te?) relative to PGM, Re and Au, and the abundance pattern for siderophile elements and chalocogens closely matches the CM2 carbonaceous chondrites. The abundance

pattern is also a reasonable match for that found in 3,900-m.y.-old Apollo 17 lunar impact breccias. It is well known that the Moon suffered intense bombardment during the first 600 m.y. of its existence, and the Earth cannot have escaped similar treatment, with the concommitant elemental enrichments.

Systematic variations in the suite of SLX of abundances of S and Se with the degree of loss of partial melt suggest that primary basaltic liquid derived from a relatively undepleted mantle source should contain 1,040 ppm S and 300 ppb Se. These values are higher than those in most fresh oceanic basalt glasses, but the S abundance is in agreement with laboratory measurements of S solubility at upper mantle temperatures and pressures. Thus, about 20-percent partial melting will remove totally the initial complement of 200 ppm S from undepleted mantle. In the absence of a free metallic iron phase, the highly siderophile elements are strongly chalcophile. Individual sulfide grains in a SLX from Kilbourne Hole, AZ, average 38 percent Fe, 23 percent Ni, 3 percent Cu, 2,300 ppm Co, 4.8 ppm Ir, 6.4 ppm Os, and 1.4 ppm Au. Thus, most of the Ir, Os, and Au (as well as Cu) is contained in sulfides that constitute only 0.04 percent by weight of the rock. It seems likely that the relatively uniform abundances of PGM in SLX over a wide range of basalt depletion may be governed by "buffering" due to their high chalcophile affinities. Complete removal of a free sulfide phase by as much as 20-percent partial melting may be a necessary precondition for removal of PGM from the mantle.

Platinum-Group Element Mineralogy of the Pole Corral Podiform Chromite Deposit, Rattlesnake Creek Terrane, Northern California

Barry C. Moring, Norman J Page, and R. L. Oscarson

The Pole Corral deposit (Red Mountain group) was selected for mineralogic studies because it contained some of the highest platinum-group element (PGE) contents found in a geochemical survey of

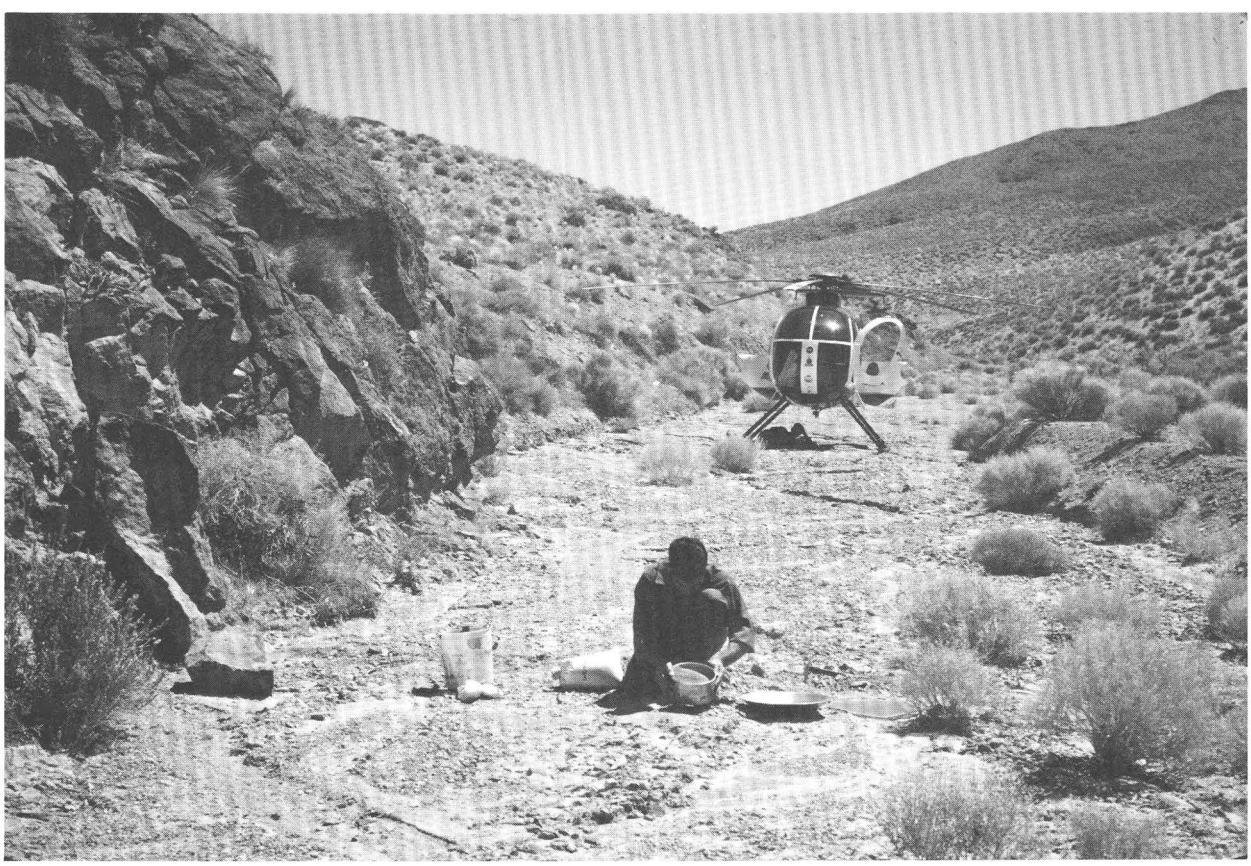

U.S. Geological Survey scientist collecting sediment from an active stream for geochemical sample to be used as part of the Walker Lake 1° x 2° CUSMAP geochemical evaluation.

280 podiform chromite deposits in California and Oregon. The deposit is located about 0.5 mi west-southwest of Little Red Mountain, which is about 7 mi (airline) southwest from the town of Beegum, CA. It occurs in serpentinized dunite hosted by serpentinized harzburgite, part of a disrupted ophiolite, in the fault-bounded Rattlesnake Creek terrane, which is a subdivision of the western Paleozoic and Triassic belt of the Klamath Mountains province. Chromitite crops out on the walls of a prospect pit and consists of 1- to 2-in.-thick layers in dunite, disrupted by faulting and shearing, with an aggregate length of about 40 ft. In 11 samples of chromitite, Pd, Pt, Rh, Ir, and Ru contents range from 1 to 15, 35 to 2,530, 3 to 74, 70 to 2,930, and 70 to 4,930 ppb, respectively, and average 4.3, 271, 23, 999, and 1,909 ppb, respectively. The mineralogy also indicates Os is present. Increased PGE contents are not associated with increased Cu (maximum 7 ppm) or Ni (maximum 1,500 ppm) contents, which suggests that the chromitites are poor in base-metal sulfides.

A back-scattered scanning electron microscope study of seven polished sections of chromitite from Pole Corral identified 24 grains of PGE minerals that were analyzed by qualitative methods. The grains ranged from about 2 to 20 m in diameter and occurred either as inclusions in chromite or at the boundary of chromite and serpentinized olivine crystals. Ten of the grains contained a single phase; the remainder contained multiple-phase grains (as many as four phases). Most of the grains consist of alloys. Ru-Fe alloy is the most common phase occurring as exsolution blebs and as single phase grains (found in 13 grains) in the chromitites. One grain of Ru-Fe alloy appears to be zoned with an Fe-rich core, and two grains have Os-rich rims. Alloys composed of various proportions of Os, Ir, and Ru occur in six grains and, within several of these, are domains enriched in Cr and Fe or composed of Pt-Fe alloy. Four grains contain Pt-Fe alloys with variable contents of Ni and Cr(?). Au-Pd alloy forms one grain. Laurite (Ru, Ir, Os)S_2 and compositions indicating the irarsite (Ir, Rh, Pt, Ru, Pd)AsS - osarsite (Os, Ru, Ir)AsS - ruarsite (Ru, Os, Ir)AsS group are the only sulfide or sulpharsenide PGE minerals identified. This mineralogy is similar to that of other podiform chromitites elsewhere in the world. Although the PGE contents of this chromitite and its mineralogy make an attractive exploration target, the tonnage distributions and PGE contents of podiform chromite deposits imply that these types of deposits will not contribute substantially to world PGE supply.

Geologic Setting of Two Sediment-Hosted Hydrothermal Mineral Localities in Escanaba Trough, Gorda Ridge

Janet L. Morton, William R. Normark, Mark L. Holmes, and Mitchell Lyle[1]

Escanaba Trough is a sediment-covered slow-spreading (2.5 cm/yr) ridge segment at the southern end of the Gorda Ridge. Two large intrusive zones at lat 40°45′ N.; long 127°30′ W. (SESCA) and lat 41° N.; long 127°30′ W. (NESCA) were mapped and sampled in July 1986 to determine their potential for hosting massive sulfide deposits. Detailed mapping of the SESCA site shows three hills less than 1 km in diameter atop a low sediment-covered ridge. The hills are erosional remnants of sediment that has been uplifted as much as 100 m. The cores of the hills might be formed of basalt, although outcrops of basalt are rare at SESCA, and the crests of the hills are covered by at least several tens of meters of sediment. The hills are bounded by steep scarps and show abundant signs of recent slumping. The NESCA site is dominated by two major hills—one steep-sided, sediment-covered hill similar to the SESCA site and the other hill 3 km in diameter that has fresh basaltic pillow flows and sheet flows on the seafloor. Extensional basins extending north and south of the volcanic hill appear to be floored by large lava lakes with many collapse structures under a thin sediment cover. The extensional basins are bounded on the west by uplifted sediment-covered blocks.

Many massive sulfide deposits, ranging in size up to 200 m across, were photographed and sampled at NESCA and SESCA. Major sulfide deposits are present around the base of the sediment-topped hills, apparently defining the original faults where uplift occurred, along sediment-covered fault scarps bounding the northern side of the volcanic hill at NESCA and along the sediment-covered slopes west of the extensional basins at NESCA. The larger deposits are partially eroded and sediment covered. Small isolated sulfide chimneys and mounds have grown on undisturbed sediment and indicate more recent diffuse hydrothermal flow through the sediment, perhaps above larger deposits contained within the sediment. Figure 1 schematically illustrates the distribution of major morphologic features and sampled hydrothermal deposits at NESCA and SESCA.

[1]Oregon State University, Corvallis, OR.

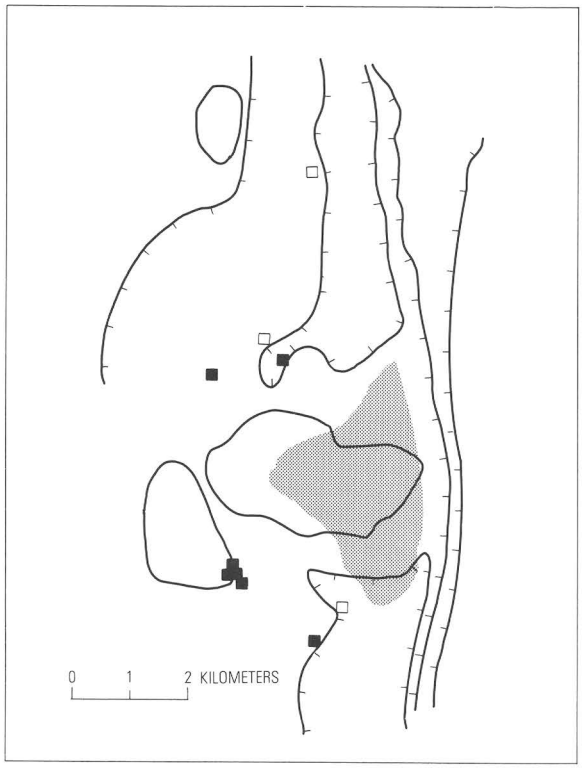

A

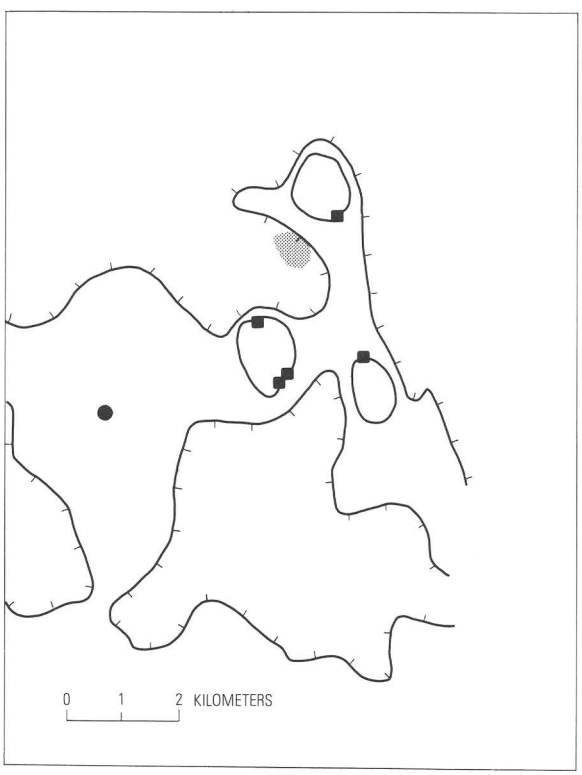

B

Figure 1. Distribution of major morphological features and sampled hydrothermal deposits. *A*, NESCA. *B*, SESCA. Hachured lines, major slopes; closed contours, hills; stipple, basalt outcrops; solid squares, dredges with massive sulfide; open squares, dredges with sulfide along veins or fractures; and solid circles, cores with massive sulfide.

Some Features on the Composition and Distribution of Geochemical Types of Placer Gold in the Koyukuk-Chandalar Mining District, Alaska

Elwin L. Mosier, John B. Cathrall, John C. Antweiler, and Richard B. Tripp

The Koyukuk-Chandalar mining district of the Brooks Range mineral belt in north-central Alaska contains numerous placer Au deposits but few known lode Au sources. Au grains, collected from 46 placer localities in the district, were analyzed for Ag and 37 trace elements utilizing direct current–arc optical emission spectroscopy. When possible, several measurements were made on each sample and averaged. Au content was determined by the summation of the 38 elements determined and subtracting from 100. Interpretation of results emphasize that the Au grains are almost invariably ternary (Au-Ag-Cu) alloys. The average Cu content is 0.040 percent, and the average Ag content and fineness [Au/(Au + Ag) x 1,000] are 10.5 percent and 893 parts per thousand, respectively, for the 46 placer localities.

Geochemical studies of placer Au from the Koyukuk-Chandalar mining district reveal striking contrasts in the Ag and Cu content of placer Au that may have a direct relation to the depositional environments of the primary Au sources. Based on Ag and Cu content, five different geochemical types of placer Au can be identified ranging from Type 1, which has high Ag content (21.2 weight percent) and low Cu content (0.007 weight percent), to Type 5, which has low Ag content (6.00 weight percent) and high Cu content (0.276 weight percent). From Type 1 to Type 5 placer Au, Au, Cu, and Au:Ag values increase systematically, and Ag, Au:Cu, and Ag:Cu values decrease systematically. A regional plot of the placer Au types shows Type 1 placers occurring in the eastern portion of the district with Types 2–5 generally occurring in order westwardly across the district, suggesting a variation in the primary Au sources that possibly could reflect a gradient of increasing depositional depths for the primary Au sources from east to west. Phase relations

for the ternary system of Ag, Cu, and Au show that higher Cu values correlate with high Au content. We hypothesize that the three elements probably were present in the ore-forming hydrothermal solutions and that phase relation for the three elements could be dependent upon the depositional environment. The 36 other trace elements determined in placer Au do not appear to correlate with the depositional environment of the primary Au source.

A comparative study of Ag content with Au grain size disclosed that smaller grain sizes generally contained higher Ag content, which suggests that some Au and Ag has been dissolved and reprecipitated on Au nuclei and (or) other minute mineral grains. The source for accreted Au could be from weathering of auriferous minerals common in the Brooks Range mineral belt. Arsenopyrite, pyrite, scheelite, and galena may contain either finely divided Au or lattice Au and commonly are found in heavy-mineral concentrates from the alluvial placers.

New Geochemical Guides to Au-Rich Co-Cu Lodes in the Blackbird Mining District, Lemhi County, Idaho

J. Thomas Nash and Gregory A. Hahn[1]

Au is a significant constituent of some lodes in the Blackbird mining district and could provide impetus for renewed mining of the Co-Cu ores. Au as native gold is present at grades in the range from about 0.5 to 20 g/t in siliceous exhalite layers that are also rich in cobaltite. The geologic association of Au with mafic volcaniclastic rocks and exhalite layers, and intimate paragenetic relation with Co-As-S minerals, and a distinctive geochemical signature [rich in Au, As, B, Bi, Co, Fe, Nb, and rare earth elements (REE)], provide a guide for evaluating sediment-hosted targets for similar Au-rich zones.

The Blackbird lodes are believed to be synsedimentary and related to volcanogenic processes operating in restricted parts of the Middle Proterozoic Yellowjacket Formation, not postmetamorphic hydrothermal veins as thought before geologic studies by Noranda Exploration, Inc., from 1978 to 1982. All lodes are stratabound within the middle part of the Yellowjacket Formation, and Au-rich ones are stratiform. The lodes are influenced by sedimentary features, such as growth faults, soft-sediment deformation, and dewatering structures, and are associated closely with mafic tuffs and coeval dikes. Geochemistry of the lodes can be reconstructed reliably in time and space because metamorphism has caused only minor changes in rock fabric and chemistry and in ore mineralogy in areas of little deformation.

All lodes are associated with tuffaceous rocks and dikes of alkali basalt composition. Beds judged to be tuffs are thinly bedded, contain 50–100 percent mafic silicates (biotite, garnet, chloritoid), and are locally rich in white mica. Chemically, these beds are rich in Fe (often more than 20 percent total as Fe_2O_3) and K (5–8 percent K_2O), as well as As-Bi-Co-Nb-Ti-Zr-REE. Au-rich Co-Cu lodes contain distinctive 1- to 10-cm-thick metachert layers, some of which contain abundant tourmaline and REE-bearing phosphate minerals. Exploration is aided by visual recognition of beds rich in mafic silicates

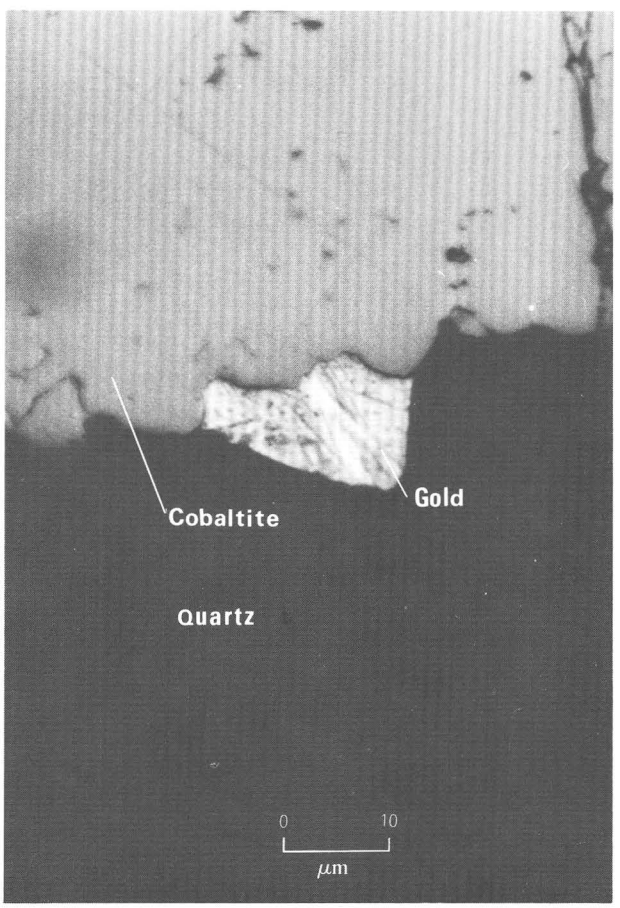

Figure 1. Photomicrograph of gold (bright, with scratches) with cobaltite and quartz from the Sunshine lode, Blackbird mining district, Idaho. The gold and cobalt minerals formed as a chemical sediment on the seafloor in association with basaltic volcanism in a process resembling a modern "black smoker."

[1]Noranda Exploration, Inc., Lakewood, CO 80215, now with Coca Mines, Inc., Denver, CO 80203.

or metachert and is supplemented effectively by geochemical surveys for Co.

Best Au grades are in layers that have abundant cobaltite or metachert. Assay data indicate a significant association with Co and As and an independence of Cu. Grades greater than 0.5 g/t appear to be in layers 1 m thick in the central and thickest part of the lode where highest concentrations of Si, Co, and As occur. Native gold grains range in size from <1 to 20 m. Most gold grains occur as inclusions in cobaltite, on cobaltite grain boundaries, or in microveinlets that cut cobaltite. Grains of gold <2 μm in size also occur in quartz of metachert bands. Grain size of gold, which influences mill recovery, seems to be largest in lodes subjected to higher metamorphic grades.

The association of Blackbird Co-Cu-Au lodes with mafic volcanic rocks at regional, district, and deposit scales provides an empirical exploration guide but also appears to explain many unusual geochemical features of these lodes. Other sediment-hosted Cu deposits generally lack associated Au, As, Bi, Co, Fe, and REE enrichments but, instead, are richer in Ag-Pb-Zn. The mafic rock association and geochemistry at Blackbird should be a useful guide to Au in Precambrian Fe-rich sedimentary rocks in which the paragenesis of gold generally is obscured by metamorphism.

Mineral-Resource Assessment of the Tonopah 1° x 2° Quadrangle, Nevada

Greta J. Orris, Gerald F. Brem, Richard F. Hardyman, David A. John, William J. Keith, Frank J. Kleinhampl, J. Thomas Nash, Donald Plouff, Norman J. Silberling, John H. Stewart, and Donald H. Whitebread

The mineral-resource assessment of the Tonopah 1° x 2° quadrangle, Nevada, produced a quantitative, probabilistic estimate of the mineral endowment of the study area. The assessment process consisted of the following stages: (1) determination of appropriate descriptive and grade-tonnage models of deposit types that are known to occur, or may occur, within the study area, (2) delineation of areas permissive for the occurrence of the selected deposit types, and (3) estimation of the number of deposits by type that may occur within the delineated areas.

Deposit types selected for evaluation in the Tonopah quadrangle include sediment-hosted (SH) disseminated Au-Ag, hot spring Au-Ag, epithermal Au-Ag vein, low-F porphyry Mo, porphyry Cu, polymetallic vein, polymetallic replacement deposits, bedded barite, simple Sb, and Fe, Cu, W, and Zn-Pb skarn deposits. Other deposit types known to occur are placer Au, turquoise, and a variety of nonmetallic commodities including magnesite, perlite, and diatomite. As a first step in the delineation of tracts permissive for the occurrence of undiscovered deposits for the major deposit types, a list of favorable criteria was compiled for each deposit type with an emphasis on those characteristics identifiable at a regional scale, and known deposits were classified into appropriate deposit types. Many of the regional scale criteria were similar for different deposit types. Because permissive lithologies, geochemistry, alteration, and associated deposit types were not diagnostic for a single deposit type, many of the delineated areas contain groups of deposit types such as low-F porphyry Mo, W skarn, and polymetallic vein deposits or SH disseminated Au-Ag, epithermal Au-Ag vein, and simple Sb deposits. Adding to the complexity of delineating areas was the problem of determining what resources might underlie Tertiary and Quaternary cover of volcanic rocks and alluvium or relatively thin low-angle fault plates at depths of less than 1 km.

Estimation of the number of undiscovered deposits was complicated by the problems of cover, Basin and Range physiography, and complex structural histories. For the SH disseminated Au-Ag, polymetallic vein, and epithermal Au-Ag vein deposit types, we estimated a 90-percent chance that one or more undiscovered deposits are present within the study area. In addition, it was estimated that there is a 50-percent chance that at least one additional deposit is present for the following deposit types: polymetallic replacement, hot spring Au-Ag, low-F porphyry Mo, and W skarn. This assessment suggests a favorable environment for undiscovered deposits including deposit types such as bedded barite and turquoise, Cu and Zn-Pb skarn, and simple Sb deposits.

Mineral-Resource Assessment of Costa Rica

Norman J Page, W. C. Bagby, J. E. Case, D. P. Cox, Donald F. Huber, Robert P. Koeppen, Stephen D. Ludington, S. P. Marsh, D. A. Ponce, Klaus J. Schulz, and D. A. Singer

The U.S. Geological Survey, Dirección General de Geología, Minas, e Hidrocarburos, and the Universidad de Costa Rica undertook a nonfuel mineral-resource assessment of Costa Rica in cooperation with the Los Alamos National Laboratory and funded by the U.S. Agency for International Development. It is based on evaluation of existing earth science data and new data gathered during 14 man-months of field studies.

To facilitate the resource assessment, rocks were grouped broadly on the geologic map. The oldest known rocks are Jurassic seafloor basalts, and the basement of the country is composed of oceanic crust formed in the Mesozoic, presumably as a result of the parting of the North and South American plates. This oceanic crust is overlain by Upper Cretaceous and Tertiary marine deposits that accumulated in a complex series of basins. A gravity profile, controlled by seismic refraction data, across Costa Rica suggests that the Pacific margin is composed of high-density stacked slices(?) of oceanic crust about 20–30 km thick, that a lower density crust increases in thickness to about 40 km below the central volcanic belt, and that crustal thickness is about 25 km along the Atlantic margin. As a result of interactions between the Caribbean and several Pacific plates, most of the country was uplifted during Miocene and later times to form the present mountainous isthmus. Uplift was accompanied by intense igneous activity related to subduction along the middle American trench. The resulting volcanic rocks cover more than one-half of Costa Rica.

The Tertiary volcanic rocks of the "gold belt" are the coalesced products of numerous volcanic centers developed from about 23 to 1 Ma. Their evolution involved (1) deposition of lava flows interlayered with abundant volcanic fragmental rocks, (2) the deposition of the overlying volcanic unit from several volcanic centers and the emplacement of the Guacimal silicic intrusion, (3) widespread rhyolite magmatism and associated hydrothermal alteration, and (4) the unconformable deposition of the andesitic Monteverde Formation at a time of renewed volcanism in the Pliocene to Quaternary. The associated Au deposits consist of (1) Au, chalcopyrite, galena, sphalerite, and pyrite in quartz veins and stockworks hosted by intermediate and felsic volcanic rocks, (2) quartz, chlorite, and sericite alteration, and (3) quartz, adularia, kaolinite, rhodochrosite, and sparse barite forming gangue. Rhyolites appear to be the heat source for the hydrothermal systems. These epithermal precious-metal deposits are similar to a Sado-type epithermal model, which has a median Au grade of 6.0 g/t and median tonnage of 300,000 t. All available data on 319 deposits and occurrences of Au and other commodities were compiled by mineral-deposit type, verified by field observations where possible, and entered into a computer file. The plotted data show that the deposit types tend to cluster in areas of similar geology.

The resource assessment consisted of (1) delineating domains according to the geologic environments that are permissive for Sado-type epithermal veins, placer Au, porphyry Cu, volcanogenic Mn, podiform chromite, Cyprus-type massive sulfides, and bauxite, (2) characterizing undiscovered mineralization by analogy with tonnage and grade models, and (3) estimating the number of undiscovered deposits of each type within the delineated domains. Other deposit types, not delineated but present, include shoreline placer magnetite, polymetallic vein, Cu skarn, Zn-Pb skarn, and hot spring S. Permissive geologic environments are also present for hot spring Au deposits and Au associated with alkalic volcanic rocks. Lateritic Ni deposits are unlikely.

Preliminary Geophysical Well Log Analysis of the Geothermal Alteration of Alluvial Sediments in the Salton Sea Basin, California

F. L. Paillet and R. H. Morin

An extensive suite of geophysical well logs was obtained during the Salton Sea Scientific Drilling Project (SSSDP). These logs included conventional and research electric, acoustic, nuclear, temperature, and caliper logs for the uppermost 6,000 ft of borehole but were limited to natural gamma, epithermal neutron, deep induction, and temperature logs for the deeper interval (6,000–10,500 ft). A major limitation in the application of geophysical logging techniques to the SSSDP program was the effect of borehole conditions on the performance of logging equipment. The geophysical probes used during the SSSDP were designed to sample a 3-ft-diameter volume of the rock and borehole fluid environment, but damage to the borehole associated with the production of geothermal fluids resulted in hole enlargements much greater than 3 ft. Most of this damage occurred during initial attempts to control circulation before logs could be run in the borehole, so that geophysical logs were of little use in characterizing the production zones at depths below 6,000 ft. The difficulty in controlling circulation also resulted in logs being run at temperatures that ranged from 280 to 310°C, which caused the mechanical failure of the caliper tool.

Analysis of geophysical logs for the upper part of the SSSDP borehole indicates that the logs provide information on the original lithology of the Salton Sea sediments. The nuclear, electric, and acoustic logs indicate variations in ratios of quartz to clay minerals in the sedimentary column that are related to variations in the depositional environment of the original sediments, such as alluvial fan, overbank

splay, mudflat, and beach and dune sand deposits. In addition, the electric logs may indicate variations in pore-fluid chemistry that could be due to the generation of hydrothermal fluids in the sediments since they were deposited. Porosity logs indicate that primary porosity is very low throughout the sediments penetrated by the upper part of the SSSDP borehole; this supports the assumption that essentially all geothermal fluid production from the lower part of the borehole is derived from fractures.

Conventional acoustic transit-time and acoustic waveform logs, vertical seismic profile (VSP) sections, and core samples for ultrasonic testing in the laboratory provide a unique opportunity to compare the dynamic properties of Salton Sea sediments at three different scales of investigation—0.5–2 in. for core samples, 1–3 ft for waveform logs, and 100–500 ft for VSP data. Data from the waveform logs and laboratory and VSP-measured compressional velocities indicate that the acoustic transit times provided by the commercial acoustic logs are incorrect. Values that range from 100 to 150 μs/ft on the log correspond to values that range from 65 to 85 μs/ft determined from waveform data. The large borehole diameter, dense drilling mud, and possible clay-mineral alteration in the vicinity of the borehole apparently affected the performance of conventional acoustic logging probes. Analysis of seismic velocities determined from acoustic waveform logs and laboratory tests of core samples indicates that progressive age and degree of alteration of sediments in the SSSDP borehole are associated with only minor changes in compressional velocity but major changes in shear velocity. These initial results support the hypothesis that the primary effect of geothermal alteration in the SSSDP borehole has been a decrease in the effective Poisson ratio of the sediments, from typical values for shaly sandstone that range from 0.28 to 0.35 before alteration to values that range from 0.20 to 0.25 after alteration.

Ophiolites, Metallogenic Models, and Terrane Models— Interrelations Observed in the Arabian Shield and Potential for "Cryptic" Mineralization

John S. Pallister

The Arabian Shield is now recognized as a mosaic of intraoceanic and continental microplates that were accreted during the Late Proterozoic. Considerable emphasis has been placed on the definition of exotic terranes and their internal characteristics as a screen for efficient mineral exploration. In addition, ophiolitic rocks, which mark terrane boundaries in the Shield, are themselves targets for certain types of ore deposition.

Based on reconnaissance field studies of the Arabian ophiolites, an intriguing mineral exploration target is serpentine-related Au and Co mineralization. Au deposits and prospects are concentrated along sutures (terrane boundaries) within the Arabian Shield. At several localities, deposits occur in quartz veins related to mafic-intermediate plutons that intrude serpentinized peridotites and carbonated or silicified serpentinite (listwänite or bibirite). This geologic setting, similar to that in the southern part of the Mother Lode system of the Sierra Nevada foothills of California, suggests that the Au may have been derived from the ultramafic rocks.

The mineralized Bou Azzer ophiolite of Morocco has produced 50,000 tons of Co (4–8 percent of world production) since 1930 and provides a useful model for mineral exploration of the Arabian ophiolites. The Bou Azzer ophiolite is approximately the same age, is exposed in a similar tectonic setting, and has common internal characteristics. Bou Azzer Co (Ni-Fe) arsenide ore bodies occur in a quartz-carbonate gangue that is an alteration product of ophiolitic peridotite. The Bou Azzer metallogenic model, developed by Marc LeBlanc and coworkers, calls for Co concentration through three main stages—serpentinization of peridotite, which results in partitioning of Co and Ni into magnetite; weathering of serpentinite to yield Co and Ni enrichments in Mn-Fe hydroxides, serpentines, and bibirite and listwänite; and remobilization and concentration of Co (Ni-Fe) arsenides and accessory Cu, Mo, and Au, followed by reprecipitation along contacts with younger plutons and within latest Pan-African age structures.

A characteristic feature of the Arabian ophiolites is the conversion of serpentinite to listwänite and bibirite along bounding fault zones. Sutures of the eastern Shield are marked by belts of these carbonated and silicified serpentinites that extend for tens of kilometers. Listwänite and bibirite derived from the Arabian ophiolites are enriched locally in Cu, As, Co, and Ni. Ancient Au mines are found along contacts between altered serpentinite and younger intrusions, a setting where all three stages of the Bou Azzer model may be met.

Most of the known metallic ore districts of Arabia were "rediscovered" in the 20th century with relative ease because of the presence of ancient workings. In contrast, Co and Ni deposits would not have

been developed by ancient man, and tell-tale mine workings would not be present. Mineral exploration has progressed in the Arabian Shield to the point that significant *new* discoveries probably will be "cryptic," either as buried deposits or of a type not formerly sought by the ancients (such as bauxite, Sn, W, and Co). Therefore, exploration based on mineralization models will become increasingly important. An obvious exploration target, based on the Bou Azzer model, is for Co and Ni associated with the very common listwänite and bibirite zones within the Late Proterozoic ophiolites.

Geophysical Mapping of Eastern U.S. Early Mesozoic Basins

Jeffrey D. Phillips and David L. Daniels

Compilation of digital aeromagnetic and gravity data for 12 areas covering the exposed early Mesozoic basins of the Eastern United States is nearing completion. This compilation is being done as part of a multidisciplinary study focusing on ore-deposit models in failed rift environments. In 10 of the 12 areas, Department of Defense gravity data files have been supplemented with newly collected gravity data and with gravity data from unpublished sources to yield sufficiently detailed coverage for preparation of complete Bouguer contour maps and bandpass filtered contour maps at a scale of 1:125,000. Available gravity coverage in the southern Hartford basin, Connecticut, and the eastern Newark basin, New Jersey, is inadequate for compilation at this scale. In 9 of the 12 areas, data digitized from older aeromagnetic contour maps are being combined with newer digitally recorded aeromagnetic data to produce regional scale contour maps and computer-generated products, such as graytone aeromagnetic intensity maps. For three areas in central and southern Virginia, digital aeromagnetic coverage is inadequate for regional compilation.

Model studies have been initiated using 2½-D algorithms along selected gravity and magnetic profiles to test aspects of published geologic cross sections for the basins; for example, in the northern Hartford basin, Massachusetts, gravity and magnetic models suggest that the floor of the basin is uneven and probably offset along normal faults that are not mapped at the surface. In addition, the dip on the eastern border fault cannot be determined accurately from the gravity and magnetic data; it may be as great as 70° or as little as 50°, depending upon the geometry of a low-density Paleozoic gneiss unit that apparently underlies the border fault. Outside the basin, the modeled configuration of a folded amphibolite layer, which is a magnetic marker bed within the Paleozoic section, agrees well with published geologic cross sections and supports the interpretation that the gneissic country rocks beneath and around the basin form continuous layers.

Because of the association of economically important magnetite skarn deposits with Mesozoic diabase in the Gettysburg basin and uncertainty regarding the distribution of diabase at depth within the basin, a detailed gravity survey was completed recently in the Harrisburg, PA, area. Bowl-shaped diabase sheets, which have a large positive density contrast with the enclosing Mesozoic sedimentary rocks, produce prominent positive gravity anomalies that can be used to estimate the thickness of the diabase sheets. Areas of maximum sheet thickness are readily apparent on the gravity map. These usually occur beneath the sedimentary cover rocks within the "rectangular" rings of exposed diabase. The Gettysburg, York Haven, and Quakertown sheets follow this pattern. The Morgantown diabase body, with its deep central gravity low, is an exception because it appears to have no significant thickness beyond its exposed rim. By delineating the areas of the Gettysburg basin that have significant thicknesses of diabase, the detailed gravity data place restrictions on the areas of the basin with high potential for undiscovered magnetite skarn deposits.

Geochemical Aspects of Ocean-Floor Hydrothermal Vent Fluids and Massive Sulfide Chimneys From the Southern Juan de Fuca Ridge

J. A. Philpotts, J. S. Kane, P. J. Aruscavage, H. Kirschenbaum, R. G. Johnson, A. F. Dorrzapf, Jr., Z. Brown, and J. S. Mee

The U.S. Geological Survey is engaged in a multidisciplinary study of the southernmost segment of the Juan de Fuca (JDF) Ridge, an active spreading center located about 400 km off the coasts of Oregon, Washington, and British Columbia. In September and October 1984, hot springs and associated massive sulfide deposits were sampled in the central axial cleft of the ridge using the deep-sea research submersible vehicle *Alvin*. The deposits have potential economic interest and provide general insight into the nature and genesis of

massive sulfides. Our JDF geochemical investigation has focussed on the bulk chemical composition and coarse concentric zoning of 16 massive sulfide chimneys and on the composition of the hydrothermal fluids. We also are evaluating the capabilities of a number of analytical techniques based on analyses of JDF sulfides and a suite of sulfide standards.

The JDF hydrothermal vent fluids, which were collected over a distance of 3.5 km along the ridge, show some small differences in composition. The fluids have the highest concentrations of many dissolved species yet reported for submarine hot springs. Relative concentrations are similar to those of fluids from 13° N. on the East Pacific Rise (EPR); this compositional signature appears to differ from that of fluids from 21° N., EPR, and the Galapagos spreading center. This dichotomy in chemistry may reflect largely the type and extent of alteration of the rocks with which the fluids are interacting.

The JDF massive sulfide chimneys are composed predominantly of ZnS; FeS_2 rims are common at some sites. Other phases include FeS, silica, anhydrite, and barite. Sulfate typically contributes less than 5 percent of total S. A unique chimney has a central orifice lined with isocubanite ($CuFe_2S_3$) and a Mg-rich rim. However, Cu exceeds 1 percent in bulk materials from only four chimneys. Radial concentration variations of elements such as Cu, Ba, and Pb may contribute to understanding the preservation of ocean-floor sulfides, many of which are vulnerable to reaction with normal seawater. Among elements of potential economic interest, Zn averages 40 percent; Pb, 0.15 percent; Cd, 0.1 percent; and Ag and Co, about 200 ppm each in the JDF chimney sulfides.

In preparing samples for analysis, acid dissolution of sulfides may result in incomplete recovery of elements such as Pb, Ba, Sr, and Ag, whereas roasting and fusion decomposition can result in loss of volatile elements. Additional flux helps to prevent sticking of high-Fe samples to graphite crucibles. Spectral and background interferences due to Zn, Fe, Cu, and so forth often dictate changes in analytical strategy. Further, silicate techniques may not be well calibrated for sulfides. Inductively

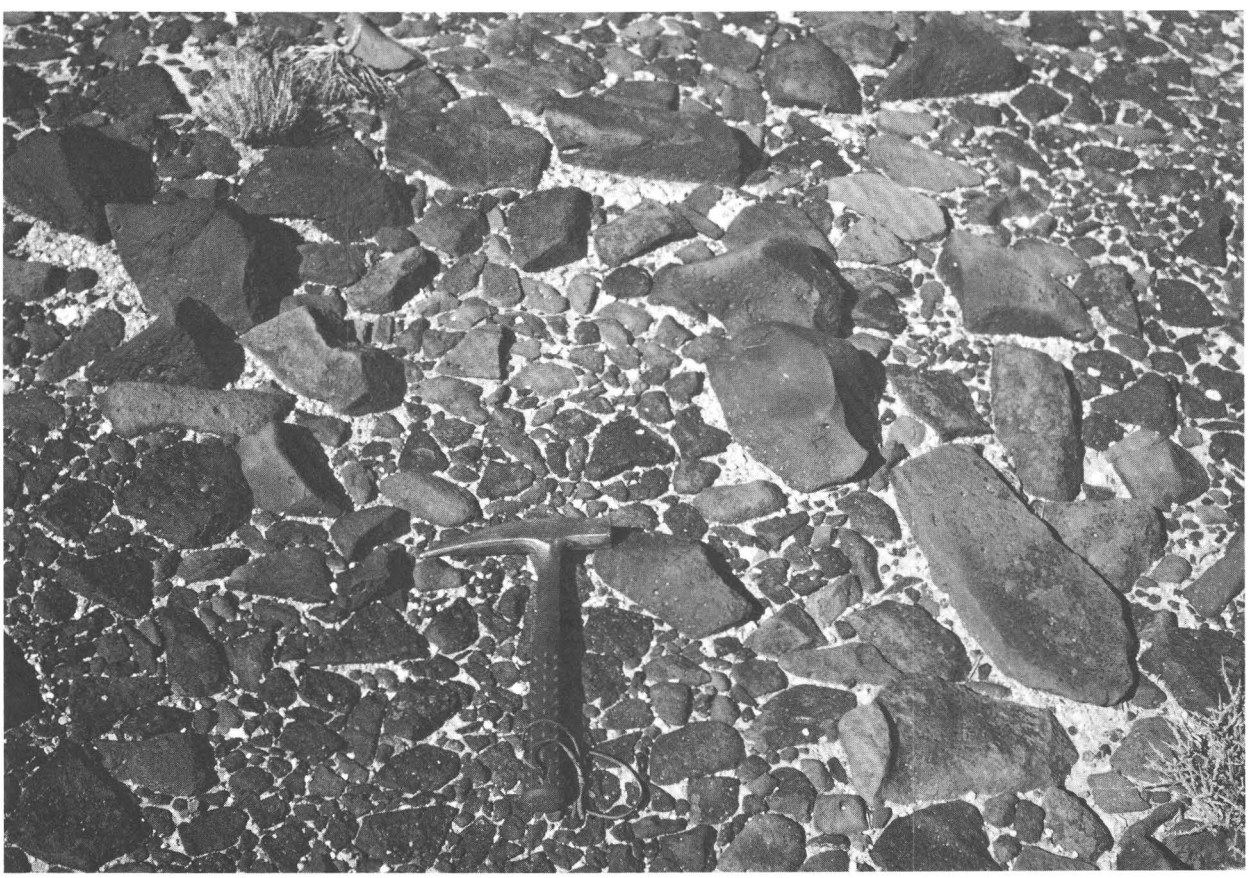

Desert pavement that formed in the semiarid environment of central Nevada. Wind has removed fine material representing the original "matrix." Pebbles and cobbles are coated with iron and manganese oxides to produce the mottled pattern.

coupled plasma optical emission spectroscopy appears to be the single most useful multielement technique for the analysis of sulfides.

"Mesothermal" Gold—A Metamorphic Connection?

W. J. Pickthorn, R. J. Goldfarb, and D. L. Leach

Worldwide "mesothermal" gold-bearing vein deposits often are found in low- to moderate-grade metamorphic rocks, typically marine in origin, in tectonically disturbed or accreted terranes. In North America, deposits of this type frequently are located along the western margin of the Cordillera in the western Sierra Nevada, Klamath, and Siskiyou Mountains of California, western British Columbia, and along the Gulf of Alaska. The U.S. Geological Survey has undertaken a multidisciplinary study of mesothermal gold deposits in metamorphic rocks in Alaska to examine the genesis of this deposit type.

The Cretaceous Valdez Group, a major component of the accreted Chugach terrane, south-central to southeastern Alaska, consists principally of tightly folded and metamorphosed graywacke and shale. Gold mineralization is found in small discontinuous quartz veins, pods, and stringers. These veins are emplaced along shear zones, faults, and joints that postdate accretion, deformation, and regional metamorphism. The veins are restricted to areas of greenschist facies metamorphism and show no consistent association with intrusive rocks. Wallrock alteration is generally absent. Fluid-inclusion analyses of gold-bearing quartz from throughout the Valdez Group yield minimum trapping pressures of 1.5 kbar and corrected homogenization temperatures ranging from 260 to 330°C. Ore-forming fluids were of low salinity, with gas contents of up to 11 mole percent. Analyses of the inclusion gas phase by Raman laser spectroscopy and quadrapole mass spectrometry indicate compositions ranging from pure CO_2 to mixtures dominated by CH_4 and N_2. Stable isotope analyses of the quartz yielded $\delta^{18}O$ values for the ore-forming fluid in the range from +6.5 to +9.6 per mil. Analyses of hydrous ore-phase minerals indicates an ore-fluid δD of approximately −20 per mil.

In southeastern Alaska, the Juneau gold belt extends for approximately 200 km along the western flank of the Coast Range batholith and coincides with the Coast Range megalineament. Approximately 75 percent of Alaska's total lode gold production was from this region, the majority from the Alaska-Juneau (A-J) Mine. Host rocks consist of metamorphosed and deformed slate, phyllite, diorite, and greenstone. Stable isotope data ($\delta^{18}O$, +9.8 per mil; δD, −20 per mil) and fluid-inclusion pressure (P)-temperature (T) estimates (P, minimum 1.5 kbar; T>200°C) are very similar to the Valdez Group deposits, however the bulk fluid composition and the structural setting are quite different. Most fluid inclusions in samples studied from the A-J contained CO_2 contents in the range from 30 to 60 mole percent with minor CH_4 and N_2. Evidence is good for boiling of the ore fluid. The A-J Mine is located along a major crustal structure, and the ore body consists of a 5.5-km-long by 100-m-wide zone of intense quartz veining; vein material often makes up more that 50 percent of the rock. Intense wallrock alteration also accompanies mineralization.

The stable isotope, fluid inclusion, and inclusion gas chemistry data are consistent with those for fluids derived from metamorphic rocks during devolatilization reactions. We suggest that prograde metamorphism during accretion released the water and volatiles, which migrated into fractures in the previously metamorphosed rocks during a decrease in the confining lithostatic pressure. The relatively small veins in the Valdez Group rocks may represent a local fluid source, whereas the intense veining and alteration suggests a larger or deeper crustal source for the A-J ore fluid. Wallrock chemistry and varying redox conditions may have been important locally in controlling gold deposition.

The Application of Conodonts to Studies of Mississippi Valley-Type Ore Deposits—A Preliminary Assessment

John E. Repetski, Joseph A. Briskey, Augustus K. Armstrong, Fred Smith,[1] Larry Wilbanks,[1] and Dave Tibbels[1]

Conodonts are microfossils that are present in and easily recoverable from many Paleozoic and Triassic marine carbonate rocks that also are the host rocks for numerous Mississippi Valley-type (MVT) metallic ore deposits. Conodonts can be exploited in minerals exploration programs because (1) they are superb stratigraphic index fossils through most of their geologic range and, therefore, can be used to correlate strata, even in drilling programs, (2) their environmental preferences and limitations can aid in detailed facies reconstructions and basin analysis, and (3) their color alteration index (CAI) and variations in their surface

[1]Jersey Miniere Zinc Co., Gordonsville, TN 38563.

texture can place constraints on interpretations of the age and spatial distribution of ore bodies and on the temperature of diagenetic and ore-bearing solutions.

Preliminary evaluation of Ordovician conodonts in the host rocks of zinc ore bodies in central Tennessee provides a case study for these developing techniques. Surface and subsurface sampling for conodonts is providing the biostratigraphic and paleoecologic framework that can be integrated with petrologic, diagenetic, and geochemical studies in progress on the surface, from cores, and underground in the mines. The regional CAI value of the host-rock formations in central Tennessee is about 1½. In a detailed traverse across an ore body in the Gordonsville Mine, central Tennessee district, CAI values range systematically from a low of 1½ to at least 2. Host rocks with the lower CAI values probably had relatively low initial permeability or were reduced in permeability during early (pre-ore) diagenesis, either or both of which would have largely isolated these rocks from the later ore-bearing hydrothermal solution(s). Furthermore, conodonts with corroded surfaces, where the etching cannot be attributed to processing techniques, are most common near the ore body, whereas vitreous noncorroded conodont elements are more common away from the body and presumably further from the etching effects of the ore-bearing fluids.

As these preliminary observations are expanded upon and are correlated more closely with ongoing study of the petrology and geochemistry in these and other areas of MVT mineralization, conodonts may prove to be valuable new tools in minerals exploration.

Evidence for Iron-Stripping and Silica-Stripping Microorganisms in Precambrian Granular and Banded Iron Formations

Eleanora I. Robbins, Gene L. LaBerge,[1] and Robert G. Schmidt

Microscopic study of a combination of thin sections and acid residues from Archean and Proterozoic iron formations from North America (Gunflint, Ironwood, Palms, Biwabik, unnamed), Australia (Brockman, Warrawoona), and Greenland (Isua) has revealed abundant morphological and mineral evidence for previously unrecognized microfossils. The morphology of micrometer-sized microstructures composed of hematite, magnetite, siderite, and chalcedonic spherules suggests the former presence of iron- and silica-stripping organisms.

Different organisms may have been involved in deposition of the different colored layers of laminated iron formations. **Black layers** are composed of hematized rods, laths, and hollow tubes that may be morphlogical evidence for an iron-stripping sheathed bacterium much like modern *Leptothrix ochracea* or perhaps *Gallionella ferruginea*, both of which precipitate ferrihydrite on their sheaths. Dispersed with the rods in magnetic black layers are tiny magnetite crystals that suggest the former presence of magnetotactic bacteria much like *Oceanospirillum*. **Red layers** contain hematite spherules that may be morphological evidence for an iron-stripping capsular bacterium much like microaerophilic *Siderocapsa*. **White layers** of chalcedonic spherules may be the remains of a silica-stripping photosynthetic chrysophyte. Silica is so pervasive in iron formation that silicic acid must have been a constituent of bottom muds. Silica bacteria much like *Pseudomonas mirabilis* or *Bacillus siliceous* may have played a part in the resolubilization of algal silica in the muds, but evaluation of the former presence of silica bacteria cannot be made on morphological grounds. **Brown layers** contain masses of globular siderite. Successive layers of globular siderite masses may be evidence for blooms of an iron-stripping bacterium or perhaps an alga. Putrefying bacteria may have played a part in the production of CO_2 and, therefore, of siderite in the bottom muds, but no unusual relict forms of putrefying bacteria remain.

In certain granular rocks, internal globular microstructures are present within the granules. Such granules may be morphological evidence for coenobial masses of a capsular iron bacterium that shares properties with *Siderocapsa*; in species of modern *Siderocapsa*, coenobial colonies coalesce into macroscopic masses and fall to the bottom in response to adverse conditions in the water column. One variety of the Precambrian granules, reminiscent of *Siderocapsa conorata*, contains tens to hundreds of internal spherules; another variety, more like *Siderocapsa eusphaera*, contains thousands of internal spherules.

The highly metamorphosed Early Archean Isua Iron-Formation apppears to contain two types of iron-walled microstructures. Rods of iron oxide appear similar to those of hematite in the younger iron formations; they may be morphological evidence for a sheath-forming iron bacterium much like *Leptothrix*. Also present are rounded, hematitic

[1]Department of Geology, University of Wisconsin, Oshkosh, WI.

microstructures averaging 10 μm that we have named *Appelocysta treubii*. Under the scanning electron microscope, they exhibit clavate to murate projections and appear to have plates and, perhaps, also sulcal grooves. *Appelocysta* may be the remains of a capsular iron bacterium as well as a thick-walled resting cyst of *Isuasphaera*.

If this morphological evidence stands the test of chemical scrutiny, then iron formation may represent the successful attempt by iron-stripping bacteria to detoxify their environment of oxygen in Precambrian oceans. The role of silica-stripping organisms in the formation of these rocks is harder to discern; silica may have been deposited initially as frustules of siliceous algae, but, if so, the transformation from opal-A to opal-CT to quartz has destroyed most fine relict textures.

Mapping Contact Metamorphic Aureoles in Extremadura, Spain, Using Landsat Thematic Mapper Images

Lawrence C. Rowan, Carmen Anton-Pacheco,[1] David W. Brickey, Marguerite J. Kingston, Alba Payás,[1] Norma Vergo, and James K. Crowley

In the Extremadura region of western Spain, Ag, Pb, Zn, and Sn deposits occur in the apices of late Hercynian granitic plutons and near the pluton contacts in late Proterozoic slate and metagraywacke that have been metamorphosed regionally to the greenschist facies. The plutons generally are well exposed and have distinctive geomorphological expression and vegetation; poor exposures of the metasedimentary host rocks and extensive cultivation, however, make delineation of the contact aureoles difficult.

Landsat Thematic Mapper (TM) images have been used to distinguish soil developed on the contact metamorphic rocks from soil formed on the stratigraphically equivalent slate-metagraywacke sequence. The mineral constituents of these soils are similar, except that muscovite is more common in the contact metamorphic soil; carbonaceous material is common in both soils. Contact metamorphic soil have lower reflectance, especially in the 1.6-m wavelength region (TM 5), and weaker Al-OH, Mg-OH, and Fe^{3+} absorption features than do spectra of the slate-metagraywacke soil. The low-reflectance and subdued absorption features exhibited by the contact metamorphic soil spectra are attributed to the high absorption coefficient of the carbonaceous material caused by heating during emplacement of the granitic plutons.

These spectral differences are evident in a TM 4/3, 4/5, 3/1 color-composite image. Initially, this image was used to outline the contact aureoles, but digital classification of the TM data was necessary for generating internally consistent maps of the distribution of the exposed contact metamorphic soil. In an August 1984 TM scene of the Caceras area, the plowed vegetation-free fields were identified by their low TM 4/3 values. Then, ranges of TM 4/5 and 3/1 values were determined for selected plowed fields within and outside the contact aureoles; TM 5 produced results similar to TM 4/5. Field evaluation, supported by X-ray diffraction and petrographic studies, confirmed the presence of more extensive aureoles than shown in published geologic maps; few misclassified areas were noted. Additional plowed fields consisting of exposed contact metamorphic soil were mapped digitally in an August 1985 TM scene.

Subsequently, this approach was used to map two 1-km-wide linear zones of contact metamorphosed rock and soil in the San Nicolas Sn-W mine area, which is located approximately 125 km southeast of the Caceras study area. Exposures of granite in the San Nicolas area are limited to a few altered granitic dikes in the mine and a small exposure of unaltered pegmatite-bearing granite in a quarry about 1.5 km west of the mine. The presence of coarsely crystalline biotite and beryl in the granite in the quarry and of contact metamorphosed slate up to 2.5 km from the nearest granite exposure suggests that only the apical part of a pluton is exposed in the quarry and that a larger shallowly buried body is probably present.

These results indicate the potential application of TM image analysis to mineral exploration in lithologically similar areas that are cultivated in spite of poor rock exposures.

[1]Instituto Geologico y Minero de España, Rios Rosas 23, Madrid 28003, Spain.

Epithermal Gold Mineralization in the Republic of Palau

James J. Rytuba, William R. Miller, and Edwin H. McKee

The Republic of Palau, a U.S. Trust Territory, is located in the western Pacific and consists of more than 200 islands alined along the 350-km-long Palau trench-arc system. The largest island, Babelthaup, is composed principally of late Eocene(?) to early

Miocene volcanic rocks. Basalts and basaltic-andesite flows and flow breccias of the late Eocene(?) Babelthaup Formation form the central and southeastern part of the island and are the oldest volcanic rocks in the arc. These volcanic rocks are characterized by high Ni (up to 190 ppm), Cr (up to 520 ppm), and Mg (up to 10.7 percent) concentrations and by low concentrations of the high-field-strength elements Zr ($\leq$ 40 ppm) and TiO_2 (< 0.6 percent). This geochemistry indicates a boninitic affinity and a similarity to the oldest volcanism in the Yap, Mariana, and Bonin arc-trench systems north of Palau. Younger basaltic andesites to dacites of the Medorm Member of the Ngeremlengui Formation occur in the western part of Babelthaup and have a K-Ar age of 35.6$\pm$2.5 Ma. Basaltic andesites of the Arakabesan Member form several small islands south of Babelthaup and have a K-Ar age of 34.3$\pm$1.5 Ma. These younger volcanics are characterized by low Ni and Cr contents and by higher amounts of high-field-strength elements than the Babelthaup Formation and belong to the island-arc tholeiite series.

Epithermal gold and base-metal mineralization occurred on the southeastern part of Babelthaup within basalt and basaltic andesite flows of the Babelthaup Formation. Mineralization consists of over 50 veins and silicified shear zones ranging in width from a few centimeters to several meters. The veins and shear zones have two preferred general orientations—north-northeast and north-northwest and are distributed over an area 1.5 by 1 km. Gold is present in all veins; channel samples across veins commonly contain 0.02–0.1 oz/ton. Te, Ag, Cu, and Zn are typically present in anomalously high concentrations in the veins. Sericite is present with quartz in the veins, and coarse crystals of epidote are locally present. Propylitic alteration is generally widespread in the country rock. Ore minerals include native gold, gold-silver-telluride, sphalerite, chalcopyrite, and, rarely, galena.

Effective geochemical sampling media in Palau were found to be heavy-mineral concentrates from stream sediments and the –80-mesh fraction of sediment from mangrove coast and swamp environments. Heavy-mineral concentrates delineated the mineralized zone through mineralogy (presence of Au, $CuFeS_2$, ZnS, PbS) and by the presence of strongly anomalous concentrations, in percent, of up to 0.07, Au; 1.5, Zn; 1.0, Cu; and 0.05, Ag. The –80-mesh fraction of sediment from the intertidal zone within the mangrove coast and swamp environments surrounding the island of Babelthaup contains anomalous amounts of Au up to 100 ppb adjacent to the mineralized zone as compared with 1–2 ppb outside the zone. Sampling of mangrove sediment combined with analysis of heavy-mineral concentrates provides an effective method for exploration for precious-metal resources in islands in the western Pacific.

Geochemistry of Precious- and Base-Metal Veins, Lake City Area, Colorado

Richard F. Sanford

Silver-gold-lead-zinc-copper veins associated with the 28-Ma Uncompahgre and the 23-Ma Lake City nested calderas near Lake City, CO, show geochemical anomalies that vary with area and with stratigraphic position. Veins hosted by Uncompahgre caldera fill contain relatively high concentrations of Ag and Au, whereas those in Lake City caldera fill have moderate Ag and Au values. Base-metal contents vary widely in both groups of veins but tend to be higher in the Uncompahgre caldera. Gold is most concentrated in veins cutting the higher parts of Uncompahgre caldera fill, but Ag shows no similar stratigraphic control. Veins cutting Proterozoic granite adjacent to the two calderas have relatively high Au concentrations. Lead isotopic ratios of galena indicate similar groupings of veins. These variations reflect local control by source rock and conditions of deposition but not age of mineralization.

Base and precious metals, as well as other trace elements, show several statistical associations that reflect the mineral content of the seven sets of veins. Groups 1 (Mo-Tl-Ba-As) and 2 (Mo-Li) are mainly within the Uncompahgre caldera; groups 3 (Cu-As-Sb-Ag-Fe-Hg-Te-Bi-Pb), 4 (Zn-Cd-Pb-Cu-Bi-Au-Fe), and 5 (U-Au-Te) are found in both calderas; and groups 6 (Th-rare earth elements-P) and 7 (Be-In-Sn-Mn) are largely limited to the Lake City caldera. Group 1 characterizes molybdenite-bearing quartz veins cutting Uncompahgre caldera fill in the southwestern part of the area. Group 2 reflects molybdenite(?) in veins of the Uncompahgre caldera in the northeastern part of the area. Group 3 reflects tetrahedrite (including Ag-, Sn-, and Te-rich varieties), tennantite, tellurides (for example, hessite), and minor base-metal minerals. This group includes the richest Ag ores. Group 4 elements are associated with low-grade base-metal ores consisting mainly of sphalerite, galena, chalcopyrite, pyrite, and minor tetrahedrite. Group 5 reflects uraninite, gold tellurides, and other tellurides and includes the most productive gold vein in the area. Group 6 characterizes thorite-monazite-apatite veinlets primarily from the Champion Mine

in the Lake City caldera. Group 7 elements are in quartz veins having barite(?) casts.

Lead isotope data from galena (Sanford and Ludwig, 1985) reveal that several separate hydrothermal cells with characteristic Pb isotope ratios operated in the area. The Pb isotopes from the Lake City caldera are relatively nonradiogenic ($^{206}Pb/^{204}Pb0$ = 18.6 and less) compared to those from the Uncompahgre caldera ($^{206}Pb/^{204}/Pb$ = 18.6 to 19.0). Galena in veins cutting Proterozoic rocks is typically the most radiogenic ($^{206}Pb/^{204}Pb$ = 19.0 and higher). Local exceptions can be explained by hydrologic variations within several hydrothermal circulation cells.

Geologic, geochemical, and radiometric evidence indicates multiple episodes of mineralization involving many local hydrothermal systems. Three broad groups of source rocks are suggested by the wallrock control on element and isotope distributions in the veins. Variations in the veins as a function of stratigraphy more likely indicate differences in conditions of transport and deposition.

Reference Cited

Sanford, R. F., and Ludwig, K. R., 1985, Lead isotopic evidence on the origin of hydrothermal veins, Lake City, Colorado: Geological Society of America, Abstracts with Programs, v. 17, p. 706.

The Red Dog Pb-Zn-Ag Deposit, Alaska—An Example of Nonexhalative Processes in the Formation of Syngenetic Massive Sulfides

Jeanine M. Schmidt and Robert A. Zierenberg

The Red Dog shale-hosted massive sulfide (SHMS) deposit of the Noatak district, northwestern Alaska, contains 77 million tonnes of 17 percent Zn, 5 percent Pb, and 82 g/T Ag. The deposit is owned by the Northwest Alaska Native Corporation; their operating partner is Cominco American, Inc. The U.S. Geological Survey, in cooperation with Cominco, has a multiyear research effort underway to study regional and deposit geology. Detailed (1 in. = 10 ft) mineralogic and textural logging of 12,000 ft of core from the Main ore body has been completed, as has reconstruction of geologic sections and petrography. Sulfide and sulfate S isotopic and fluid-inclusion studies are to follow.

The Red Dog deposit, hosted by siliceous black shale and chert of Carboniferous age, has a stratigraphic footwall that includes grey micrite and calcareous black shales and is overlain by barite and variably baritic gray and green chert and shale of Pennsylvanian to Permian age. The deposit, which consists of imbricated sulfide sheets overlying Cretaceous sandstones, was disrupted by northward-directed thrusting during the Jurassic-Cretaceous Brooks Range orogeny. Massive sulfides and pervasively silicified rocks are relatively rigid compared to the enclosing shales, so that much of the deposit is undeformed internally and preserves many primary and early diagenetic features.

Although Red Dog is classified as a SHMS deposit, it differs from other Pb-Zn deposits of the Noatak district and from other SHMS deposits worldwide. Silicified wallrocks and barite are common at Red Dog but minor in other Noatak district deposits. Silica and sphalerite are more abundant than Fe-sulfide phases. The δS^{34} values of Red Dog ores are near zero, and those from the nearby Lik deposit and many other SHMS have heavy (positive) δS^{34} values near contemporaneous seawater sulfate. Red Dog contains only rare laminated or bedded sulfides, is up to 150 m thick, and has no sediment interlayers or multiple sheets of sulfides. Much of the sulfide is semimassive with a "pseudobreccia" texture of remnant islands of an earlier generation silica sulfide, surrounded by irregular replacement fronts of later stages of mineralization; sulfide veining of sulfide is common.

The earliest phases of mineralization, which are best preserved at the edges of the deposit, where mineralization was less intense, provide evidence for ore genesis. Diagenetic growth of barite in unconsolidated mud was common before sulfide deposition. Early and massive barite commonly are replaced by sulfides and (or) by silica. Much of the silica rock and siliceous massive sulfide formed by replacement of unconsolidated mud, which produced polyhedral aggregates of quartz with cores of inclusion-rimmed hexagonal growth zones. Stylolites are common in calcareous shales, barite, silica, and semimassive ores.

Although many textures of the Red Dog deposit are the result of mineralization in unconsolidated sediment and below the sediment-water interface, other features suggest classic "exhalative" processes. Rarely preserved sedimentary structures indicate scour and resedimentation of sulfides. Tube-shaped trace fossils are interpreted as vent fauna that lived at or near the sediment-water interface during sulfide deposition. Subsurface mineralization at Red Dog may have contributed to the large size and high grade of the deposit because an overlying sediment and (or) silica cap effectively confined the hydrothermal fluid and prevented the loss of metals by dispersion in a buoyant plume.

The Saxapahaw, North Carolina, Gold Occurrences—Search for a Deposit Model and New Remote Sensing Techniques

R. G. Schmidt, Alba Payás,[1] Pablo Gumiel,[1] and J. P. D'Agostino

Nonuniform distribution of gold within and near zones of intense siliceous high-alumina alteration near Saxapahaw, Alamance County, NC, suggests a model for gold mineralization that may be useful for exploration in the region. Remote sensing using Landsat Thematic Mapper (TM) data from forests and cultivated fields is proposed as a useful exploration tool.

The Carolina slate belt is a complex of late Precambrian to Cambrian metamorphosed volcanosedimentary epiclastic and volcanic rocks extending 600 km from central Georgia to southern Virginia. Near Saxapahaw, it is roughly 60 km wide and includes abundant dacitic crystal tuffs with lithic clasts.

Three types of intrusive rocks have been distinguished within the study area; two of these were intruded before greenschist facies regional metamorphism. The complex quartz diorite pluton at Saxapahaw, an elliptical body 3 x 10 km, may have influenced gold distribution. From relict grains of unreequilibrated plagioclase, we interpret at least part of the pluton to be postmetamorphic.

Intense siliceous premetamorphic high-alumina alteration is present in a very large northeast-trending zone intersected at right angles by the elongate quartz diorite pluton at Saxapahaw. The Snow Camp segment of the altered zone, southwest of the pluton, is 13 km long and several kilometers wide. Less well defined altered zones continue to the northeast of the pluton for 8 km. Within both segments, crystal tuffs have been converted to quartz-sericite or quartz-paragonite rock and, where alteration was most intense, to highly siliceous masses depleted in Na, K, and Ca and containing pods of quartz-pyrophyllite-andalusite-pyrite, locally minable as ore-grade pyrophyllite rock. This alteration is commonly texture destructive and has trace concentrations of Cu, Mo, and Sn associated with it.

Significant gold is restricted to sites 2–5 km distant on both sides from the pluton at Saxapahaw, which suggests that gold may have been introduced or remobilized by a hydrothermal system driven by the heat of the pluton. The most favorable environments for precipitation seem to have been present in siliceous sericite-bearing zones, but the paucity of gold in the southwestern part of the early siliceous high-alumina alteration system suggests that gold mineralization postdates that alteration event. We propose that introduction or mobilization of gold probably took place in preexisting altered zones and may even have been postmetamorphic and related to younger intrusive rocks.

The study of Landsat TM data has permitted delineation of known and new areas of intense hydrothermal alteration. Spectrally anomalous soils in plowed fields have been correlated with potassic altered subvolcanic intrusive bodies. Deciduous forests in areas of intense hydrothermal alteration have a distinctive appearance on digitally processed falsecolor TM images.

We suggest that spacial juxtapositions of large siliceous alteration zones and young plutonic bodies be identified because of their potential for

Stibiconite, $Sb_3O_6(OH)$, along a fracture in silicified Paleozoic carbonaceous limestone from the Enfield Bell gold mine, Jerritt Canyon district, Nevada. Stibiconite is an alteration product of stibnite and is a good mineralogical indicator of the presence of antimony, which is commonly enriched in sedimentary-rock-hosted disseminated gold deposits.

[1]Instituto de Geologico y Minero de España, Rios Rosas 23, Madrid 28003, Spain.

containing undiscovered gold deposits. TM and other Landsat-derived data have been particularly useful tools for finding areas of hydrothermal alteration.

Microcomputer Systems for Geologic Map Compilation and Drafting

Gary I. Selner, Richard B. Taylor, and Bruce R. Johnson

The advent of relatively inexpensive microcomputers and affordable high precision digitizers and plotters makes possible office-scale digital systems for aquisition, editing, and plotting of map data. GSDRAW and GSMAP (Selner and others, 1986) are programs for microcomputers that assist geologists and illustrators in compilation and publication drafting of geologic maps and illustrations. These programs attempt to do for geologic maps what digital word processing has done to facilitate composition and publication of text. As a set of practical "graphics programs" designed to produce geologic maps and other illustrations, they enable digital compilation of graphical elements, ease the process of modification in response to second thoughts and editorial comments, enable scale and projection changes, and lead from initial compilation to publication without redigitizing or redrafting.

GSDRAW is based on storage of X-Y coordinate data unique to each illustration, and GSMAP is based on storage of geodetic coordinates (latitude-longitude); otherwise, the two programs are very similar. GSDRAW is used for illustrations, cross sections, and maps where either latitude-longitude grid is not available or the use of a latitude-longitude system is not necessary. GSMAP is used for geologic maps using Universal Transverse Mercator or Lambert Conformal Conic map projections. A basic set of line types (such as thrust fault) and geologic symbols (such as strike and dip, foliation, lineation) has been included. Additional symbols can be added as needed by computer-oriented users. These programs are designed for plotter output. Screen graphics are used to assist digitizing and editing.

GSDRAW and GSMAP have been designed for use on IBM PC and compatible microcomputers, plotters using Hewlett-Packard Graphic Language plot commands, and GTCO digitizers (modifications for other kinds of digitizers are relatively simple).

Additional programs of interest to geologists that utilize the same hardware environment are either available or in the development process. The source code and compiled versions are included with the open-file reports that document the programs.

Reference Cited

Selner, G. I., Taylor, R. B., and Johnson, B. R., 1986, GSDRAW and GSMAP—Prototype programs for the IBM PC or compatible microcomputers to assist compilation and publication of geologic maps and illustrations: U.S. Geological Survey Open-File Report 86–447A, B, 8 p.

Comparative Studies of Modern and Ancient Sediment-Hosted Massive Sulfide Deposits

Wayne C. Shanks III

Sediment-hosted mafic volcanic-associated massive sulfide deposits are of economic interest because of their size and polymetallic nature, in some cases including relatively high precious-metal contents. Tectonic setting, local structure, depositional environment, metal and sulfur sources, and chemical state of the ore fluid and water column are factors that control ore formation. Metal and sulfur sources and ore fluid chemistry can be inferred from stable isotope studies of some ancient deposits, but, for highly deformed and metamorphosed deposits, study of modern analogs is of paramount importance.

Guaymas Basin, formed by active rifting in the Gulf of California, is filled with several hundred meters of siliceous-calcareous biogenic sediment and interlayered turbidites. Diabase sills and dikes of midocean ridge basalt (MORB) affinity intrude the sedimentary sequence to within a few meters of the sediment-water interface. Seawater hydrothermal circulation surrounding the sills and dikes alters the sediments to greenschist facies assemblages and produces up to 312°C vent fluids. Hydrothermal mounds and elaborate "pagodalike" chimney structures are dominantly calcite, barite, anhydrite, pyrrhotite, marcasite, and silica; sphalerite, galena, and chalcopyrite are important "ore" minerals. Sulfur isotope values of sulfides range from −3.7 to +6.7 per mil; ranges are smaller for each of three clusters of deposits related to separate diabase sills. Sulfide in the deposits is derived from the following sources: (1) basaltic sulfide with sulfur isotope values near 0 per mil, (2) sedimentary bacteriogenic sulfide with strongly negative values, and (3) isotopically heavy sulfide from hydrothermal reduction

of seawater sulfate. Carbon isotope values of hydrothermal calcite ranges from −9.6 to +14.0 per mil (Peedee belemnite), indicating 30- to 50-percent derivation from marine organic carbon in the sediment column. Oxygen isotope values of 7.3–10.8 per mil (Standard Mean Ocean Water) give temperatures from 214 to 311°C (for equilibrium isotopic exchange with 2.0 per mil water) in good agreement with measured vent temperatures.

The newly discovered massive sulfide deposits on Gorda Ridge, within the Exclusive Economic Zone off northern California, occur in a somewhat different setting where basaltic volcanic domes penetrate to the seafloor through 0.5–1 km of sedimentary cover. Massive, extensive hydrothermal deposits rich in marcasite, pyrrhotite, barite, and talc flank and overlie the domes; some samples are extremely rich in Cu, Zn, Pb, and Ag. These deposits have little calcite or anhydrite due to lack of carbonate in the underlying sediments. Sulfur isotope values of sulfides (1–10 per mil) reflect only basaltic and seawater components; underlying sediments are not reducing and lack isotopically light biogenic sulfides. Large deposit extent may be related to the large thermal mass of the volcanic domes.

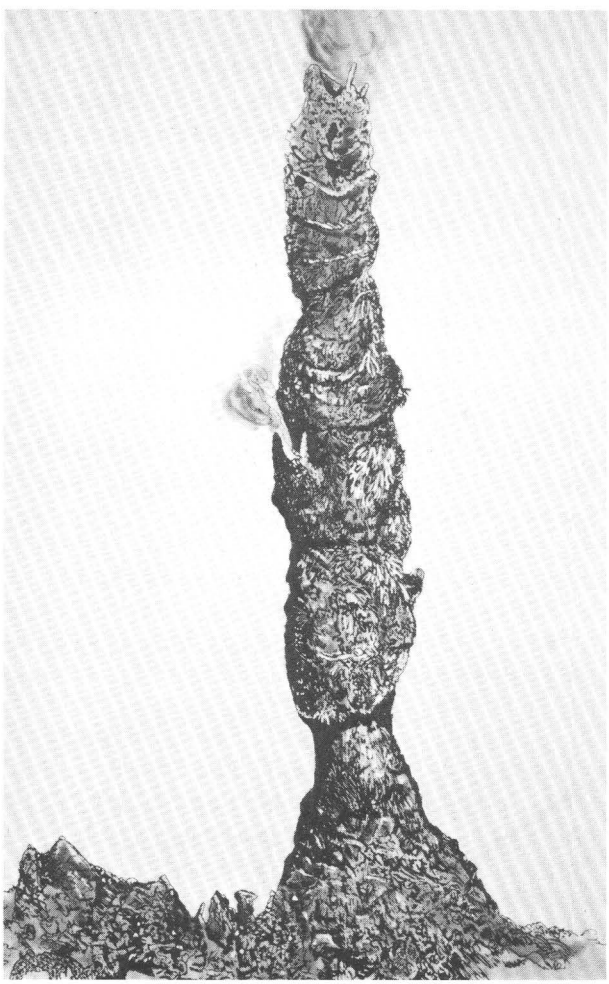

Interpretive drawing of a 9-mm-high chimney from the Vent 1 site, southern Juan de Fuca Ridge, based on a photomosaic assembled from *Alvin* external photographs. Drawn by Calvin Fontaine.

Possible ancient analogs of the Guaymas and Gorda deposits include the Besshi and related deposits, Japan; Goldstream, British Columbia; and Ducktown, Gossan Lead, and Elizabeth in the U.S. Appalachians. The Elizabeth deposit and other deposits of the Vermont copper belt occur in intensely deformed and metamorphosed Ordovician(?) dominantly metapelitic rocks with minor metavolcanic rocks. The Elizabeth and Ely deposits, which occur in the noncalcareous Gile Mountain Formation, have sulfur isotope values ranging from 4.3 to 9.4 per mil. The Gove and Cookville deposits, which are contained within the Standing Pond Volcanics, and Pike Hill, which is in the calcareous metapelites of the Waits River Formation, have sulfur isotopic values from 1.5 to 4.7 per mil. Standing Pond Volcanics, a thin extensive unit of MORB affinity, has disseminated sulfides with isotopic values from 0.5 to 1.6 per mil. Two- and three-component sulfur source models, as in the modern deposits, also may be applied to the massive sulfides of the Vermont copper belt.

Electronic Structures and Spectra of Minerals—Basic Research To Help the Development of Spectroscopic Remote Sensing and Geophysical Exploration Techniques

David M. Sherman

Many exploration techniques that exploit the spectroscopic and other physical properties of minerals have been based largely on empirical grounds. To help develop new assessment techniques, however, we must know the physical basis for these properties. Such information is provided by the electronic structures of minerals.

The electronic structure of a solid defines the energies and wavefunctions of its electronic and vibrational states. Transitions between such states give rise to the absorption bands observed in the infrared, visible, and near-ultraviolet spectra of minerals. Such spectra, in turn, are used in spectroscopic remote sensing techniques for the identification of minerals on the Earth's surface. The electronic structure of a solid also determines its

magnetic and electrical properties and, ultimately, its chemical behavior.

Of particular interest are the electronic structures of transition metal oxides, silicates, and sulfides. These phases cause absorption bands in the visible region of remotely sensed spectra and the electrical or magnetic anomolies observed with geophysical exploration techniques. These phenomena are a direct consequence of the partially occupied 3d electronic orbitals of transition-metal cations. The electronic structures of transition metal oxides and silicates are best obtained by using a "cluster molecular orbital" approach. Here, one calculates the electronic structure of a finite cluster of atoms that represents some structural unit of the crystal; for example, much of the electronic structures of Mn oxides can be understood in terms of the electronic structures of MnO_6 clusters. Such clusters represent the Mn coordination polyhedron, and, from their electronic structures, we can interpret the ultraviolet and visible region spectra of manganese oxides and silicates. The reason that small clusters can often give an accurate description of the electronic structures of minerals is because in nonmetals, each electron tends to be localized to a single atom. This is in accordance with the partial ionic character of most transition metal oxides and silicates.

In a number of minerals, however, the metal d-electrons are not localized. When this happens, electrons can hop among different metal cations by way of thermally and optically activated processes. Optically activated electron hopping results in strong absorption bands in the visible spectral region of minerals and is responsible for the strong colors and pleochroism of numerous transition metal silicates. Thermally activated hopping (restricted to mixed valence minerals) can result in semiconduction as in magnetite. Indeed, probably all bulk electronic conduction with activation energies less than 1.0 eV in oxides and silicate minerals is due to thermally activated electron hopping. Understanding the nature of electron hopping in minerals, therefore, is important for understanding their electrical and spectroscopic properties.

The research being done to address these problems consists of (1) electronic structure calculations on transition metal coordination polyhedra (for example, FeO_6, MnO_6 clusters), (2) measurement and interpretation of the ultraviolet, visible, and near-infrared spectra of transition metal oxides and silicates, and (3) electronic structure calculations on larger clusters to understand the nature and mechanisms of electron hopping processes.

Alteration and Mineralization in the Monterrosas Copper-Iron Deposit, Peru

Gary B. Sidder

At the Monterrosas Mine, copper-iron ore is hosted by gabbro and diorite of the Late Cretaceous Coastal Batholith of central Peru. Chalcopyrite, pyrite, and magnetite in variable proportions, with gangue of actinolite, sodic scapolite, apatite, tourmaline, and quartz, form the vertical tabular ore body, which is about 430 m long, 3–20 m wide, and at least 110 m deep. Minor amounts of cubanite and pyrrhotite are present as blebs and as intergrowths with chalcopyrite in pyrite. The ore body contains 1.9 million tons that average about 2 percent Cu. The grade of Cu ranges from 0.2 to 15 weight percent. Au (0.03 oz/ton), Ag (0.7 oz/ton), Co ($\leq$5,000 ppm), and Mo ($\leq$200 ppm) are present in recoverable quantities, and Ni ($\leq$200 ppm) and Ga ($\leq$200 ppm) occur in anomalously high concentrations. Fe, as massive magnetite, attains grades of 60 percent or more; however, it is not recovered.

Alteration effects are widespread in gabbro and diorite and become more intense with increasing proximity to the ore zone. Secondary minerals, such as actinolite, sodic scapolite, epidotes, diopside, sphene, magnetite, chlorites, apatite, sericite, sulfides, and tourmaline, formed as late magmatic to hydrothermal replacements of the primary magmatic assemblage (labradorite-andesine, diopside, actinolitic hornblende, ilmenite, and apatite) and as fracture fillings. The abundance of alteration minerals decreases from >70 to <10 modal percent away from ore. Boundaries between the ore zone and altered gabbro-diorite wallrocks are indistinct. At the periphery of the ore body, a zone of finely to coarsely crystalline actinolite ($\leq$5 cm) that contains disseminated and stringer oxide and sulfide minerals is immediately adjacent to actinolitized gabbro-diorite wallrocks. This zone grades into one of massive magnetite that also hosts stringers and blebs of sulfides and actinolite; this, in turn, grades into a central zone that consists of massive sulfide with minor magnetite, actinolite, and other gangue. The size of the two outer zones may differ on either side of the high-grade sulfide zone, and the width of the ore zone changes along the strike.

Metasomatic exchange of major and minor elements between hot saline fluids and gabbro and diorite characterizes the mineralization. Metasomatism involved the addition of FeO_t, K_2O, and MgO and the ore-forming metals to the host rocks, with

the accompanying depletion of SiO_2, CaO, Na_2O, TiO_2, and, possibly, Al_2O_3. These gains and losses define an alteration index that is correlative with the distance to ore, the intensity of alteration, and the concentration of Cu. The metal-enriched, saline (53+ to 43 weight percent NaCl), magmatic ($\delta^{34}S$, 1.6–3.3 per mil) hydrothermal (500+ to 350°C) fluid migrated into mineralized parts of gabbro and diorite along fractures.

Textures, such as bent and broken crystals of plagioclase, a continuum from deuteric to hydrothermal alteration, and cross-cutting relations between ore and alteration minerals, indicate that mineralization was initiated during late magmatic crystallization of the gabbro and diorite magma. The proposed genetic model suggests that progressive crystallization of primary magmatic minerals resulted in the residual concentration and segregation of Fe, H_2O, Cl, P, and other volatiles and metals. Faults and fractures produced by magmatic pressures and (or) tectonism provided channelways for movement of the mineralizing fluids to depositional sites also within gabbro and diorite. Deposition of ore and alteration minerals resulted from decreases of temperature and acidity because of metasomatic reactions between the hydrothermal fluids and the early formed gabbro-diorite wallrocks. Thus, the Monterrosas deposit is similar to other amphibole-rich Cu-Fe deposits in Peru and Chile and resembles some skarnlike replacement deposits of Fe.

Mineral-Resource Assessment of the Glens Falls 1° x 2° Quadrangle, New York, Vermont, and New Hampshire

John F. Slack

A multidisciplinary study of the Glens Falls 1° x 2° quadrangle was carried out under the auspices of the U.S. Geological Survey Conterminous United

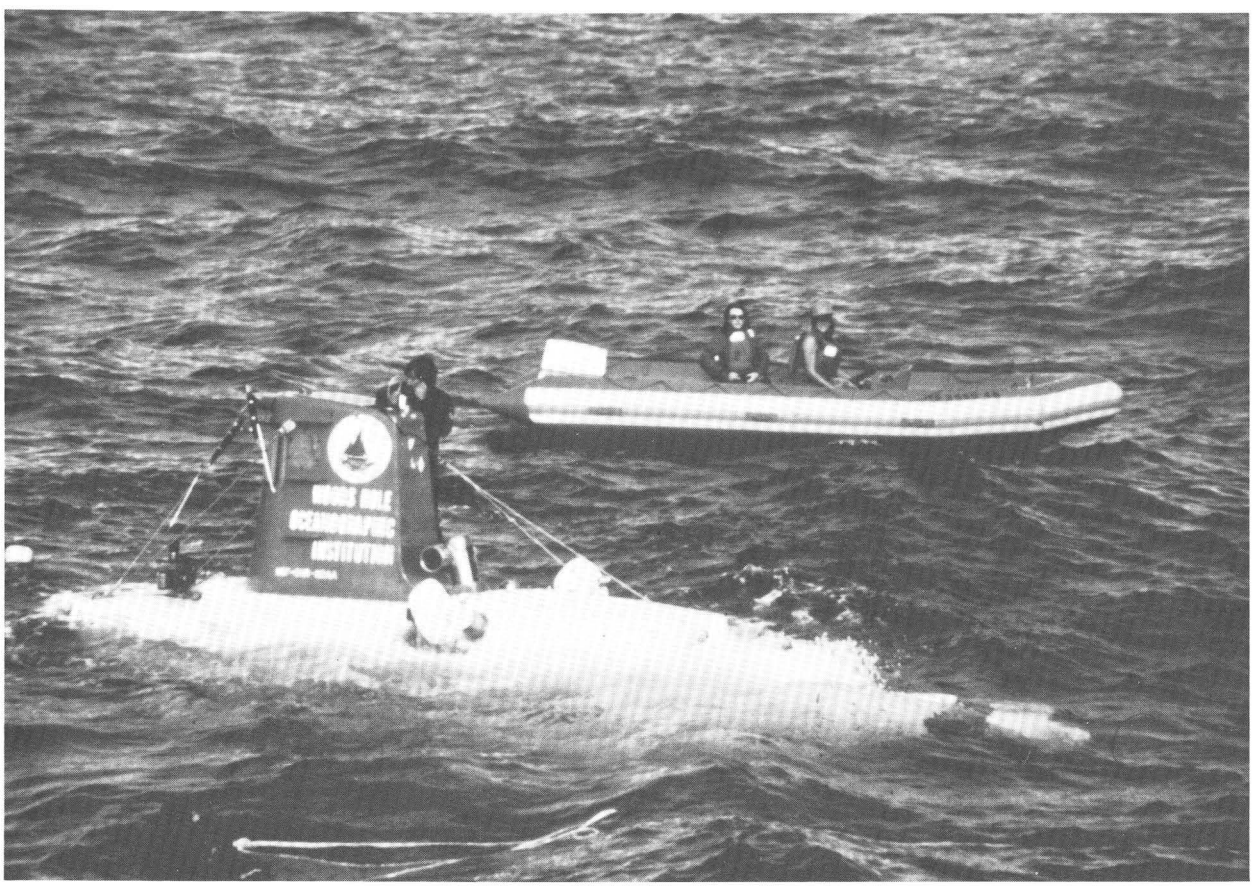

Alvin after surfacing from a U.S. Geological Survey research dive. The research vessel is met by crew members in wet suits who will secure lines on the submersible vessel, which is owned by Woods Hole Oceanographic Institution and funded by the National Science Foundation, the Office of Naval Research, and the National Oceanographic and Atmospheric Administration.

States Mineral Assessment Program (CUSMAP) from 1982 through 1986. The overall mineral-resource assessment is based on a variety of new data acquired during the CUSMAP project. Included are (1) geologic mapping, (2) regional geochemical sampling (principally panned concentrates), (3) magnetic, electromagnetic, and gravity surveys, (4) Landsat and radar lineament studies, (5) geobotanical remote sensing, (6) compilation of the locations of known mines, prospects, and mineral occurrences, and (7) topical studies of individual mineral deposits.

The assessment reported here involves qualitative rather than quantitative methods of mineral-resource appraisal. Lacking detailed grade and tonnage data for a variety of metal commodities and deposit types, a simplified technique of diagnostic and permissive recognition criteria is employed to assess mineral-resource potential. Three main criteria are used—favorable geology, geochemical anomalies, and known mineral occurrences. These criteria are integrated with applicable ore deposit models to evaluate potential for a variety of metallic mineral deposits; nonmetallic deposits, although important, are not considered. Areas with one recognition criterion are ranked as having low resource potential; areas with two or three criteria are assigned moderate or high resource potential, respectively.

Metallic mineral resources in the Glens Falls quadrangle include previously known deposits and also several newly recognized deposit types. In the former category are (1) volcanogenic massive sulfides (Elizabeth, VT), (2) stratabound low-Ti magnetite deposits (Hammondville, NY), (3) discordant gold-quartz veins (Taggart, VT), (4) high-Ti magnetite deposits in anorthosite and gabbro (Moose Mountain, NY), (5) residual iron and (or) manganese deposits (Brandon, VT), (6) stratabound uranium deposits in Grenville basement rocks (Jamaica, VT), (7) small gold-rich pyrrhotite replacement deposits (Cuttingsville, VT), (8) uranium in Carboniferous two-mica granites (Sunapee, NH), and (9) small vein deposits containing a variety of metallic commodities (Holts Ledge, NH, Thetford, VT).

Areas having moderate to high resource potential for previously unrecognized (in part, speculative) deposit types in the quadrangle include (1) volcanogenic gold in the volcanic belts of east-central Vermont and west-central New Hampshire, (2) porphyry-related gold associated with the alkaline intrusive complex (Cretaceous) at Cuttingsville, VT, (3) stockwork (or possibly Carlin-type) gold in black slates and limestones of the Taconic allochthons in New York and Vermont, (4) sedimentary-exhalative (sedex-type) polymetallic sulfides in the Taconic allochthons, (5) vein- and (or) greisen-type tin-tungsten deposits associated with Devonian and (or) Carboniferous granitoid intrusions in western New Hampshire and parts of eastern Vermont, (6) tin-tungsten-molybdenum-fluorine in late (extensional) faults in the eastern Adirondacks, NY, and in western New Hampshire, (7) skarn-type tungsten deposits related to Devonian granitoids in eastern Vermont, (8) concentrations of rare earth elements associated with some of the stratabound (low-Ti) magnetite deposits of the eastern Adirondacks, (9) possible volcanogenic gold in aluminous, graphitic, and pyritic metasedimentary sequences of the eastern Adirondacks, (10) stratiform (Irish-type) lead-zinc-silver deposits in the early Paleozoic shelf sequence of western Vermont and eastern New York, and (11) uranium concentrations in peat in western New Hampshire and central Vermont.

$^{40}Ar/^{39}Ar$ Thermochronology of Mineral Deposits—Information on Age, Duration, Number of Episodes, and Temperature of Mineralization

Lawrence W. Snee

High-precision $^{40}Ar/^{39}Ar$ age-spectrum dating, a variant of the conventional K/Ar technique, is proving useful for solving some of the long-standing problems in economic geology, which have been, until recently, unresolvable. These problems include the age, duration, number of episodes, and temperature of mineralization. The method can provide mineral dates with very small analytical errors (~0.25 percent), thus offering the level of precision needed for dating the episodes of mineralization and alteration of hydrothermal systems. This technique also provides information about the distribution of Ar in the mineral or "whole rock" analyzed, whether the material formed before, during, or after an alteration event. Even strongly altered wallrock minerals can often yield meaningful geochronological data. With advantages for high precision and application to altered or unaltered materials, questions of the actual duration of a mineralization event can be addressed. In many cases, $^{40}Ar/^{39}Ar$ age-spectrum dates provide geothermometric, as well as geochronologic, information because such dates are actually determinations of the time and temperature at which a mineral closed to the diffusion of Ar. In this respect, $^{40}Ar/^{39}Ar$ data are unique in that they link temperature and time, providing a

"thermochronology." These time-temperature data are fundamentally significant to the understanding of ore-forming processes. Two areas where this technique has provided valuable data are a Sn-W mine in Panasqueira, Portugal, and the central Idaho batholith.

In a study of the Hercynian-aged Panasqueira Sn-W deposit, highly precise age differences were distinguished. Muscovite samples with an age difference as small as 2.2 Ma (0.7 percent of the mineralization age) are statistically distinct. Statistics are even better for comparison of multiple samples from separate events; that is, a difference of 0.9 Ma (0.3 percent) can be resolved. The total duration of thermal activity for the Sn and W ore-forming stages was at least 4.20 ± 5 Ma (1 σ). Within that time-span, the age and duration of the first substage of the oxide-silicate stage, greisenization, and silica cap alteration, in that order, are resolvable. Minor Ar loss from all dated samples occurred during later reheating, probably during the later, longer lived pyrrhotite alteration stage. Studies of cross-cutting relations and fluid-inclusion homogenization temperatures (Kelly and Rye, 1979) resulted in calibration of the Ar-retention temperature of muscovite. By combining the Ar retention temperature of muscovite with the age spectrum characteristics of the muscovite from a thermally complex area, constraints on the temperatures and relative durations of thermal episodes can be defined.

In several mining districts in the central Idaho batholith a complex series of hydrothermal events occurred during the Cretaceous. High-precision $^{40}Ar/^{39}Ar$ age-spectrum dates that range from 78 to 70 Ma were determined for muscovites and adularia from sulfide-bearing quartz veins with associated Au, W, Sb, Hg, Pb, and Ag. Even though Eocene hydrothermal activity has been considered important in this area, age spectra of muscovites and microclines collected near Eocene dikes, plutons, and volcanic centers indicate Cretaceous ages modified by partial ^{40}Ar loss incurred during post-Cretaceous events. Thus, after Cretaceous time, except in areas near intense Eocene thermal activity, the central Idaho batholith remained below 130°C (Ar-retention temperature of microcline). The ages of the quartz-vein deposits are similar to emplacement and cooling ages of Cretaceous plutons. The $^{40}Ar/^{39}Ar$ data provide constraints for the cooling history of plutons and quartz veins and thus yield evidence for depth of formation and genesis of the mineral deposits.

Reference Cited

Kelly, W. C., and Rye, R. O., 1979, Geologic, fluid inclusion, and stable isotope studies of the tine-tungsten deposits of Panasqueira, Portugal: Economic Geology, v. 74, no. 8, p. 1721–1822.

A Link Among ^{34}Sulfur-Rich Pyrite in Greenish-Gray Shales, Ferric Iron From Smectite as It Converts to Illite, Kinetics of Sulfur Redox Reactions, and the Genesis of Mississippi Valley-Type Deposits

Charles S. Spirakis and Allen V. Heyl

Theoretical arguments supported by chemical and isotopic data (Maynard, 1980) indicate that shales deposited during rapid sedimentation (shallow basin-margin environments) have low amounts of organic matter (<0.3 percent), are green to grey in color, and contain isotopically heavy S (up to +29 per mil) in pyrite. The similarity of these isotope values to S isotope values in Mississippi Valley-type (MVT) deposits suggests that greenish-grey shales are a possible sulfur source. However, mobilization of S from pyrite requires oxidation. One of the few oxidizing agents of significant abundance in pyrite-bearing shales is ferric Fe, much of which is bound initially in smectite but is released as smectite converts to illite. The conversion reaction is triggered by heat in excess of about 80°C. Released ferric Fe initially will oxidize organic matter to produce organic acids and CO_2; in shales with a high ratio of smectite to organic matter, sufficient ferric Fe will remain after the oxidation of organic matter to oxidize S in pyrite. Kinetics indicate that, even to temperatures as high as about 230°C (well above the regional temperatures around ore districts), the oxidation yields long-lived metastable concentrations of partly oxidized S species rather than sulfate. Addition of the partly oxidized S-bearing solution from shales to basinal solutions containing Pb and other metals can produce the mineralizing solutions. Experiments have shown that at temperatures of MVT sulfide mineralization, partly oxidized S species will be reduced quickly to sulfide by organic matter (a ubiquitous component of the deposits). Because reduction of partly oxidized S species in the mineralizing solution by organic matter at the sites of mineralization is rapid, sulfide S is produced without fractionation of isotopes. Therefore, precipitated sulfide

minerals have isotopic values similar to the S isotopes in pyrite in greenish-grey shales. Although sulfate from evaporite minerals or from the oxidation of pyrite (*IF* sulfate, rather than partly oxidized species, were to form) would contain isotopically heavy S, the kinetic inhibition of sulfate reduction at temperatures of mineralization precludes sulfate reduction as a sulfide source—a constraint exacerbated by the requirement of near complete reduction of the S species to obtain the heavy S in the ores.

The organic acid- and CO_2-bearing, but S-poor, solutions initially released during the clay conversion reaction may contribute to the presulfide-stage dissolution of carbonates associated with MVT deposits. The large quantities of Mg and Si released from the conversion of smectite to illite provide sources of these elements for the characteristic dolomitization and silicification of ore zones and solution pathways.

The proposed scheme incorporates the relation between depositional environment and the chemical and isotopic character of shales with the chemistry of clay conversion reactions and with the kinetics of S redox reactions into a model that explains the genesis of the deposits as an aspect of the evolution of sedimentary basins. The model is consistent with the evidence for a single mineralizing solution (rather than mixing at the sites of mineralization) and with the evidence for reduction of a S species by organic matter at the sites of mineralization but is not constrained by the prohibitively slow reduction of sulfate.

Reference Cited

Maynard, J. B., 1980, Sulfur isotopes of iron sulfides in Devonian-Mississippian shales of the Appalachian Basin—Control by rate of sedimentation: American Journal of Science, v. 280, p. 772–786.

Neutralization Of Acidic Ground Water Near Globe, Arizona

Kenneth G. Stollenwerk and James H. Eychaner

Acidic solutions related to mining and milling processes are seeping into ground water in the Globe-Miami area of Arizona. As a result, a plume of acidic ground water containing large concentrations of dissolved solids and metals is moving through the shallow aquifer system of the area. The contaminant plume is about 17 km long and 600 m wide. The aquifer consists of alluvium and conglomerate derived from granite, schist, granite porphyry, and volcanic rocks and discharges about 0.3 m^3/s of water to a perennial stream. Sediment size ranges from clay to boulders, and calcareous cement content increases with age of sediment. This study was designed to evaluate the potential effects of the acidic plume on water quality downgradient from the plume and in the underlying freshwater aquifer.

Maximum concentrations of selected constituents in the plume are 3,000 mg/L Fe(II), 200 mg/L Cu, 300 mg/L Al, and 16,400 mg/L dissolved solids; the minimum pH in the plume is 3.3. Using the geochemical computer program PHREEQE, solute speciation indicates that aqueous sulfate complexes in conjunction with low pH are responsible for the solubility of the metals. Adjacent uncontaminated water has trace concentrations of metals, as little as 400 mg/L dissolved solids, and neutral pH.

Samples from 16 polyvinyl chloride-cased observation wells are representative of uncontaminated, contaminated, transition, and neutralized water. Chemical reactions with sediments and mixing with uncontaminated water neutralizes the acidic water. The reactions form a transition zone between contaminated and neutralized ground water where gypsum replaces calcite and most metals precipitate. Abundant gypsum crystals and sediments with ferric hydroxide coatings have been recovered from well cuttings. Although the most significant and rapid reactions involve carbonate minerals, alteration of igneous and metamorphic minerals collected from the plume indicates that they also affect solute composition.

Solubility differences result in a chromatographic effect where more soluble elements have been transported a greater distance. Increased Mn and sulfate concentrations have been measured in the perennial streamflow leaving the study area, 81 km downvalley from the acidic plume.

Trace-Element Source for Contamination of Agricultural Drainage Flowing Into Kesterson National Wildlife Refuge, Merced County, California

R. R. Tidball, R. C. Severson, J. M. McNeal, P. H. Briggs, and K. R. Kennedy

Agricultural drainage water derived from the San Luis irrigation district, San Joaquin Valley, CA, is contaminated by Se that has caused high mortality

among nesting birds and aquatic life in Kesterson National Wildlife Refuge. Several hundred soil samples were collected in the irrigation district (Panoche Creek fan study area in fig. 1) and throughout the San Joaquin Valley to identify possible source areas for Se and other elements. All samples were analyzed for total concentrations of 48 elements. Se and Hg anomalies were identified within the irrigation district with maximum values of 4.5 and 2.5 ppm, respectively. A second Se anomaly occurs in the Antelope Hills area in western Kern County, CA, with maximum values of 2.5 ppm, but this area is not a source for Kesterson.

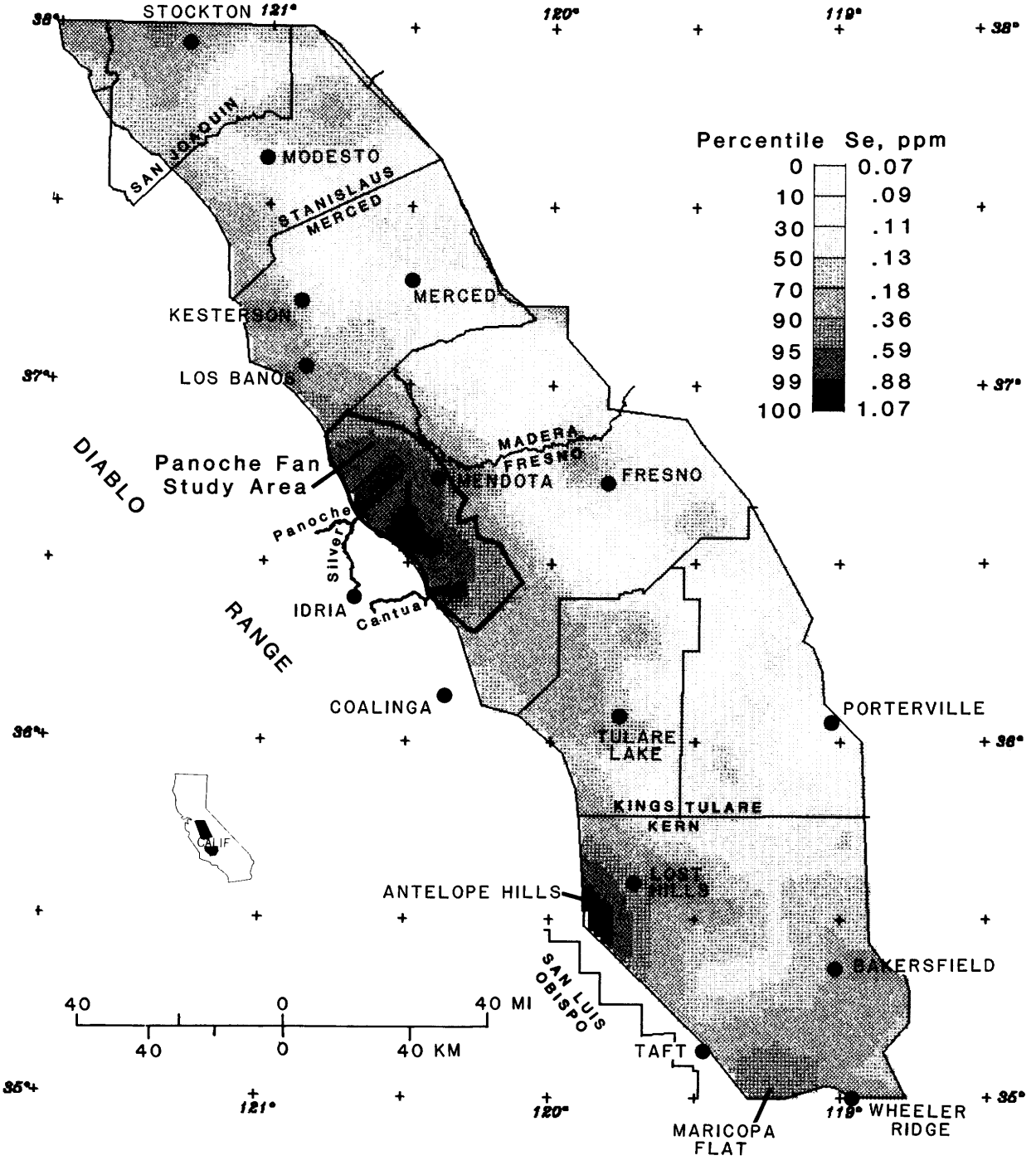

Figure 1. Map of total selenium at 0–30 cm depth in soils of the San Joaquin Valley, CA. Gray scales delineate percentiles of the frequency distribution.

R-mode factor analysis showed associations of (1) Se with S, which reflect their common occurrence, (2) Ni, Mg, Cr, Co, Mn, and Fe, which indicate a serpentine source, and (3) C and Hg, which indicate that organic matter and Hg-rich sediments occur together. Hg is dispersed on the Panoche Creek fan that probably originates from the New Idria Hg district. The present host for Se in the interfan area between Panoche and Cantua Creeks appears to be mudflow-type deposits derived from adjacent fine-grained sedimentary rocks. Se in a broad halo around the New Idria Hg district may have migrated into the surrounding sedimentary rocks.

Some Characteristics of Gneiss-Hosted Gold Deposits of Southeastern California

R. M. Tosdal and D. B. Smith

In southeastern California, gneiss-hosted gold mineralization occurs at the American Girl and Padre Madre Mines in the Cargo Muchacho Mountains and at the Mesquite Mine and Black Mountain Prospect in the Chocolate Mountains. The style of gold mineralization is distinct from epithermal detachment fault-related gold deposits, such as at the nearby Picacho Mine.

Two distinct amphibolite facies gneiss units host the gold deposits. The older unit consists of quartzofeldspathic gniess, which is derived from silicic volcanic and sedimentary protoliths; this unit is known locally as the Tumco Formation. Euhedral and embayed quartz and plagioclase blastophenocrysts suggest the protolith is composed, in part, of pyroclastic rocks or hypabyssal porphyry intrusive rocks. The younger gneiss unit consists of metamorphosed granitoids, ranging in composition from diorite to granite, that intruded the supracrustal rocks before and during(?) regional metamorphism. Granite gneiss is associated spatially with several of the mineralized zones; in these locations, the granite gneiss is structurally higher than the quartzofeldspathic gneiss. The gneiss units and mineralized zones share the same fabric and are intruded by late- and post-kinematic aplite and pegmatite. Discordant U-Pb zircon dates for both gneiss units indicate Jurassic ages for their protoliths. The pegmatites are undated but are related spatially to the granite gneiss.

The gold occurs in shallowly dipping, tabular to lenticular bodies that are subparallel with the foliation. The bodies are along contacts between the two gneiss units or entirely within the quartzofeldspathic gneiss. The gold is either disseminated or in siliceous zones composed of ptygmatically folded and boudinaged quartz-magnetite layers or veins.

Metamorphic mineral assemblages and textures in the Cargo Muchacho district suggest two stages of synmetamorphic(?) hydrothermal alteration. The older assemblage is quartz + magnetite + biotite ± hornblende ± K-feldspar ± sulfide minerals and always occurs in well-foliated gneiss. Locally, the younger assemblage is superposed on the older assemblage in the quartzofeldspathic gneiss. Aluminous minerals, such as muscovite, biotite, and kyanite, along with quartz, ilmenite, rutile, tourmaline, and rare accessory minerals, compose the younger assemblage. These rocks are schistose, where micaceous and granofelsic, but vuggy, where composed of kyanite and quartz. Late stage and postmineralization alteration and deformation features include pyrophyllite replacing kyanite; local brittle fractures filled with clay, chlorite, and carbonate minerals; and limonite replacing sulfides and magnetite.

Geochemical anomalies from the mineralized areas are subdued and rather sporadic. Mineralized rocks in all areas have the following suite of elements in common: Au, Ag, As, Sb, Hg, W, Zn, and Te. In the Cargo Muchacho district, Cu, Bi, B, and F also are associated with gold mineralization.

A variety of genetic models have been proposed for one or more of the gneiss-hosted gold deposits. These are (1) metamorphosed gold-bearing chemical sediments, (2) metamorphosed epithermal deposits, (3) epithermal mineralization related to mid-Tertiary detachment faults, (4) mesothermal mineralization related to granitic rocks, either a peraluminous granite at depth or the exposed gneissic granite, or (5) synmetamorphic and synplutonic hydrothermal mineralization related to the exposed gneissic granite, which is interpreted as a synmetamorphic intrusion. Insufficient data is available to prove any of these genetic models.

Geochemical and Crystallographic Constraints on the Formation of the Vanadium-Uranium Ores of the Colorado Plateau

Richard B. Wanty, Joan J. Fitzpatrick, and Martin B. Goldhaber

The Colorado Plateau physiographic province contains many large deposits of V and U hosted in fluvial sandstones of the Salt Wash Sandstone

Member of the Upper Jurassic Morrison Formation; the deposits also are enriched in Fe. Although the deposits have been mined principally for U, they are actually V deposits with secondary U; on the average, V is two to five times more abundant than U on a weight basis. The ores formed epigenetically as these elements were transported in moderately oxidizing low-temperature waters to chemically reduced rocks that contained detrital plant fragments. The ore-mineral assemblage consists of coffinite and uraninite, with associated V oxide, vanadiferous chlorite, and vanadiferous illite-smectite. Fe is present in the V-bearing phases. Because U, V, and Fe have redox-sensitive solubilities, the geochemistry of these elements was studied to determine specific chemical processes that formed the ore.

Valence-specific analyses for V and Fe in the ore show that V(III) is more abundant than the more oxidized forms. Approximately two-thirds of the Fe is in the ferric (+3) state in the oxide and clay minerals. X-ray diffraction analysis of the V oxides (heavy fractions, >2.89 gm/cm^3) from unoxidized samples stored under N_2 show the presence of montroseite [(V,Fe)OOH] and the more oxidized paramontroseite (VO_2). The two phases were distinguished from each other on the basis of unit cell size and intensity differences between key reflections as indicated by the calculated intensity profiles for the two minerals. From a consideration of the diffraction characteristics of the paramontroseite, it appears that two generations are present—a good crystalline primary paramontroseite and a poorly crystalline oxidation product of primary montroseite.

V and U together are soluble under moderately oxidizing conditions as vanadyl (VO^{2+}) or uranyl (UO_2^{2+}) ions. Fe is soluble under reducing conditions but in the absence of dissolved sulfide. These elements may coexist in waters that are mildly oxidizing but anoxic; such a fluid probably transported the metals. V most likely was transported as VO^{2+} or some complex thereof. Possible ions that may have complexed the VO^{2+} include oxalate, fluoride, or carbonate. U probably was transported as UO_2^{2+}, most likely in a complex with carbonate. Dissociation of the complexes occurred in response to changes in pH or ionic strength, or possibly by bacterial metabolism of organic ligands, within the host rocks. Once removed from their complexes, V and U were able to react with H_2S, which was produced locally in the mineralizing zone by bacterial reduction of sulfate. The U was reduced and precipitated with silica in coffinite. The VO^{2+} either hydrolyzed and precipitated as paramontroseite or was reduced by the H_2S to form V(III), which precipitated as montroseite. Fe substituted in the V minerals because of its similar ionic size and charge. The fact that the Fe is mostly ferric indicates that the activity of H_2S could not have been very high, although the presence of ore-stage pyrite indicates that at least some of the Fe was reduced.

Geochemical Exploration Studies in the Glens Falls 1° x 2° Quadrangle, New York, Vermont, and New Hampshire

Kenneth C. Watts, Jr.

A regional geochemical survey of the Glens Falls 1° x 2° quadrangle was completed recently as part of the mineral-resource assessment under the Conterminous United States Mineral Assessment Program. A total of 1,286 heavy-mineral concentrates from the active sediment channels of small streams were collected. These data were supplemented by the collection of other forms of geochemical data and by published ground- and surface-water data from the National Uranium Resource Evaluation Program. Data from the nonmagnetic fraction of the heavy-mineral concentrates have produced the most useful mineral-resource information and are the chief basis of the findings reported here, although the other data have been integrated into the interpretations.

The Glens Falls area is separable into seven stratigraphic-tectonic areas composed of Precambrian and Paleozoic rocks with distinctive geologic history and somewhat dissimilar environments for the formation of mineral deposits. Several previously unrecognized zones of multielement anomalies of regional extent are shown to crosscut these terranes. These broad zones of anomalies evidently are related regionally to deep and shallow tectonic features and to specific lithostratigraphic units suggestive of stratabound metal occurrences.

One regional set of northeast-trending zones of anomalous elements that includes Pb, Cu, Sn, and Ba transects tectonic-stratigraphic terranes and coincides with N. 60°–65° W. radar lineaments that other workers interpret as a deep-seated continental fracture system that is printed through cover rocks.

Another regional zone has a geochemical signature of anomalous Sr, Ba, Nb, B, Fe, Pb, and Cu, is probably Mesozoic in age, trends east to west, and chemically overprints the geochemical signature of the older, regionally metamorphosed Precambrian

and Paleozoic rocks. This geochemical overprint appears to be related to rifting, and hydrothermal activity accompanied by the emplacement of postkinematic, alkalic plutons of the White Mountain series that have potential for precious base and rare metal deposits.

The regional geochemical data were interpreted in greater detail utilizing the following: (1) element associations and zonations determined by comparison of single-element map plots and R-mode factor analyses, (2) mineralogy of the samples, and (3) supplementary geochemical data. Interpretations were made by using ore-deposit models most appropriate to each of the geologic settings.

R-mode factors that account for the most data variance, in order of decreasing contribution for the overall quadrangle, include (with the most strongly loaded elements in order) (1) V, Nb, Ti, B, Mn, Cr, Cu, Fe, and Mg—largely a rutile-tourmaline association, (2) La, Mg, Sc, Y, and B—an accessory mineral association that, at least in part, is related to pegmatites, (3) Ni, Co, As, Fe, and Cu—a pyrite-pyrrhotite association, (4) Sn, Pb, Sb, Ba, and Cu—a barite association chiefly found in the allochthonous, eugeosynclinal sequence of the Taconic Ranges, (5) Ca, Sr, Mn, and Co—a carbonate-oxide mineral association that, at least in part, is derived from zones of hydrothermal carbonization not related geographically to the distribution of the main calciferous lithologies, and (6) W, Bi, Mo, and Be—a scheelite association most typical of areas east of the Connecticut River where it is associated with domes and metavolcanics.

Discrete areas of multielement anomalies probably are related to (1) the location of metavolcanic centers and proximal hydrothermal vent areas (Cu, Pb, B, Bi, W, As, Co, Fe, Sn, Ag, and Mo), (2) zones in metasedimentary basins once occupied by anoxic seafloor depressions and hydrothermal vents (Pb, Zn, Cu, Ag, Sn, and Sb) that may grade laterally into oxidized facies equivalents characterized by anomalous Ba (barite) and Mn, and (3) areas of skarn and vein deposits associated with exposed plutons and concealed cusps (Cu, Pb, W, Bi, As, Co, and Mn).

The Apex Mine, Utah—A Colorado Plateau-Type Solution-Collapse Breccia Pipe

Karen J. Wenrich, Earl R. Verbeek, Hoyt B. Sutphin, Bradley S. Van Gosen, and Peter J. Modreski

The Apex Mine, in southwestern Utah's Beaver Dam Mountains, is in the southern Basin and Range province near the Colorado Plateau's western edge. Oxidized ore was mined intermittently from the Apex between 1884 and 1949 for Cu, Pb, Ag, and minor Zn and Au, as it was from numerous mines in the Grand Canyon area. Most of the old Grand Canyon Cu mines are in the oxidized zone of U- and base-metal-bearing breccia pipes that formed by collapse of overlying sedimentary rocks into solution caverns within the Mississippian Redwall Limestone. Most of the U ore occurs within the sandy breccia matrix formed by comminution of Pennsylvanian and Permian sedimentary rocks. Similarly, the Apex Mine is in a collapse breccia formed by solution, presumably of the underlying Redwall Limestone. In the past, this breccia was attributed to fault brecciation, but the following observations suggest instead that it formed by solution collapse: (1) the breccia clasts are polylithologic, are oriented nearly randomly, and range widely in size from pebbles to large slabs, (2) the breccia occurs in large, irregular masses whose shape and distribution bear no relation to fault position, (3) much of the breccia consists of a chaotic jumble of blocks in loose contact with large voids between individual blocks, and (4) individual clasts are not sheared, and the breccia exhibits no planar fabric suggestive of faulting. The faults, in fact, postdate this collapse breccia; in several places, masses of breccia have been brought into sharp fault contact against solid bedded limestone.

Despite these similarities between the Plateau breccia pipes and the thoroughly oxidized Apex Mine in 1985, processing of Ge and Ga ore (averaging about 600 ppm Ge and 300 ppm Ga) began from the Apex, making it the world's first primary producer of these two metals. Similar concentrations of Ga and Ge are unknown in the Colorado Plateau U-bearing breccia pipes, although few samples have been analyzed for Ge. The only Ga concentrations found to exceed 100 ppm came from two samples from the Ridenour Mine, a U-rich breccia pipe on the Hualapai Indian Reservation. In addition to Ga and Ge in the Apex Mine, Au is enriched within goethite- and jarosite-rich ore. Concentrations of Au in 7 of 21 samples from the breccia zone range between 8 and 33 ppm, suggesting that Au may be a viable byproduct from the Apex. Although such high Au concentrations are rare in the U-rich Colorado Plateau breccia pipes, they do occur in the oxidized zones of the Copper Mountain and the Chicken Mines (both on the north rim of the Grand Canyon). In both occurrences, and at the Apex mine, Au is associated with high Zn, specifically hemimorphite and smithsonite.

A wide assortment of Cu, Pb, Zn and As minerals can be found at the Apex Mine. Along with minerals such as azurite, malachite, chrysocolla, brochantite, conichalcite, and aurichalcite (for which the Apex has long been popular with mineral collectors), other minerals identified by earlier workers and additional ones identified during this study are adamite, anglesite, cerussite, chalcopyrite, cobaltian adamite, covellite, cuprian adamite, cuprite, duftite, galena, goethite halloysite, hematite, hemimorphite, jarosite, plattnerite, plumbojarosite, and rosasite. Most of this mineral suite is similar to that of the Tsumeb solution-collapse breccia pipe in Namibia. In addition, the suite of base-metal elements is similar to that of the Colorado Plateau breccia pipes, and, although primary unoxidized ore minerals of these base metals, such as galena and chalcopyrite, are rare in the Apex Mine, they are present.

Additional solution collapse breccia pipes have been identified in the Beaver Dam Mountains. Because breccia pipes on the Colorado Plateau tend to occur in clusters, there appears to be significant economic potential for more ore bodies similar to the Apex in this part of the Basin and Range. The major difference between ore bodies in the Beaver Dam Mountains and those on the Colorado Plateau is that the Apex type tends to be oxidized extensively and lacks U-bearing ore. The absence of U-bearing minerals may be due to (1) complete oxidation of the ore body during the Basin and Range faulting and tilting, such that any U minerals present would have been oxidized, dissolved, and transported away by oxidizing fluids, (2) the U-bearing fluids may not have migrated this far north, or (3) the hydrologic environment of the host rock in the Basin and Range may not have been favorable to U deposition during the Triassic.

Preliminary Results of Geophysical Studies Near the Creede Mining District, Colorado

David L. Williams, William D. Stanley, and Victor F. Labson

Gravity, aeromagnetic, magnetotelluric (MT), and audiomagnetotelluric (AMT) surveys recently have been completed in the region around the Creede mining district, Colorado. The gravity and aeromagnetic surveys offer good coverage of the region, but MT coverage consists of a single reconnaissance profile in the southern part of the district. The AMT survey was limited to the area of the northern moat of the Creede caldera. Only preliminary aeromagnetic maps are currently available.

The region around Creede contains at least four large and diverse calderas of late Oligocene age known as the central San Juan caldera complex. Apparently, the calderas were emplaced through older volcanic rock overlying Precambrian basement and, in some instances, Mesozoic sedimentary rocks. The ash flows of the Bachelor and San Luis calderas and postcaldera lake sediments and volcaniclastics of the Creede Formation are the important host units of mineralization.

In general, the caldera-generated ash-flow tuffs that make up most of the terrain have a strong remanent magnetizations. In places, these magnetizations are destroyed by high-temperature alteration, permitting aeromagnetic methods to detect such alteration zones. Intrusive rocks and the Creede Formation are typically less magnetic than unaltered ash-flow tuffs. The ash-flow tuffs have an average density of about 2.4 gm/cm^3, whereas intrusive rocks generally are denser than 2.6 gm/cm^3, and the Creede Formation is closer to 2.2 gm/cm^3.

The gravity and regional aeromagnetic signatures of the individual calderas are diverse, with the La Garita caldera, oldest and largest of the group, showing gravity and magnetic highs. The Bachelor caldera, whose intracaldera ash-flow tuff hosts much of the Creede mineralization, has a slight gravity low and indefinite aeromagnetic signature. The Creede caldera is the most clearly delineated, with pronounced gravity and magnetic highs. The anomalies for the Creede caldera define details of ash-flow tuff thickness and the resurgent Creede pluton. The San Luis caldera, youngest of the group, has a gravity high and a rather complex aeromagnetic signature.

In addition to the regional aeromagnetic survey, a detailed helicopter aeromagnetic survey was flown over the mining district and preliminary maps show fine structures that may be identified with faults, veins, alteration zones, shallow intrusions, and breccia pipes.

An AMT survey of the Creede Formation just south of the mining district was designed to map the thickness and lithology of the Creede Formation and was successful in achieving these goals. Fine-grained ashy lake sediment could be distinguished easily from coarser volcaniclastics and colluvium. Travertine bodies in the sediments also were detected easily. The reconnaissance MT profile extended from the Creede caldera moat across the Bulldog Mountain region to the area between Nelson Mountain and the Equity Mine. Preliminary

interpretations of the data reveal no major pluton underneath the mapped location of the Bachelor caldera crossed by the MT profile. However, a highly resistive body (3,000–12,000 ohm-m) detected north of Nelson Mountain at depths of 2–3 km is interpreted to represent a pluton, possibly associated with the southern edge of the San Luis caldera. The northern extent of this resistive body is not known because of the limited extent of the MT survey.

Textural Association of Platinum-Group Minerals From the J-M Reef, Stillwater Complex, Montana

M. L. Zientek and R. L. Oscarson

The mineralogy, grain size, and textural associations of platinum-group element (PGE) minerals have been determined for a sample collected from the J-M Reef of the Stillwater Complex, MT, by backscattered electron microscopy combined with qualitative and semiquantitative energy dispersive X-ray analysis. Approximately 160 PGE mineral grains were observed in the 5-cm^2 area constituting this sample. At least 14 minerals are present and consist of Pd, Pt, and Rh sulfides; Pt and Pd tellurides; and Pt-Fe, Pt-Pd-Sn, Pd-Pb, Pd-Hg, Au-Pt-Pd alloys. Moncheite, Pd tellurides, and Pt-Fe alloy are the most common; michinerite, plumbopalladinite, and potarite, which have not been reported previously from the Stillwater Complex, are also present. Four distinct textural occurrences of these minerals are characterized by differing proportions of minerals and grain size. PGE minerals may occur as inclusions in base-metal sulfide (BMS), either totally surrounded by BMS or, more commonly, directly against the BMS-gangue contact. This is the textural occurrence most commonly described from the Merensky Reef, Bushveld Complex, South Africa. Fourteen percent of the observed grains fall in this category; moncheite and Pt-Fe alloy are most common in this group. The maximum dimension of all grains in this group averages 41 μm. Associated with many PGE-mineral inclusions in BMS are PGE minerals included in the adjacent silicate gangue. This occurrence accounts for 10 percent of the grains and is dominated by moncheite. The grain size, which is much finer than those included in BMS, averages 4 μm. Approximately 6 percent of the PGE minerals occur in chalcopyrite, which occurs in irregularly shaped clusters of grains included within bronzite. Pd tellurides dominate this occurrence, with an average grain size of 1.5 μm. Most of the grains of PGE minerals (70 percent) occurred in discontinuous stringers or veinlets with or without BMS. Their mineralogy is dominated by Pd tellurides and a very high proportion of the phases observed other than moncheite. Au alloys, vysotskite, palladian pentlandite, and potarite are characteristic of these veinlets. Grain size, which is quite fine, averages 4 μm. These veinlets probably represent the end product of the crystallization of a PGE-enriched immiscible sulfide liquid; serpentinization and associated veining postdate these veinlets.

For this sample, PGE concentrations were estimated by summing the contribution to whole rock abundance made by each grain. Simple grain shapes (circles or rectangles) utilizing measured grain dimensions were used in these calculations. The calculated concentrations were 7 ppm Pd and 55 ppm Pt. The actual concentrations, determined by combined fire assay-atomic absorption analysis, are 37 ppm Pd and 55 ppm Pt.

PGE minerals account for all the Pt grade but only one-fifth of the Pd grade. The remaining Pd occurs in solid solution with pentlandite. The Pd content of previously analyzed J-M Reef pentlandites ranges from 1,870 to 13,600 ppm (Cabri and others, 1984). Semiquantitative analyses of pentlandite from the veinlets in this sample range from 3.5 to 8.7 weight percent Pd.

Reference Cited

Cabri, L. J., Blank, Herma, Goresy, A. E., Laflamme, J. H. G., Nobiling, Rainer, Sizgoric, M. B., and Traxel, Kurt, 1984, Quantitative trace-element analyses of sulfides from Sudbury and Stillwater by proton microprobe: Canadian Mineralogist, v. 22, p. 521–542.

Comparison of the Turner-Albright Ophiolite-Hosted Massive Sulfide, Southwestern Oregon, to Active Hydrothermal Deposits on the Southern Juan de Fuca Ridge

Robert A. Zierenberg, Randolph A. Koski, Wayne G. Shanks III, William E. Seyfried, Jr.,[1] and Michael D. Strickler[2]

The Turner-Albright volcanogenic massive sulfide and associated altered volcanic rocks represent a well-preserved, relatively unmetamorphosed analog of the active seafloor hydrothermal systems developed at the southern Juan de Fuca spreading center. The deposit consists of several Cu-Zn-Ag-Au-Co-rich

[1]University of Minnesota, Minneapolis, MN.
[2]Lithologic Resources, Grants Pass, OR.

massive sulfide bodies in the lower part of the extrusive sequence of the Late Jurassic Josephine ophiolite. Basalt occurs as pillowed and massive flows, thick ponded lava lakes, talus, and hyaloclastite breccias. These basalts typically contain phenocrysts of fresh clinopyroxene; plagioclase, which is partially replaced by albite, chlorite, and pumpellyite; and titanomagnetite, which is altered totally to sphene and leucoxene. The formerly glassy groundmass of these rocks was metamorphosed beneath the seafloor to chlorite, pumpellyite, prehnite, and albite by circulation of heated seawater.

A second, more primitive, lava series occurs as thick units of hyaloclastite breccia spatially associated with the sulfide horizons. These lavas contained phenocrysts of olivine, chromium spinel, and plagioclase and typically have plumose to dendritic relect quenched textures in the groundmass. However, these basalts have been altered hydrothermally by the ore-transporting fluids, and the least-altered rocks are now essentially two component mixtures of Fe-rich chlorite and quartz. The chlorite-quartz rocks were altered at approximately 350°C from a fluid depleted in Mg and enriched in $\delta^{18}O$ by approximately 2 per mil, similar to hydrothermal fluids sampled at modern ridge crests. Increased alteration results in total replacement of the basalt by quartz. Intermediate stages of alteration often preserve the original volcanic textures.

Typical sulfide intervals contain massive sulfide at the top and grade downward through semi-massive sulfide to mineralized basalt. Much of the sulfide-bearing rock has fragmental textures. The down-hole decrease in sulfide content is accompanied by an increase in the proportion of altered volcanic fragments and a decrease in the degree of alteration of the fragments. Pyrite is the dominant sulfide, but sphalerite-rich intervals are common, especially at the tops of ore intercepts where primary growth banding often is preserved. Cu-rich zones show invasion and replacement of preexisting sulfides by chalcopyrite on all scales from entire core samples to individual color bands in sphalerite crystals. Sulfur isotope values for the sulfides are generally between 1 and 8 per mil.

Only a small portion of the sulfides formed by true exhalative processes above the seawater-basalt interface; most formed below the seafloor from hydrothermal fluid that infiltrated and partially replaced basaltic hyaloclastite and talus breccia. The geologic setting and geochemical processes that led to the formation of the Turner-Albright deposit are similar to the active hydrothermal deposits forming at the southern Juan de Fuca Ridge, where only the upper Zn- and Ag-rich portion of the system is exposed for sampling by research submarines.

The paleokarst, which formed in the Mississippian Redwall Limestone, is so extensive that many caves, such as this one along Diamond Creek, AZ, were used during the Late Mississippian as passages by channels of the Surprise Canyon Formation. This 80- x 140-ft cave formed in the Thunder Springs Member of the Redwall with the top reaching into the Mooney Falls Member. Collapse of the overlying late Paleozoic sedimentary rocks into such caves formed breccia pipes, some of which were mineralized by U-bearing fluids about 200 Ma (age determined by Ken Ludwig). The extensive karst in the Redwall Limestone permitted considerable flushing of the soluble and fine-grained portions of the breccia pipes, such that total downdropping in some pipes exceeds 700 ft. This particular cave is an important part of the Hualapai Indian heritage. As H. F. Dobyns and R. C. Euler stated in *The Walapai People*, "A cave in the steep north wall of Diamond Creek Canyon contained a rich deposit of red mineral pigment. Mixed with deer tallow, this pigment formed a fine face cream and body coating to protect skin against sunburn and cold. Its bright [red] color made it a very precious commodity that the Northeastern Pai sold in intertribal trade for good prices. . . .Mining was dangerous and difficult. Miners constructed tall ladders of notched logs to prop against the nearly vertical cliff wall so they could climb from the nearest ledge [shown at the bottom of the photograph as the sloping ledge of the Devonian Temple Butte Formation] up to the narrow opening into the cave." Research was funded by the Bureau of Indian Affairs in cooperation with the Hualapai Tribe.

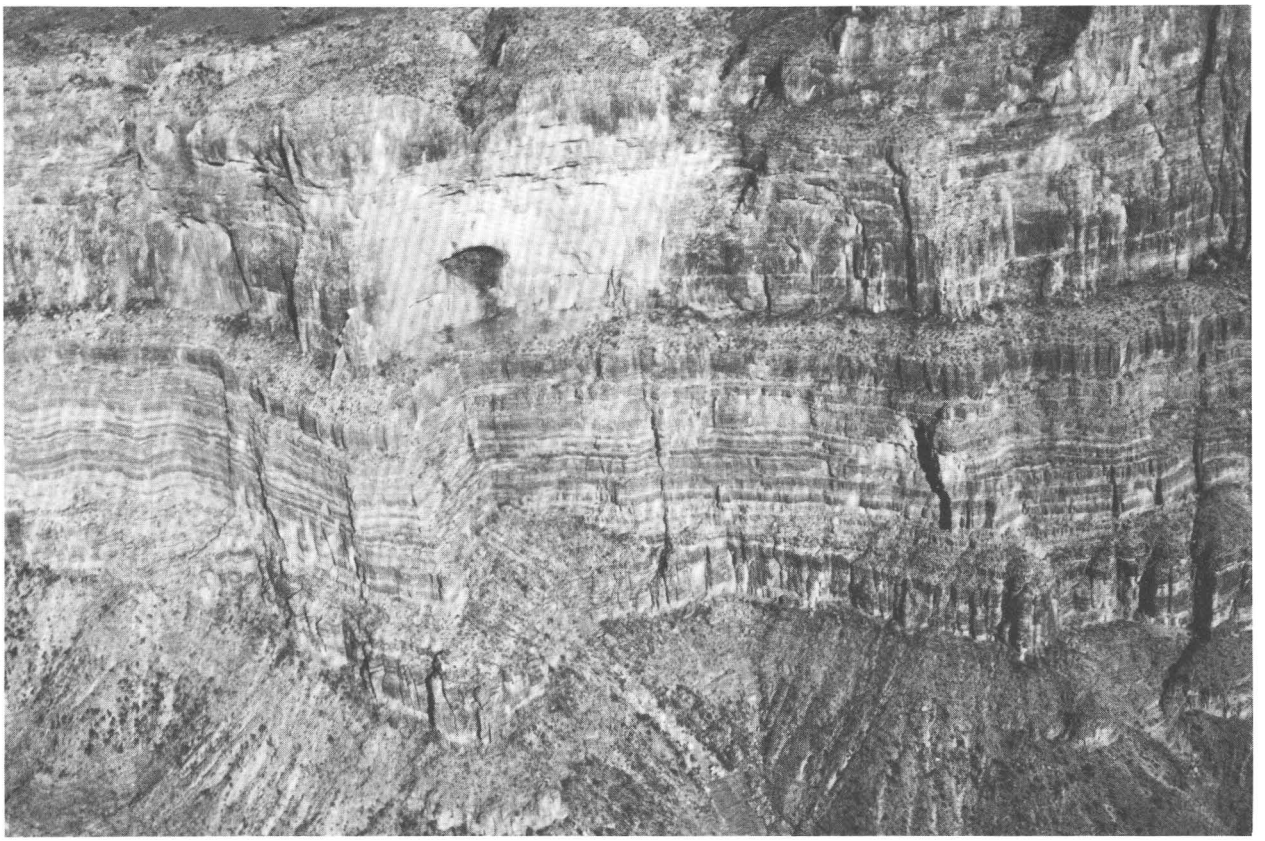

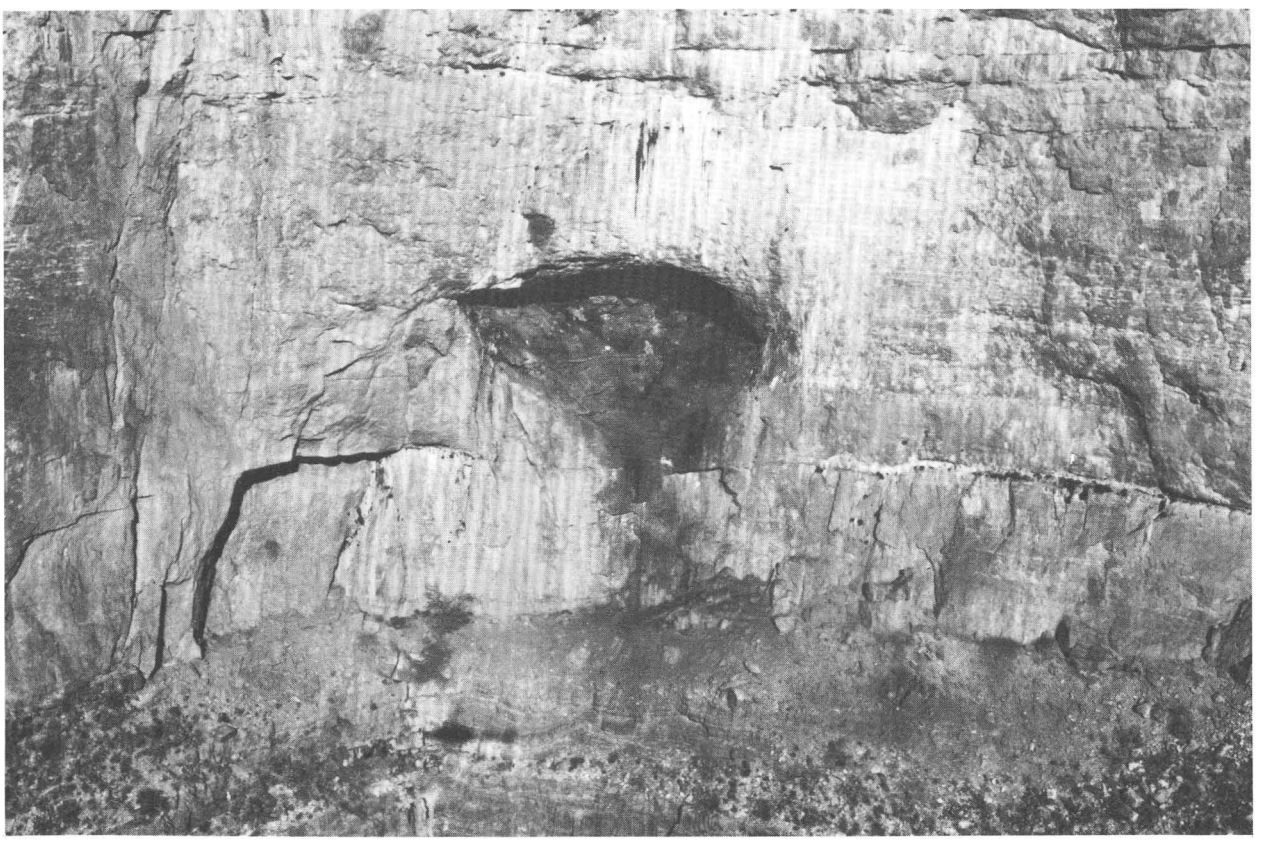

ORGANIZATION OF THE U.S. GEOLOGICAL SURVEY

Office	Name	Telephone	City
Office of the Director			
Director	Dallas L. Peck	703/648–7411	Reston
Associate Director	Doyle G. Frederick	703/648–7412	Reston
Assistant Director for Research	Bruce R. Doe	703/648–4453	Reston
Assistant Director for Engineering Geology	James F. Devine	703/648–4423	Reston
Assistant Director for Administration	Jack J. Stassi	703/648–7201	Reston
Assistant Director for Programs	Peter F. Bermel	703/648–4430	Reston
Assistant Director for Intergovernmental Affairs	John J. Dragonetti	703/648–4427	Reston
Chief, News Media Service	Donovan B. Kelly	703/648–4459	Reston
Assistant Director for Information Systems	James E. Biesecker	703/648–7108	Reston
National Mapping Division			
Chief	Lowell E. Starr	703/648–5748	Reston
Geologic Division			
Chief Geologist	Robert M. Hamilton	703/648–6600	Reston
Water Resources Division			
Chief Hydrologist	Philip Cohen	703/648–5212	Reston

ORGANIZATION OF THE GEOLOGIC DIVISION

Office of the Chief Geologist			
Chief Geologist	Robert M. Hamilton	703/648–6600	Reston
Associate Chief Geologist	William F. Cannon	703/648–6601	Reston
Assistant Chief Geologist for Program	Benjamin A. Morgan	703/648–6640	Reston
Assistant Chief Geologist, Eastern Region	Jack H. Medlin	703/648–6660	Reston
Assistant Chief Geologist, Central Region	Harry A. Tourtelot	303/236–5438	Denver
Assistant Chief Geologist, Western Region	Carroll Ann Hodges	415/323–8111	Menlo Park
Office of Mineral Resources			
Chief	Glenn H. Allcott	703/648–6100	Reston
Chief, Branch of Alaskan Geology	Donald J. Grybeck	907/786–7403	Anchorage
Chief, Branch of Eastern Mineral Resources	Bruce R. Lipin	703/648–6327	Reston
Chief, Branch of Central Mineral Resources	David A. Lindsey	303/236–5568	Denver
Chief, Branch of Western Mineral Resources	Edwin H. McKee	415/323–8111	Menlo Park
Chief, Branch of Geochemistry	Byron R. Berger	303/236–1800	Denver
Chief, Branch of Resource Analysis	Lawrence J. Drew	703/648–6125	Reston
Chief, Branch of Geophysics	Frank C. Frischknecht	303/236–1212	Denver
Office of Energy and Marine Geology			
Chief	Terry W. Offield	703/648–6470	Reston
Chief, Branch of Petroleum Geology	Dudley D. Rice	303/236–5711	Denver
Chief, Branch of Coal Resources	Harold J. Gluskoter	703/648–6401	Reston
Chief, Branch of Sedimentary Processes	Thomas D. Fouch	303/236–1644	Denver
Chief, Branch of Pacific Marine Geology	Monty A. Hampton	415/323–8111	Menlo Park
Chief, Branch of Atlantic Marine Geology	Robert B. Halley	617/548–8700	Woods Hole
Office of Regional Geology			
Chief	Eugene H. Roseboom	703/648–6960	Reston
Chief, Branch of Eastern Regional Geology	Gregory S. Gohn	703/648–6900	Reston
Chief, Branch of Central Regional Geology	Glen A. Izett	303/236–1250	Denver
Chief, Branch of Western Regional Geology	Robert O. Castle	415/323–8111	Menlo Park
Chief, Branch of Isotope Geology	John N. Rosholt	303/236–7880	Denver
Chief, Branch of Astrogeology	Hugh H. Kieffer	602/527–7015	Flagstaff
Chief Branch of Paleontology and Stratigraphy	Richard Z. Poore	703/648–5288	Reston

Office	Name	Telephone	City
Office of Earthquakes, Volcanoes, and Engineering			
Chief	John R. Filson	703/648–6714	Reston
Chief, Branch of Engineering Seismology and Geology	Thomas C. Hanks	415/323–8111	Menlo Park
Chief, Branch of Global Seismology and Geomagnetism	Robert P. Masse	303/236–1510	Denver
Chief, Branch of Seismology	William L. Ellsworth	415/323–8111	Menlo Park
Chief, Branch of Geologic Risk Assessment	Albert M. Rogers	303/236–1585	Denver
Chief, Branch of Tectonophysics	Wayne R. Thatcher	415/323–8111	Menlo Park
Chief, Branch of Igneous and Geotheranal Processes	L. J. Patrick Muffler	415/323–8111	Menlo Park
Office of Scientific Publications			
Chief	John M. Aaron	703/648–6077	Reston
Office of International Geology			
Chief	A. Thomas Ovenshine	703/648–6047	Reston

Addresses

U.S. Geological Survey
Reston, VA 22092

U.S. Geological Survey
Box 25046
Denver Federal Center
Denver, CO 80225

U.S. Geological Survey
345 Middlefield Road
Menlo Park, CA 94025

U.S. Geological Survey
Branch of Alaskan Geology
4200 University Drive
Anchorage, AK 99508–4667

U.S. Geological Survey
2255 North Gemini Drive
Flagstaff, AZ 86001

U.S. Geological Survey
Quissett Campus, Building 13
Woods Hole, MA 02543

INDEX

T

V

W

Z

☆U.S. G.P.O. 1987-181-407:40062